GMD2 Groundwater Flow Model

High Plains Aquifer Modeling Maintenance Project

Funded by the

Kansas Water Office (Kansas Water Plan), KAN0078739

and

Equus Beds Groundwater Management District # 2, KAN0078734

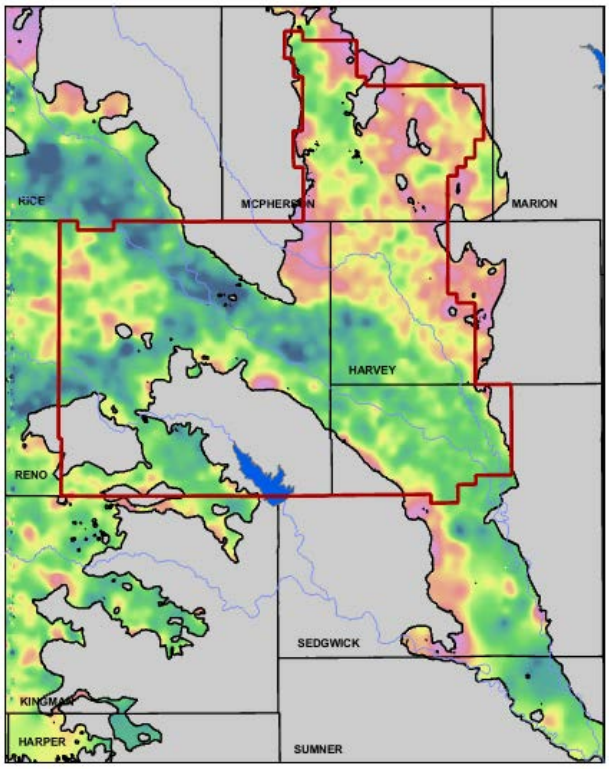

Brownie Wilson, Gaisheng Liu, Geoffrey C. Bohling, and James J. Butler, Jr.

Kansas Geological Survey Open-File Report 2020-1

January 2020

GEOHYDROLOGY

KU KANSAS GEOLOGICAL SURVEY
The University of Kansas

GMD2 Groundwater Flow Model

High Plains Aquifer Modeling Maintenance Project

This project was funded by the

Kansas Water Office (Kansas Water Plan)

And

Equus Beds Groundwater Management District # 2

Kansas Geological Survey Open-File Report 2020-1
January 2020

Kansas Geological Survey, Geohydrology Section
University of Kansas, 1930 Constant Avenue,
Lawrence, KS 66047
http://www.kgs.ku.edu/

Disclaimer

The Kansas Geological Survey does not guarantee this document to be free from errors or inaccuracies and disclaims any responsibility or liability for interpretations based on data used in the production of this document or decisions based thereon.

TABLE OF CONTENTS

Introduction 1
Project Overview 1
Description of Study Area and General Model Setup 2
Previous Geohydrologic Studies 2
Physiographic Setting 4
Model Design 4
Active and Inactive Areas 9
Review and Setup of Data and Parameters 10
Precipitation and Temperature Data 10
Geology and Lithology 12
Aquifer Characteristics 12
Bedrock Surface 15
Lithologic Characterization 17
Water Levels 21
Boundary Conditions 27
Stream Characteristics and Flow 29
Water Right Development 32
Estimation of Historic Water Use 34
Irrigation Return Flow 36
Model Calibration and Simulation 41
Model Characteristics 41
Predevelopment Pumping 41
Transient Pumping and Irrigation Return Flows 43
Stream Characteristics 43
Drains 43
Evapotranspiration 43
Time-Varying Specified-Head Boundaries 43
Precipitation Recharge 44
Hydraulic Conductivity and Specific Yield 46
Model Calibration 49
Sensitivity Analysis 53
Transient Model Results 54
Water Levels 54
Streamflow 54
Model Budgets 73
Comparison with Sustainability Assessment, KGS OFR 2017-3 74
Model Scenarios 78
Scenario 1: No Change in Water-Use Policy 78
Scenario 2: Enhancing Extreme Wet and Dry Climatic Events 81
Scenario 3: Reoccurring Droughts 83
Comparison of All Scenarios 85
Acknowledgments 88
Appendix A, Lithologic-Based Model Layers 89
References 94

INTRODUCTION

Equus Beds Groundwater Management District No. 2 (GMD2) was formally established in 1975 and was the second of five such local management districts in Kansas authorized under the Groundwater Management District Act of 1972. GMD2 overlies the Equus Beds aquifer, a groundwater system in south-central Kansas that represents the easternmost portion of the much larger High Plains aquifer (HPA), which in turn covers parts of South Dakota, Wyoming, Nebraska, Colorado, Kansas, New Mexico, Oklahoma, and Texas. Like much of the HPA, irrigation is the dominant water use, although the Equus Beds aquifer is also a primary water source for large municipal allocations, such as for the cities of Wichita and Hutchinson, along with other significant industrial uses. The management goal of GMD2 is to balance groundwater withdrawals with annual recharge to prevent unsustainable groundwater mining while also protecting from and remediating groundwater contamination.

Project Overview

The Kansas Water Office (KWO) and GMD2 contracted with the Kansas Geological Survey (KGS) in the summer and fall of 2017 to develop a numerical groundwater model primarily for the GMD2 area and, secondarily, for the Arkansas River alluvial aquifer south of the district to Belle Plaine, Kansas. The primary objective of the model is to better understand the hydrologic system and water-table changes occurring in the underlying HPA in response to historic water uses. The model will be used to simulate future water use and possible climatic scenarios to estimate their effects on the Equus Beds.

The project period covered October 2017 through January 2020. The calibrated transient model was completed in the fall of 2019. This final report was completed in January 2020. As the model was being developed, the KGS provided several progress reports to GMD2, Kansas Water Office (KWO), and, occasionally, Kansas Department of Agriculture, Division of Water Resources (KDA-DWR) staff.

DESCRIPTION OF STUDY AREA AND GENERAL MODEL SETUP

The study area includes all of GMD2 in south-central Kansas and the Arkansas River alluvial aquifer to the south of the district. The model domain extends from the Smoky Hill River valley on the north to the confluence of the Arkansas and Ninnescah rivers (a little more than thirty miles south of the GMD2 southern boundary) on the south and to roughly six miles east and to six miles west of the district boundaries (fig. 1). The total area covered by the model is 5,567 square miles, and it is completely positioned within Kansas. Groundwater-based irrigation represents the largest appropriation of water, although the area is also home to municipal well fields for the cities of Wichita, Hutchinson, McPherson, and Newton and surrounding communities along with several rural water districts and industrial sites. The entire GMD2 boundary and the Arkansas River alluvium to the south of the district within the model's active area lie within the Equus-Walnut Regional Planning Area for the Kansas Water Authority and Kansas Water Plan.

Previous Geohydrologic Studies

Several KGS bulletins report on the geology and groundwater resources of the model area, including Williams et al. (1949) (all of McPherson and parts of Reno, Harvey, and Sedgwick counties), Fent (1950) (Rice County), Bayne (1956, 1960) (Reno and Harper counties), Lane (1960) (Kingman County), Walters (1961) (Sumner County), and Lane and Miller (1965) (Sedgwick County). In addition to characterizing the groundwater conditions in the region, these bulletins provide valuable historic well records and lithologic logs that are among the key data used to construct and calibrate the model.

The U.S. Geological Survey (USGS) has conducted a series of studies on the Equus Beds aquifer. Recently, Stone et al. (2019) found the water-quality characteristics of the aquifer over the 15-year period from 2001 to 2016 did not change significantly relative to historical ranges of variability. Kelly et al. (2013) developed a numerical groundwater flow model across the core area of GMD2 to assess the influences of the City of Wichita's Artificial Storage and Recharge project on the aquifer, especially related to chloride transport from the Arkansas River and Burrton oilfield to the city's well field.

Butler et al. (2017) of the KGS assessed the sustainability of GMD2 by applying a data-driven, water-balance approach, which used annual water-level measurements and reported groundwater usage to determine what average level of usage is needed to stabilize water levels in the near term. The analysis by Butler et al. (2017) also produced estimates of aquifer net inflow and specific yield, both of which are incorporated in this study to improve the accuracy of model construction and calibration.

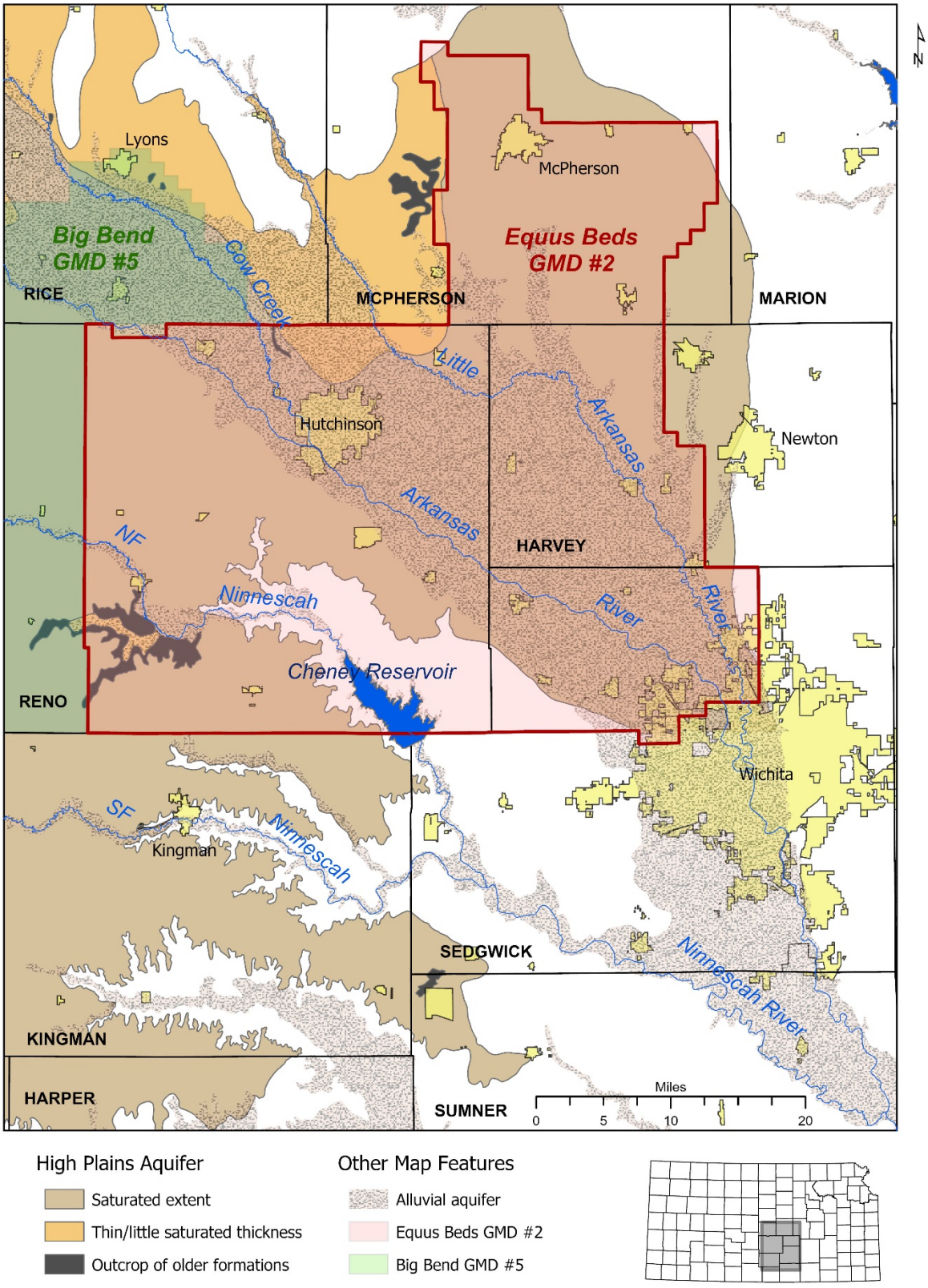

Figure 1. Map of GMD2 model area.

Physiographic Setting

The core of the active area of the model lies within the Arkansas River Lowlands physiographic region, characterized as relatively flat alluvial plains formed from deposits of the Arkansas River (fig. 2). The Arkansas River Lowlands dissect the Wellington-McPherson Lowlands region, which lies primarily to the north of the model's area in McPherson County. This region is characterized by relatively flat to rolling alluvial plains, which are composed of unconsolidated sand, silt, clay, and gravel deposited by streams during the Pleistocene Epoch when the Equus Beds aquifer was formed. Wind-deposited sand dunes (also referred to as sand hills), most of which were formed by sands transported from the Arkansas River valley by the south wind during the last glacial period, are also present in local parts of Rice, Reno, and Harvey counties. Southwestern portions of Reno County, western Kingman, and northwest Harper County constitute the easternmost extent of the High Plains physiographic region in Kansas. The Red Hill region in the southwest portion of the study area lies almost completely within the inactive portion of the model.

A land cover classification map compiled by the Kansas Biological Survey in 2015 shows that cropland is the primary land-cover type (fig. 3). The cities of Wichita, Hutchinson, and McPherson have the largest municipal footprint, while grasslands are found primarily in the sand hills northeast of Hutchinson and along stream courses.

Model Design

This project used MODFLOW, the modeling software that was developed by the USGS based on a finite-difference approximation of the flow equation (Harbaugh et al., 2000; Niswonger et al., 2011). MODFLOW is one of the most widely used groundwater flow models in the world. It can be used to simulate the effects of many processes, such as areal recharge, stream-aquifer interactions, drains, evapotranspiration, and pumping. Input files for the MODFLOW model were created with assistance from scripts written in Fortran (https://www.fortran.com/). The model was run by entering the executable file name in a Windows command prompt.

The model uses uniform and equally spaced square cells, 400 x 400 feet in size (~3.67 acres). There are 1,106 rows and 877 columns, resulting in 969,962 individual model grid cells. The grid spacing is much finer than those used in past KGS modeling activities (Wilson et al., 2015; Liu et al., 2010; and Wilson et al., 2008) to accommodate any future contaminant transport models. The GMD2 model uses one convertible layer that allows both confined and unconfined properties of the aquifer to be simulated, depending on water levels. The streamflow-routing package (SFR in MODFLOW) was used to compute stream-aquifer interactions (Prudic et al., 2004) by subdividing streams into a series of segments and reaches.

Time-varying specified-head boundaries are located along most edges of the model. Specifically, they are used on the western edge to represent the HPA, on the northern edge where the model comes into contact with the Smoky Hill River alluvial aquifer, and on the southeastern edge of the Arkansas River alluvium (fig. 4). The head values for these boundaries are determined by a spatial and temporal interpolation of the water-level observations from nearby wells.

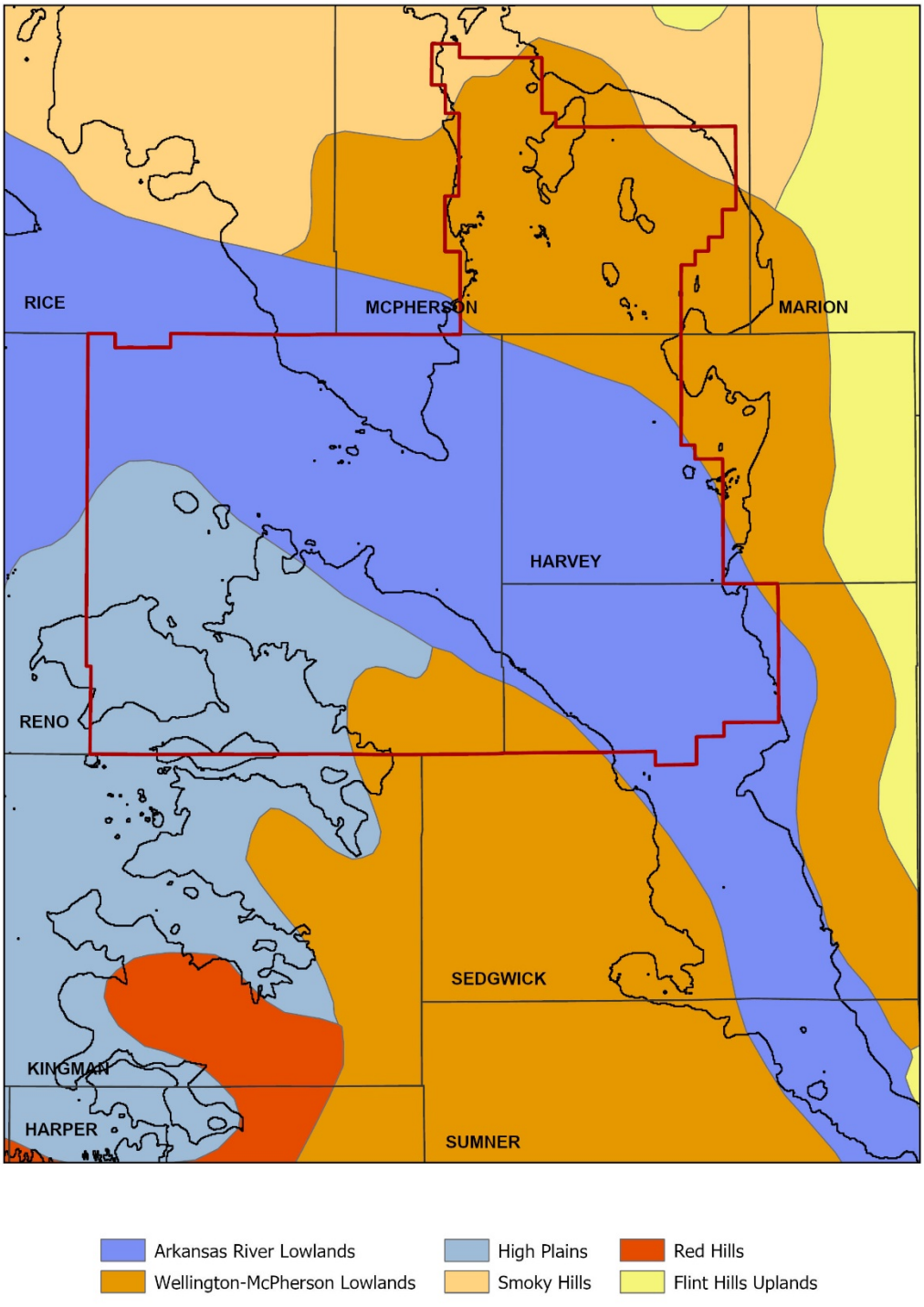

Figure 2. Physiographic regions in the model area. The irregular, thicker black line represents the active area of the model discussed in this report, and the red line represents the boundaries of GMD2.

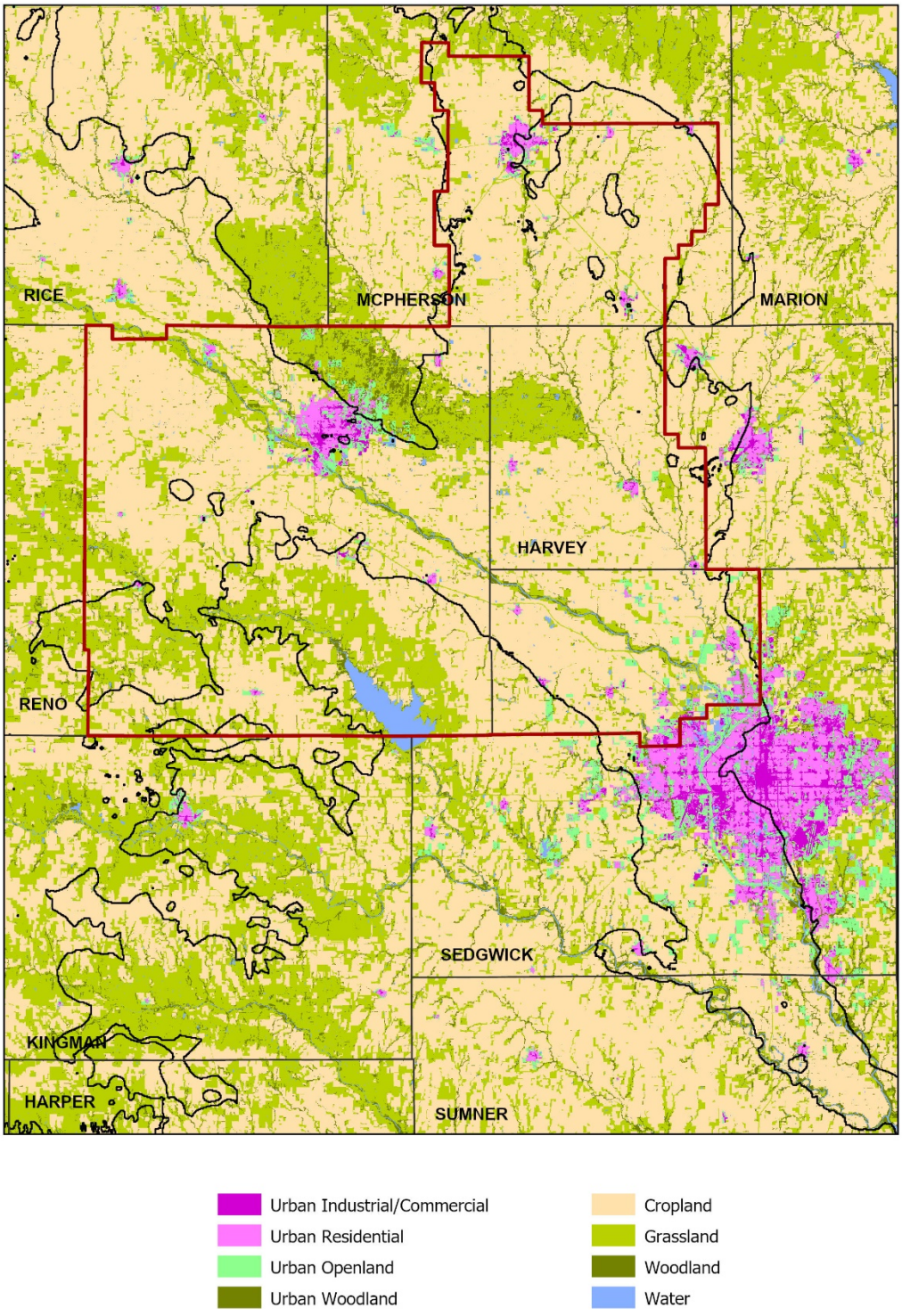

Figure 3. Land use/land cover classifications in the model area, 2015. The irregular, thicker black line represents the active area of the model, and the red line represents the boundaries of GMD2.

Constant head boundaries also are used in selected cells within the active area of the model to help prevent cells drying out during model runs (fig. 4). These cells are distributed along portions of the edges of the inactive bedrock area. At these cells, the interpolated water levels during the predevelopment time are used and fixed as constant through the transient simulations. This is a reasonable assumption as all of these constant cells are adjacent to bedrock areas with thinly saturated sediments and no significant pumping. The surface runoff from the nearby bedrock area is likely able to recharge and keep these cells constantly saturated with time. Remaining boundary edges are set to no-flow cells, which prevents flow between active and inactive areas of the model.

Streams cells allow for stream/aquifer interactions to take place and are set up for the Arkansas River, Little Arkansas River, Cow Creek, South and North Fork Ninnescah rivers, and Ninnescah River. Drain cells are specified for Big Slough Creek, from which water from the aquifer can discharge to the surface depending on water-table elevations. If water levels drop below the land surface, this connection is broken and the drains become inactive.

The lower vertical boundary of the model is the Permian-aged bedrock (mainly shale), which has much lower permeability than the aquifer and is treated as a no-flow boundary. The upper boundary of the model is the land surface, where water may enter or leave the aquifer through areal recharge, evapotranspiration, and stream-aquifer interactions. Land surface elevations are based on classified bare-earth LiDAR digital elevation models provided by the KGS Data Access and Support Center (DASC).

The modeling work was divided into two major steps. First, a steady-state simulation was generated for the predevelopment period before 1945. Data used for predevelopment simulation for most of GMD2 were typically from 1940 to 1950, during which large-scale, intensive pumping activities were not present. For areas south of the district in Kingman, southern Sedgwick, and northern Harper and Sumner counties, additional data representing the 1950s were used to fill in spatial data gaps. Second, a transient simulation was conducted for the period between 1945 and 2017 to replicate the historic evolution of the groundwater system and stream-aquifer interactions. The predevelopment step established the initial conditions for the subsequent transient simulation.

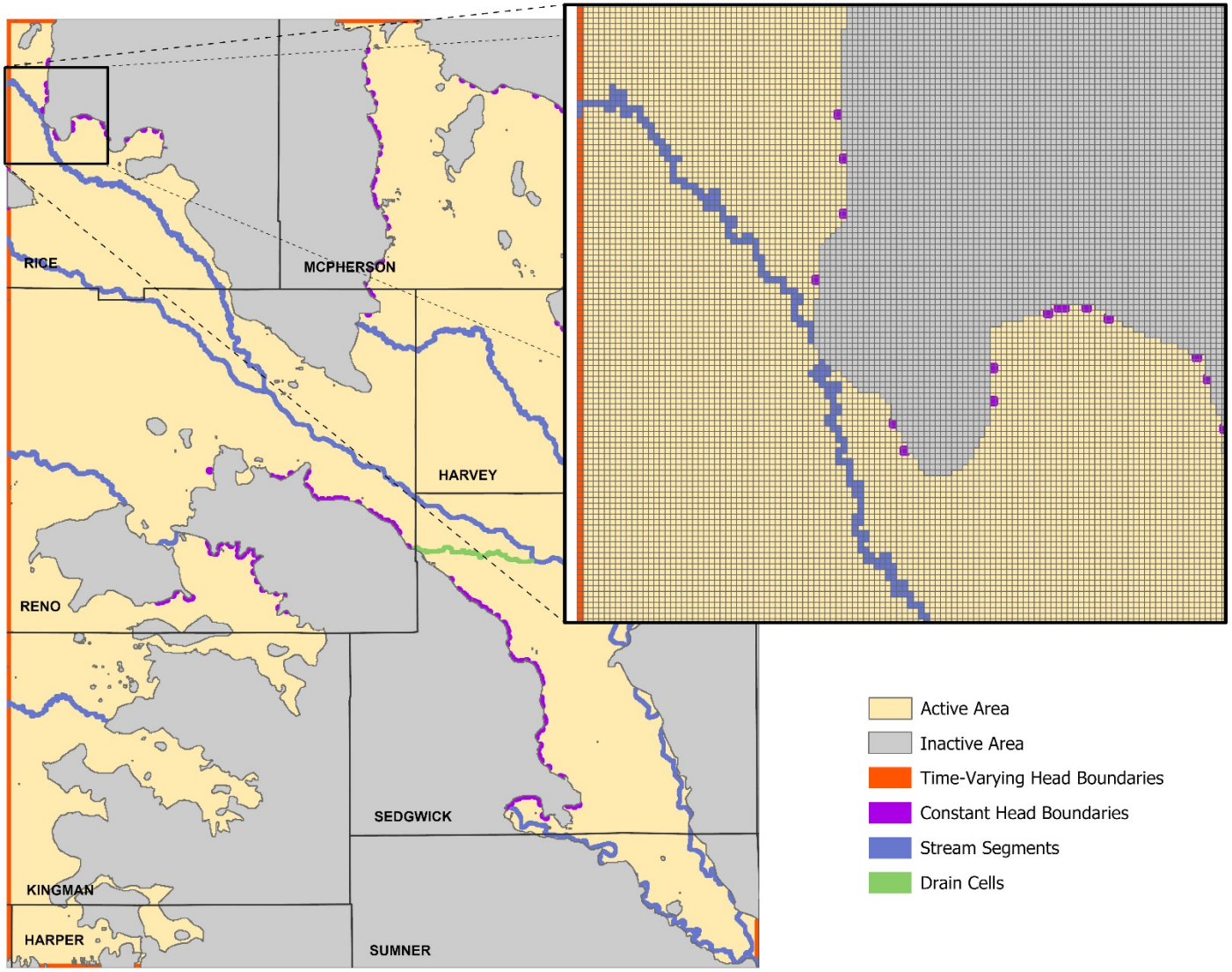

Figure 4. Model boundaries, grid cells, active area, and special model cells.

The model takes advantage of detailed information from the KGS HyDRA program, in which the lithological descriptions from thousands of drillers' logs have been digitally transcribed and categorized into common groups. The lithological groupings were then spatially interpolated to develop three-dimensional grids of lithological categories. Next, based on representative hydraulic conductivity (K) and specific yield (SY) values assigned to each lithological category, estimates of K and SY were computed for each model cell according to where the water level intersects the lithological grid. More than 26,000 lithologic logs were used in this process. In GMD2, as the water-level change is not as significant as in other areas of the HPA, K and SY estimates are not dynamically adjusted with year-to-year water-level fluctuations. In other words, the hydraulic conductivity and specific yield computed with predevelopment water levels are used for the subsequent transient simulation.

The model was calibrated to match predevelopment water levels and long-term hydrographs of selected wells, especially the water-level change over time. Low flow conditions in the identified stream cells were used to calibrate the streambed properties. The recharge-precipitation relationship, evapotranspiration rate, hydraulic conductivity, and specific yield are all treated as calibration parameters due to their relatively large uncertainties and significant influence on model results.

Active and Inactive Areas

Most groundwater models of this type include "active" and "inactive" areas. The actual groundwater flow calculations are conducted only within the active cells. In this study, the extent of the HPA in and around GMD2 and the Arkansas River alluvial aquifer represents the active area. "Inactive" cells are those where aquifer material is not present or is very thin (such as the HPA extents in northern Rice and western McPherson counties) or that have a substantial area of bedrock outcroppings, such as those in southern Reno County west of Cheney Reservoir. The number of active cells in the model is 436,840, giving a total active model area of 2,507 square miles, a little over 45% of the model domain.

REVIEW AND SETUP OF DATA AND PARAMETERS

Precipitation and Temperature Data

Monthly precipitation and temperature data were downloaded from the PRISM Climate Group at Oregon State University (http://prism.oregonstate.edu) in June 2018. PRISM provides raster-based grids (roughly 4 x 4 km) for the entire continental United States, and the data compare very favorably with similar precipitation-based data processing undertaken in past KGS activities (Wilson and Bohling, 2003; Wilson et al., 2008; and Liu et al., 2010).

The monthly PRISM grids for each year from 1942 to 2018 were processed to compute the annual average, minimum, and maximum precipitation and temperature for each year along with averages for the "summer" period (April to September) and the "winter" period (October to March). The "summer" and "winter" periods represent the irrigation and non-irrigation seasons, respectively. The output for each of these processing steps was a new raster-based grid, which was then overlain on the model area and the values assigned to each of the model cell centers.

The average summer and winter precipitation over the model area from 1945 to 2017 is 21.48 and 8.98 inches, respectively (fig. 5). The highest summer precipitation year was 1951 followed closely by 2016, with 37.03 and 36.08 inches, respectively, and the lowest period of precipitation was in the winter of 1967 with only 2.04 inches of precipitation.

Figure 6 shows spatial patterns in the normal precipitation (average precipitation over the period of the last three full decades, 1981 to 2010). The model area has a northwest-to-southeast gradient, with precipitation levels slightly lower in the Rice County area and increasing towards their maximum levels in southeast Sedgwick and northeast Sumner counties.

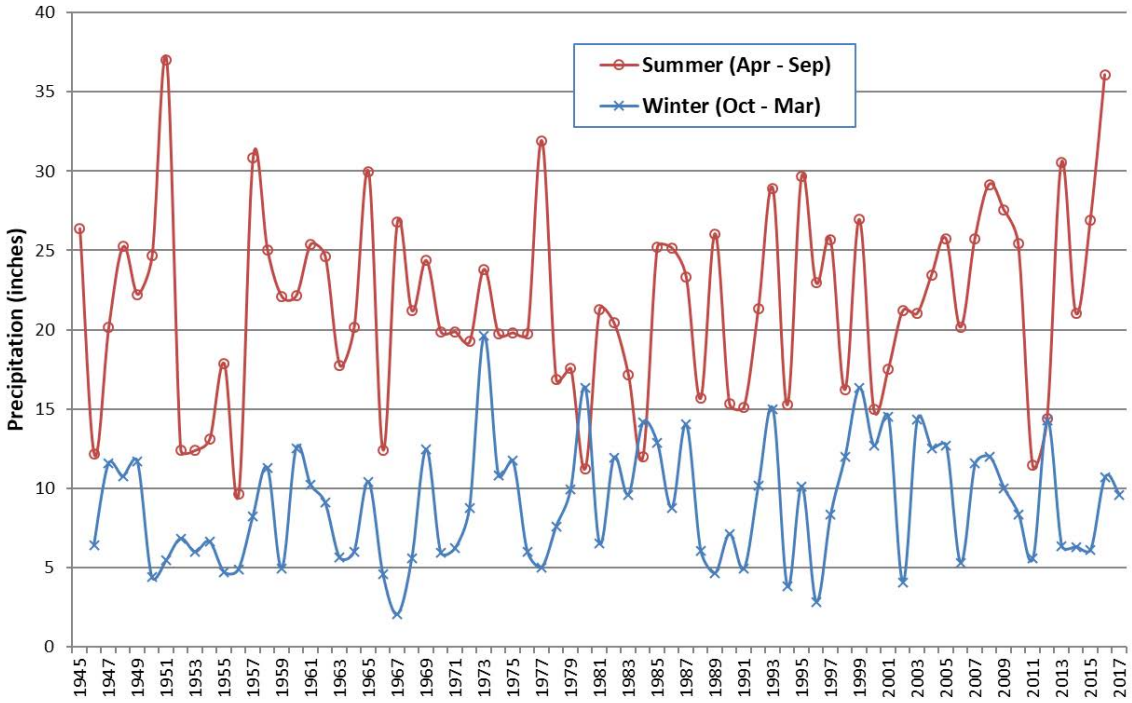

Figure 5. Average summer and winter precipitation over the model area.

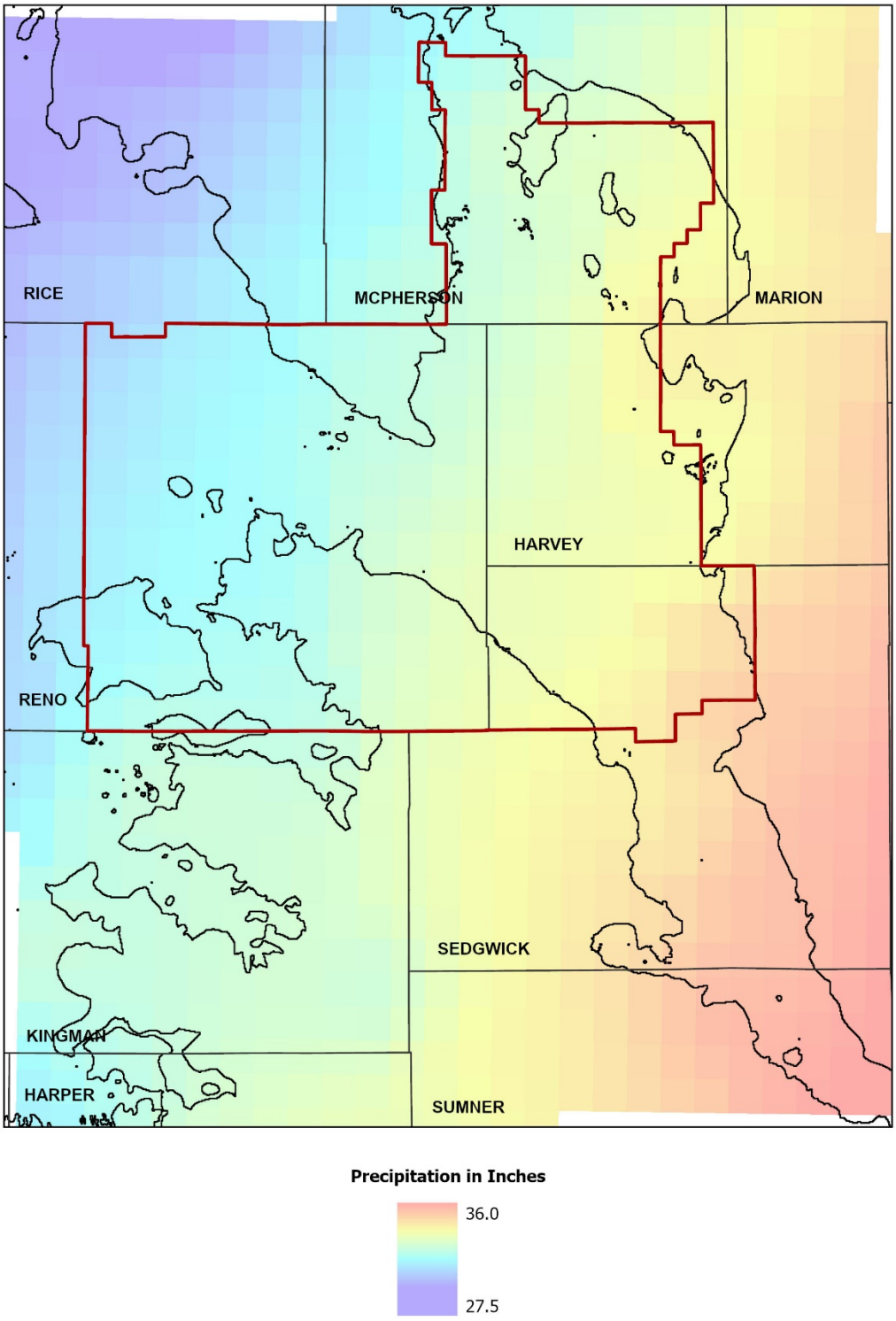

Figure 6. PRISM normal precipitation (average for 1981 to 2010).

Geology and Lithology

Surficial geologic formations, those at or near the surface, in the model area are sedimentary in nature and range from Permian to recent in age. The oldest are the Permian-aged Nippewalla and Sumner Groups that crop out in areas east and south of GMD2. Cretaceous-aged material, specifically the Kiowa Shale, Cheyenne Sandstone, and Dakota Formation can be found near or at the surface in Rice, McPherson, and Marion counties. The majority of the active area of the model is formed by the Arkansas River valley and its associated alluvial deposits. The valley is bounded by undifferentiated Pleistocene deposits, mainly loess, dune sand, and older alluvial deposits (fig. 7), and includes the water-bearing McPherson Channel, a relatively deep, stream-cut channel that runs to the north.

Aquifer Characteristics

The Equus Beds aquifer represents the eastern extent of the High Plains aquifer system. “Equus” is Latin for horse, and the aquifer derives its name from fossils of a type of now-extinct horse found in the area. Together with the hydrologically connected deposits of the Arkansas River alluvial aquifer, the Equus Beds aquifer is the primary water source for almost all groundwater uses in the active area of the model. The aquifer was formed when the ancestral channels of the Arkansas and Smoky Hill rivers, along with the subsidence areas from the dissolution of underlying salt formations, were filled with Pleistocene-aged deposits from streams and eolian processes. The unconsolidated sands and gravels are interspersed with discontinuous layers of silt and clay. The intent of this project is to simulate groundwater conditions in the unconsolidated material, and no distinction is made between the HPA and alluvial deposits. The core area of the model is concentrated over the thickest portions of the aquifer (fig. 8).

Given the nature of the overlying soil, generally flat topography, and shallow depths to water, most of the Equus Beds aquifer recharges readily. However, much of the McPherson Channel, the area north, south, and west of the City of McPherson, is overlain by silt deposits that reduce the groundwater recharge rate relative to other areas in the district.

Water quality in the area is generally suitable for most uses; however, the area does have several sites of contamination from both natural and human-induced sources. Oil field brine contamination is a significant issue in western Harvey County, particularly due to its proximity to the City of Wichita’s well field. Naturally occurring saline waters from the dissolution of underlying Permian-aged salt formations also can present significant water-quality threats if the overlying freshwater systems are overly pumped (e.g., upwelling of the more saline waters can be induced).

Cretaceous- and Permian-aged formations that underlie the Equus Beds are not considered in this study. The Wellington Formation and Ninnescah Shale compose the bedrock floor throughout the area. These units are water bearing but typically yield small quantities of highly mineralized water. The Dakota aquifer system, which is also water bearing, is found in the northern extents of the model domain, outside the active area, and can be highly variable in both quantity and quality (Whittemore et al., 2014). There are no known Dakota wells within GMD2. All water-level and water-right data known to be associated with Cretaceous and Permian strata were removed before calculations and simulations were performed for the model.

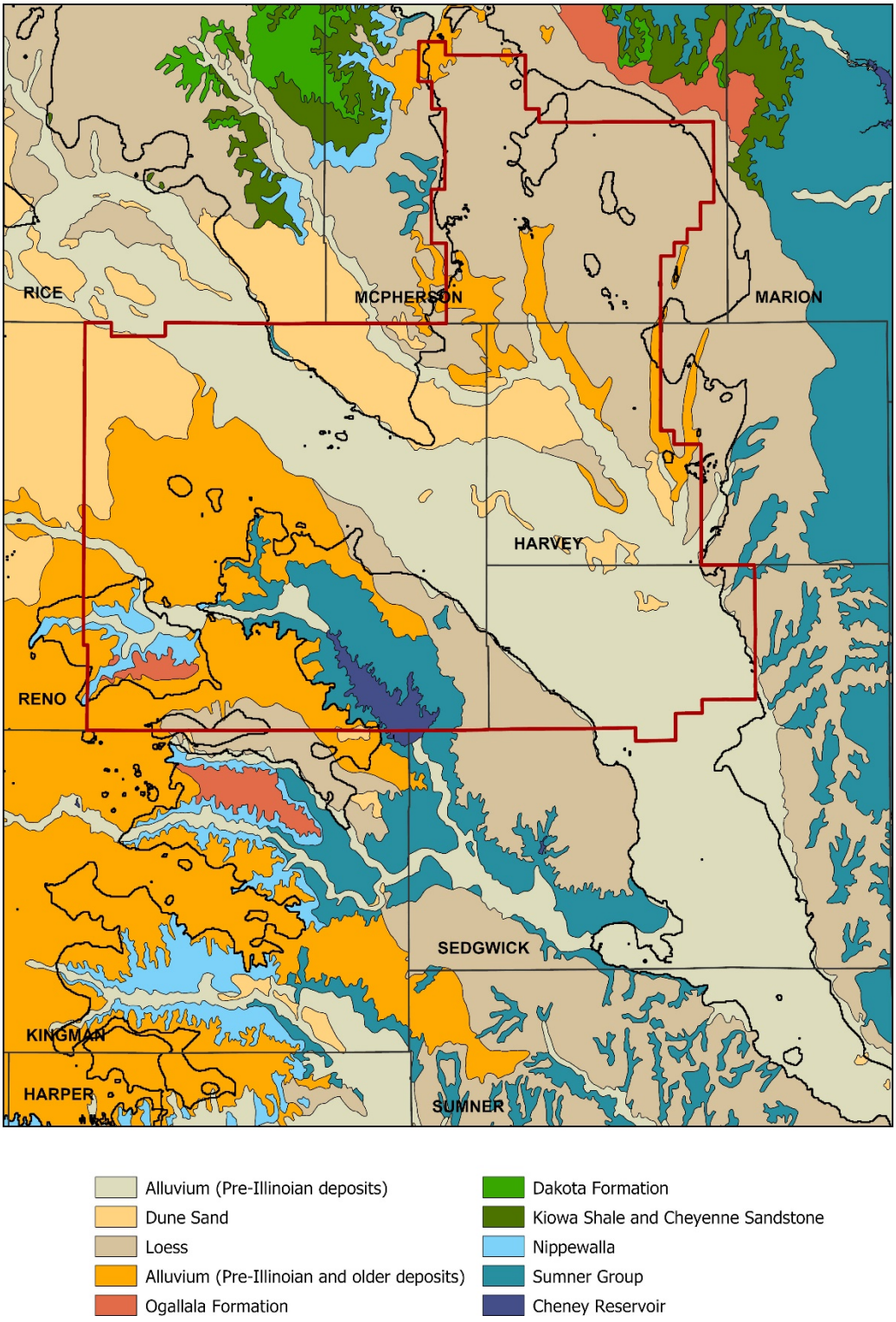

Figure 7. Surficial Geology.

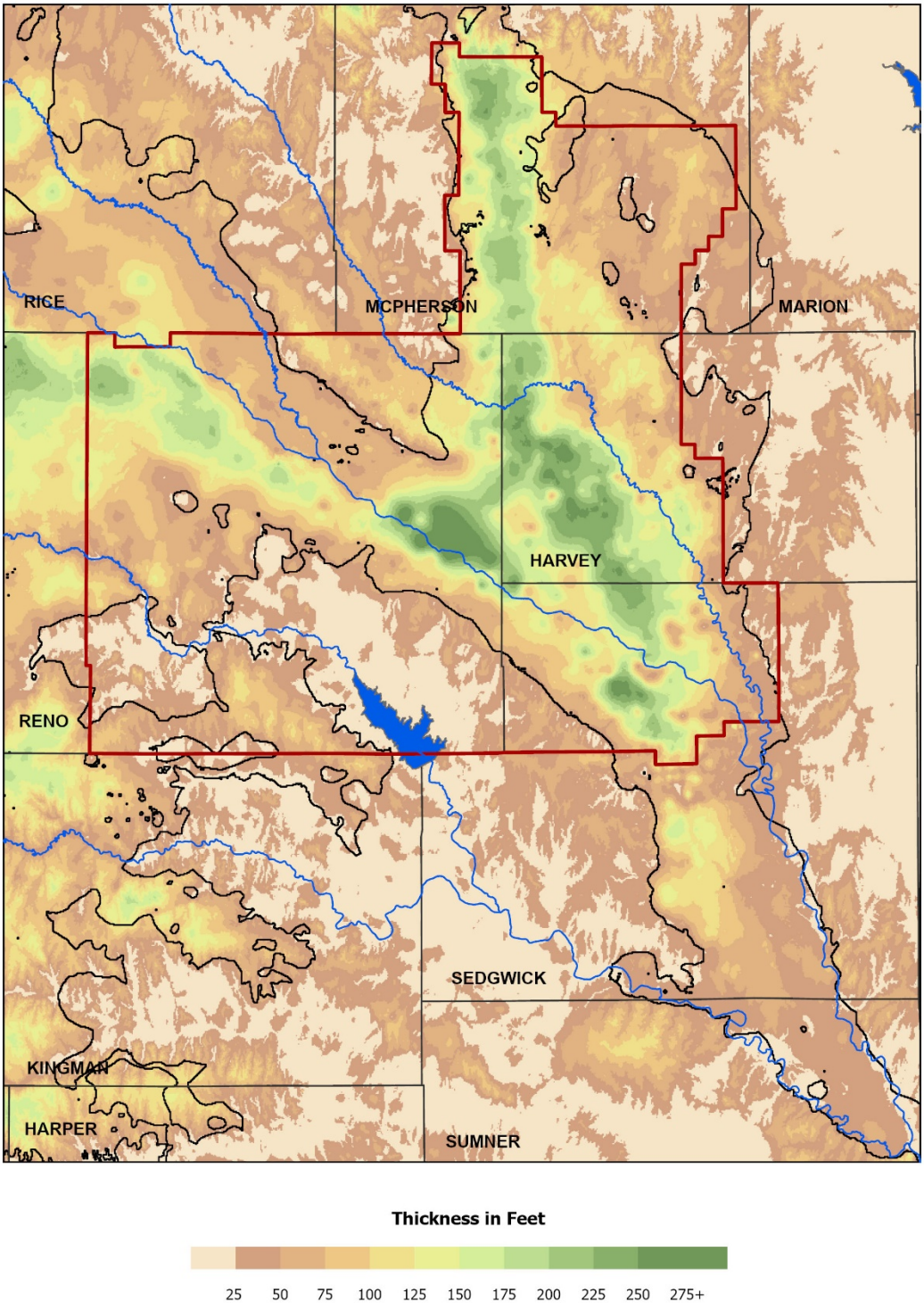

Figure 8. Thickness of unconsolidated sediments.

Bedrock Surface

Data for the bedrock surface were obtained from DASC's High Plains Aquifer Base GIS layer. This data set merges two estimates of the bedrock elevations: one from a study by Macfarlane and Wilson (2006) covering the Ogallala portion of the High Plains aquifer in Kansas and a second from a similar but unpublished project completed in 2009 for the Kansas GIS Policy Board covering the extent in south-central Kansas. Both bedrock projects used lithologic logs obtained from water well completion records, county geologic bulletins, and geophysical logs stored at the KGS, along with additional data from the USGS. The bedrock elevations from additional water-well completion records completed after 2009 were included to better characterize the surface in selected areas of the model.

The bedrock elevations were interpolated to form a continuous raster-based surface (fig. 9). The model cells were overlain on the interpolated surface and the average bedrock elevation within each model cell computed and assigned as the bottom elevation of the cell. In a few areas primarily along the fringes of the active area, the bedrock was manually adjusted to be at least 10 feet below the land surface.

The bedrock surface elevation follows the same general slope as the land surface, with highs located along the northwestern portions of the model and lower values in and along the Arkansas River valley running toward the southeast. The bedrock depth in the active area of the model averages 97 ft and ranges from near the land surface to more than 300 ft in core areas of GMD2, namely northwestern Sedgwick County, western Harvey County, and east-central Reno County.

A three-dimensional version of the bedrock surface (fig. 10) facilitates visualization of the bedrock topography, especially the ancestral channel of the Arkansas River, which runs through the core of GMD2. Another prominent topographic subsurface feature is the McPherson Channel in the northern portion of the model area. This channel represents the ancestral paleovalley of the Smoky Hill River, which flowed to the south between present-day Marquette and Lindsborg during the early Pleistocene Epoch (Williams and Lohman, 1949). It is believed that sometime during the Pleistocene, headwater erosion of the streams in the Kansas River watershed captured the drainage from the Smoky Hill and reversed its flow to the north.

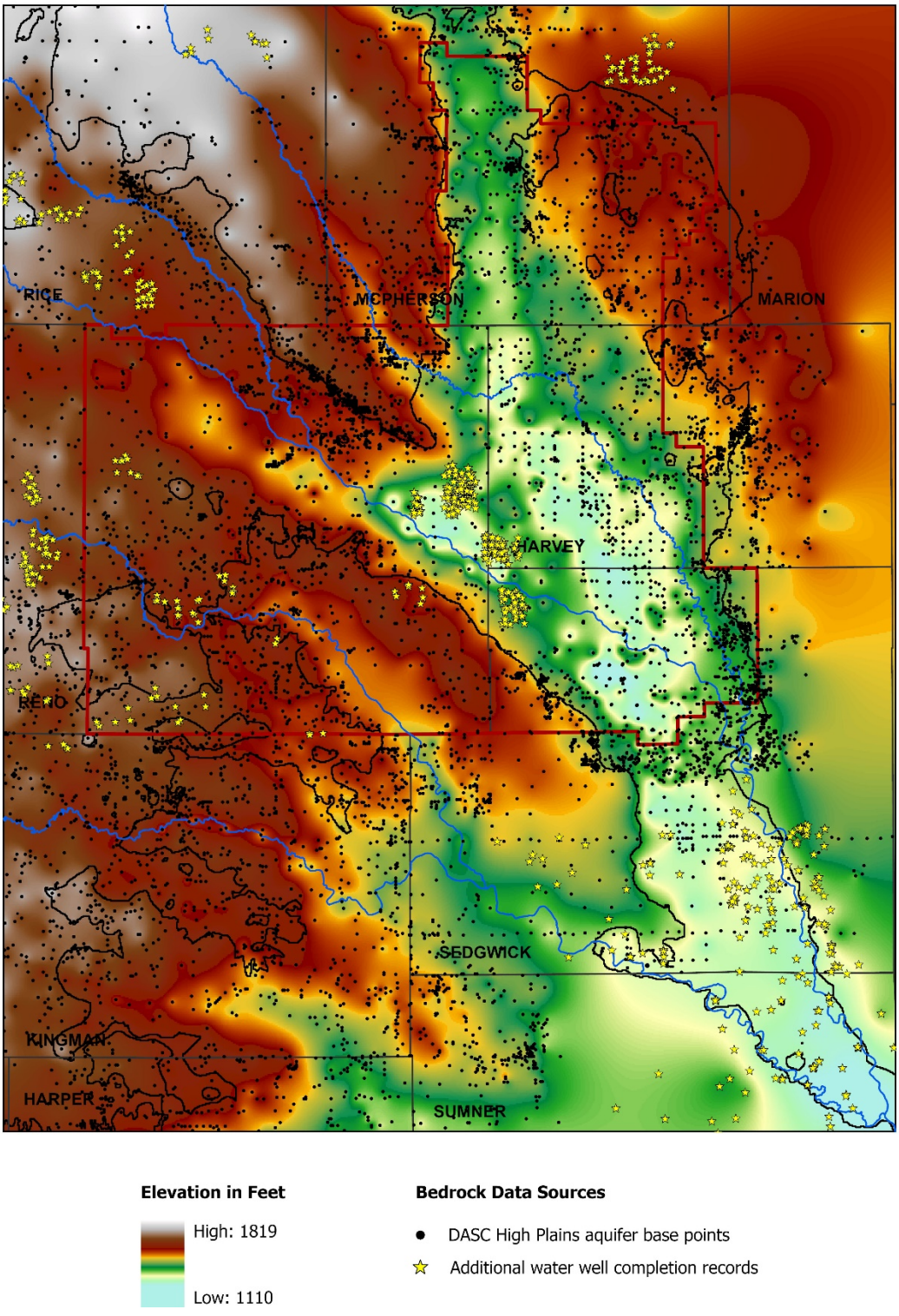

Figure 9. Elevation of the bedrock surface interpolated from well logs.

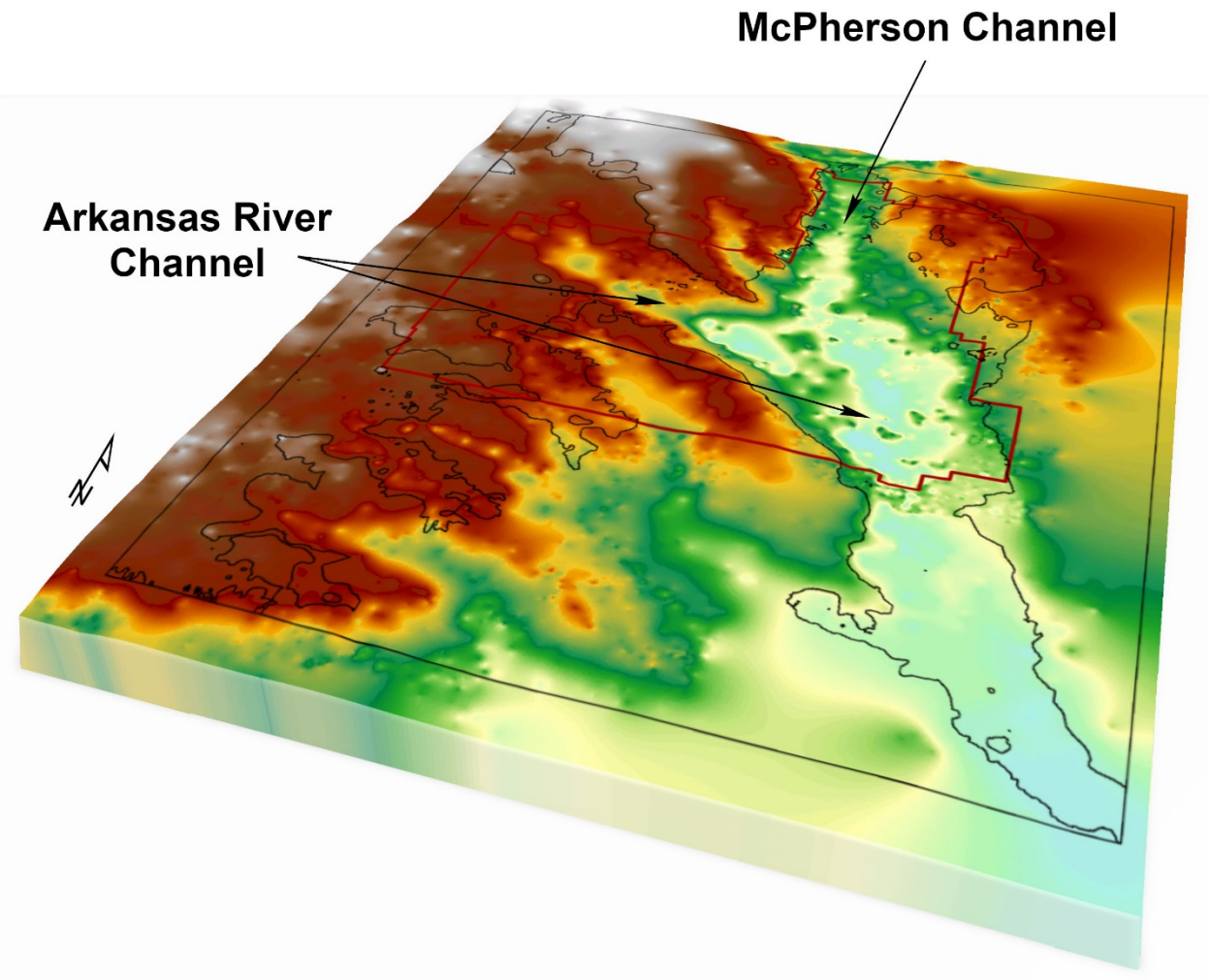

Figure 10. Three-dimensional view of the interpolated bedrock surface, looking north-northwest (see fig. 9 for color scale).

Lithologic Characterization

The KGS has established methods to extract and categorize information from drillers' logs with the current version of the process known as the Hydrostratigraphic Drilling Record Assessment (HyDRA) (Bohling, 2016). Lithologic descriptions and interval depths have been transcribed and stored in Oracle, an enterprise-level relational database management system, from which they are extracted and categorized into similar descriptive groupings. The lithological groupings are spatially interpolated to produce a three-dimensional grid, with each grid cell containing the proportions of different groupings. Using representative values for each lithological group, vertically averaged K and SY are computed for the saturated interval between the predevelopment water table and bedrock surface.

A little more than 26,200 well logs were used in the HyDRA process (fig. 11), from which the lithological descriptions were assigned to 71 standardized lithology codes. In some cases, the description for an individual depth interval may be represented using multiple lithology codes. In

these cases, the percentage contribution of each lithology is assigned according to rules based on the number of lithologies in the interval and their order of appearance in the description. The standardized lithologies, in turn, were further categorized into five groups, each representing a set of lithologies expected to exhibit similar values of aquifer permeability (K) and specific yield (SY) (table 1).

With the lithological groupings in place, HyDRA segments each lithologic well location into 10-ft intervals, starting from the interpolated predevelopment water table (described in the next section of this report) to bedrock. The proportion of each of the five lithology categories occurring within each 10-ft interval is estimated based on the driller's log. The five category proportions in the 10-ft intervals are then interpolated into a three-dimensional grid across the model's active area, so that each 3-D grid cell contains a set of values representing the category proportions within that cell. A summary representation of this information, the proportion-weighted average category, is shown in fig. 12. A special program was written to intersect MODFLOW-formatted water table and bedrock elevation grids with the three-dimensional proportional grids and then write out the vertically averaged K and SY values to MODFLOW-formatted grid files, based on the category proportions within the intersected grid cells and the K and SY values assigned to each category.

Table 1. Standardized Lithologies Categories.
The K and Sy values are estimated after model calibration. The district-wide average SY estimate from the sustainability study (Butler et al., 2017) is used for setting bounds of SY during calibration.

Category 1 K=1.2E-5 ft/d SY=4.7E-5	Category 2 K=5.0E-4 ft/d SY=5.0E-4	Category 3 K=8.1 ft/d SY=5.0E-3	Category 4 K=200 ft/d SY=0.125	Category 5 K=400 ft/d SY=0.175
shale clay bedrock red bed siltstone	fine silty clay fine to medium silty clay silty clay medium silty clay fine to coarse silty clay medium to coarse silty clay fine sandy clay fine to medium sandy clay medium sandy clay sandy clay fine to coarse sandy clay medium to coarse sandy clay coarse sandy clay clayey silt fine silt silt top soil overburden marl calcified material (limestone/caliche)	fine sandy silt fine to medium sandy silt medium sandy silt sandy silt fine to coarse sandy silt medium to coarse sandy silt coarse sandy silt gravelly clay sandstone	clayey sand fine silty sand fine to medium silty sand silty sand medium silty sand fine to coarse silty sand medium to coarse sandy silt coarse silty sand unknown cemented sand and/or gravel fine sand fine to medium sand	sand medium sand fine to coarse sand fine to medium coarse sand medium to coarse sand coarse sand clayey gravel silty gravel

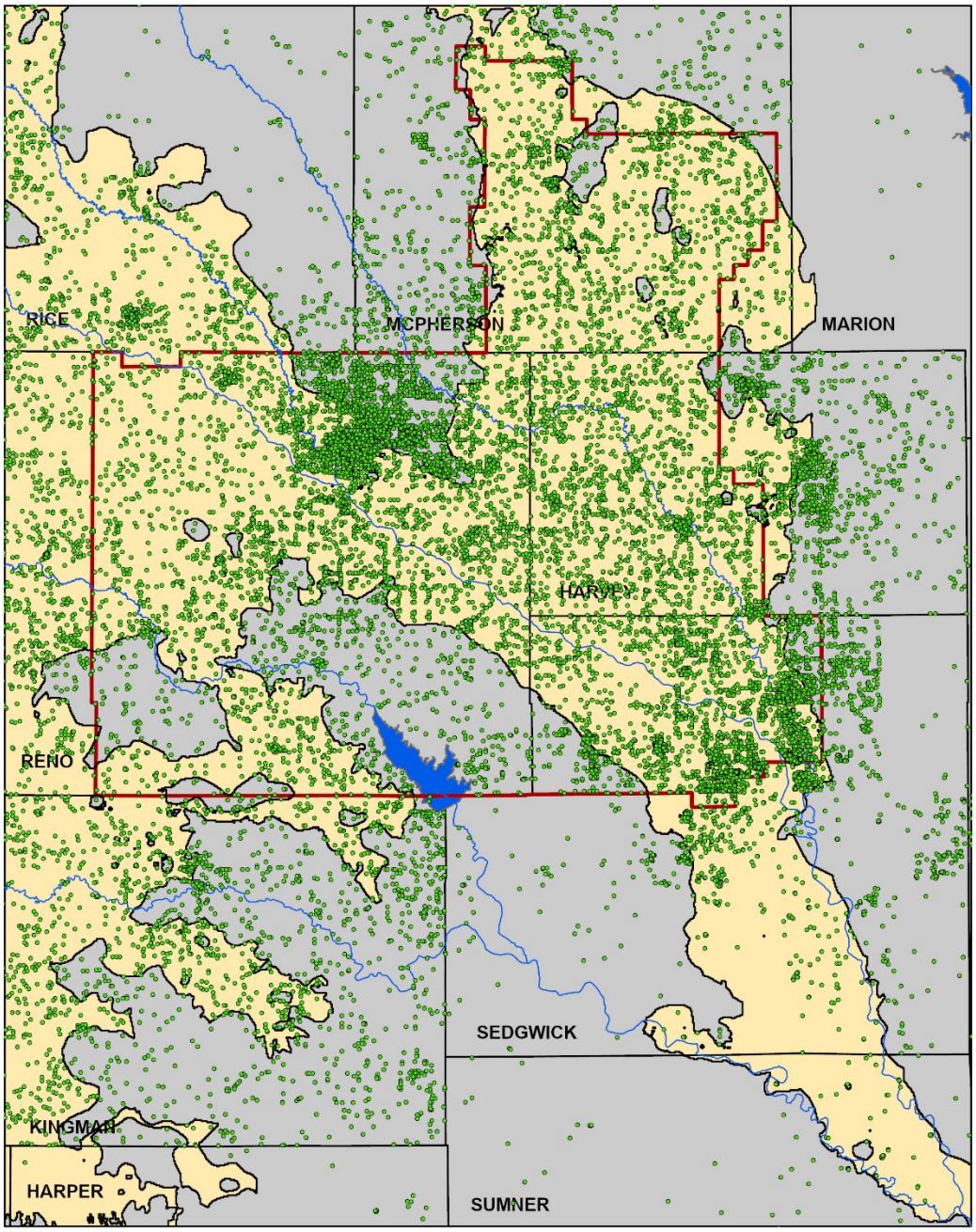

Figure 11. Distribution of lithologic logs used in HyDRA.

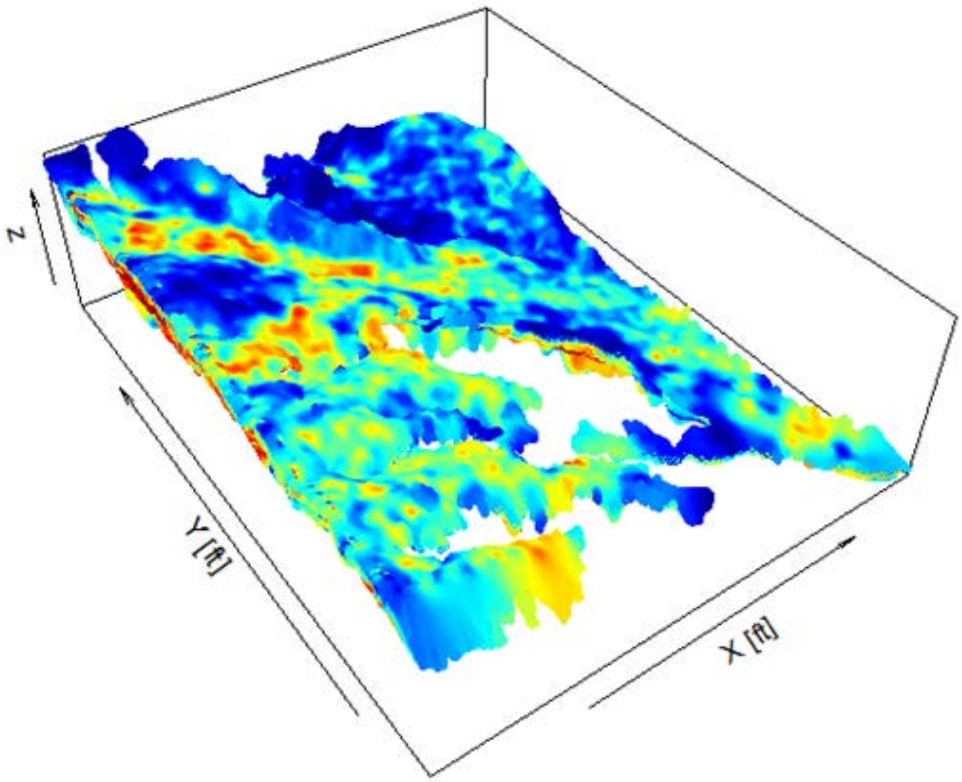

Figure 12. Three-dimensional proportion-weighted average lithology categories. The dark blue colors indicate finer grain sizes whereas light green to yellow and red represent coarser grain sizes.

Water Levels

Estimates of the predevelopment water table were compiled primarily from the "Well Records" listings found in county-based geologic bulletins. Most of the depth-to-water measurements in these reports were made from the late-1930s to the mid-1950s and are considered to represent conditions before the aquifer was heavily developed. Measurements from groundwater wells known to be screened in the Cretaceous or Permian systems were not included. The water levels from bulletin wells were interpolated to create a continuous gridded surface representing the predevelopment water table.

The model cells were overlain on the gridded surface and the average predevelopment water-table elevation within each model cell was computed (fig. 13). In a few areas, primarily along the fringes of the active area and stream channels, the predevelopment water table was manually adjusted to be at least 5 feet below the land surface and/or 5 feet above the bedrock.

Like the bedrock surface, the predevelopment water-table elevation follows the same general slope as the land surface, trending from highs along the western edge of the model to lows in the southeast. The overall predevelopment depth-to-water varies across the model's active area (fig. 14). The depth to water along much of the Arkansas River valley is typically 10 feet or less with greater depths in the McPherson Channel to the north. The depth to water in GMD2 within the active area of the model averages 19.8 feet and ranges from near the land surface to 104.7 feet.

The average predevelopment saturated thickness of the Equus Beds aquifer within the GMD2 boundary and active area of the model is 95 ft and ranges from close to 0 to just over 300 feet. The 2017 average winter saturated thickness of 93 ft in GMD2 is generally similar (fig. 15). There are areas of local groundwater declines, most notably in the McPherson Channel, where water levels have slowly dropped more than 20 feet since predevelopment.

The Equus Beds aquifer has the greatest concentration of water-level measurements in Kansas. In addition to the wells measured annually as part of the state's Cooperative Water Level Program and those measured by the USGS, GMD2 has more than 700 additional monitoring sites, for both water levels and water-quality samples (fig. 16). Many of these measurement locations are nested sites with sets of wells screened at various depths in the aquifer. GMD2 measures most of its wells on a quarterly cycle, and the Water Information Storage and Retrieval Database (WIZARD) (http://www.kgs.ku.edu/Magellan/WaterLevels/index.html) serves as the primary database repository for that information.

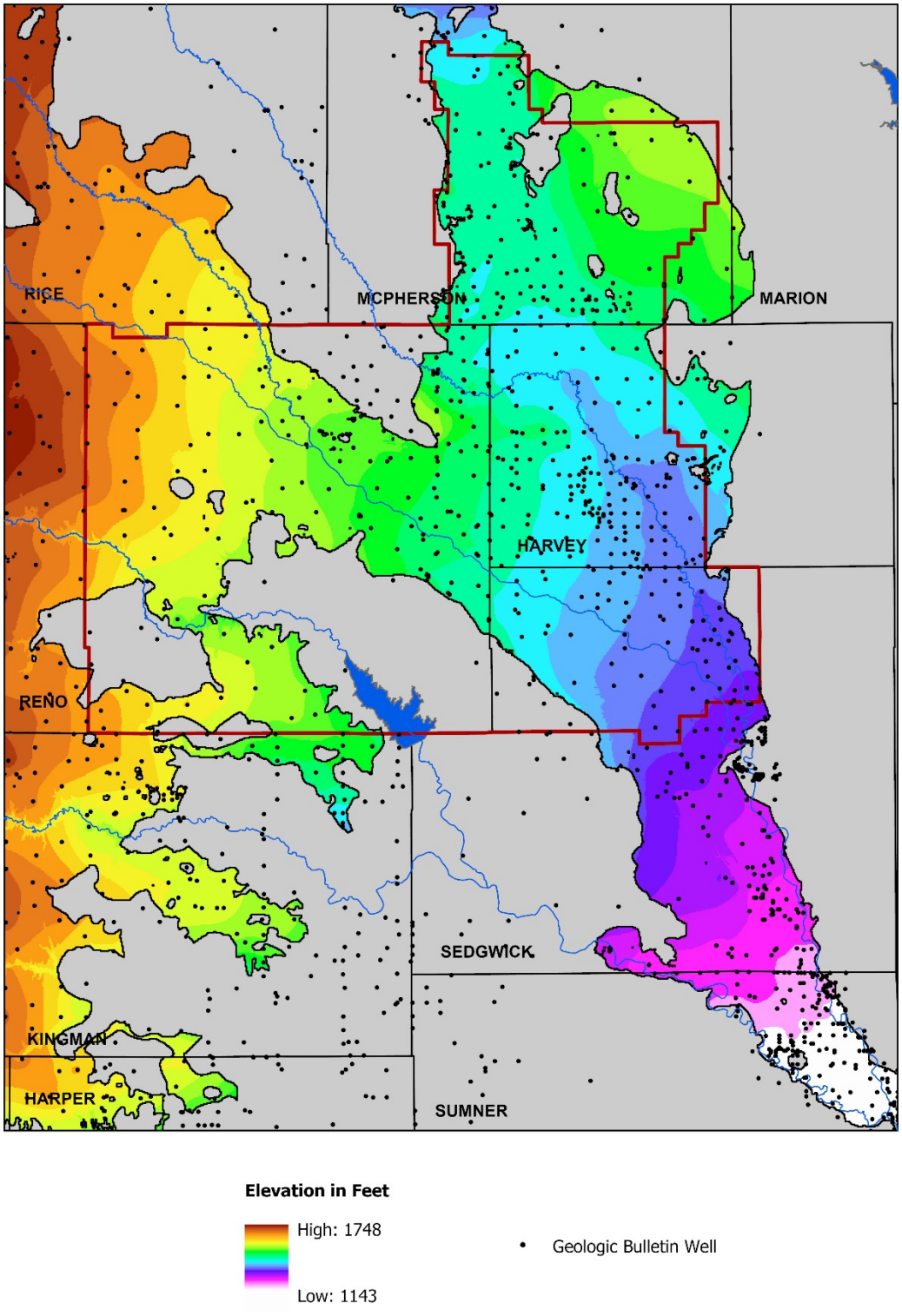

Figure 13. Interpolated predevelopment water table.

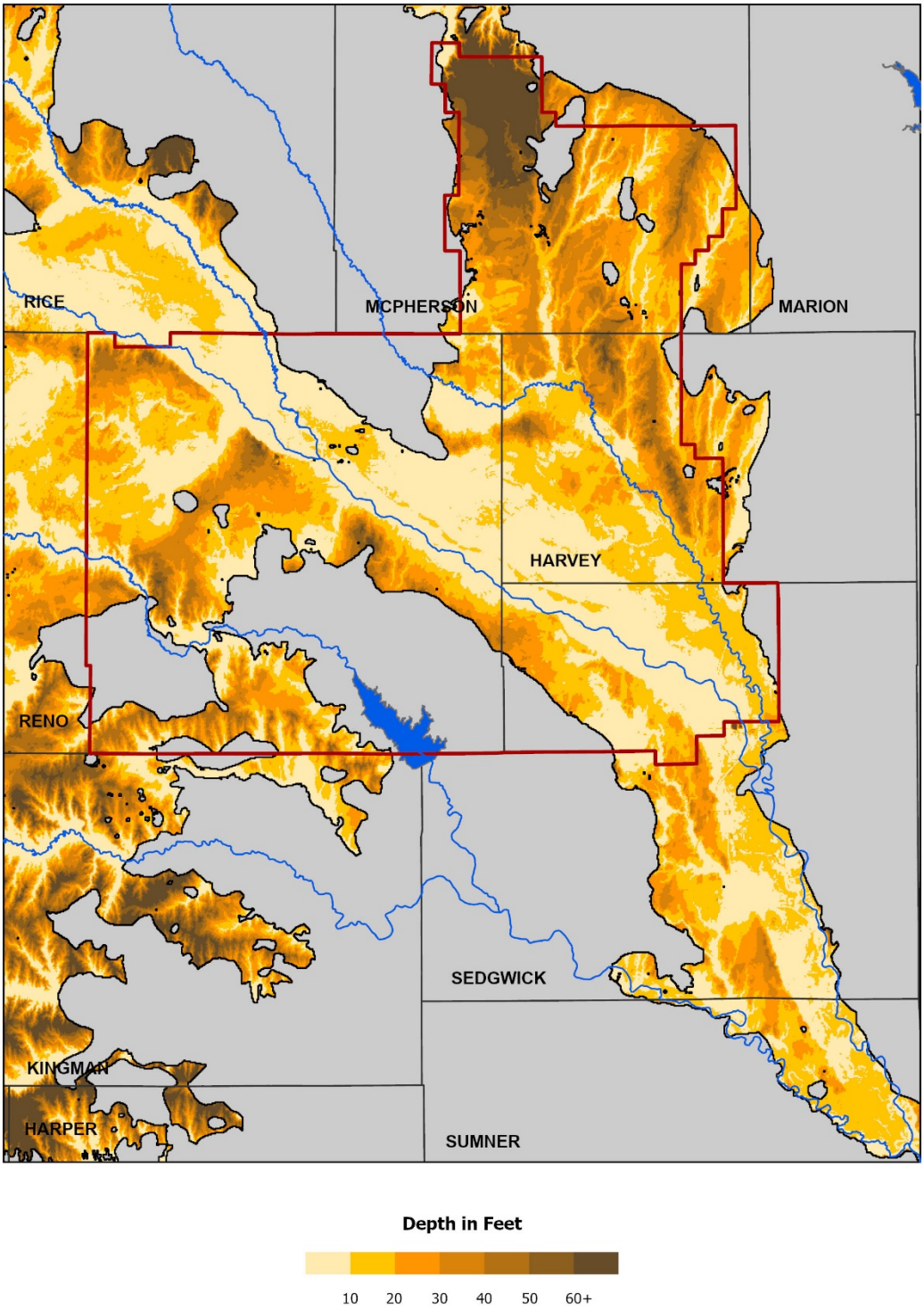

Figure 14. Interpolated predevelopment depth to water.

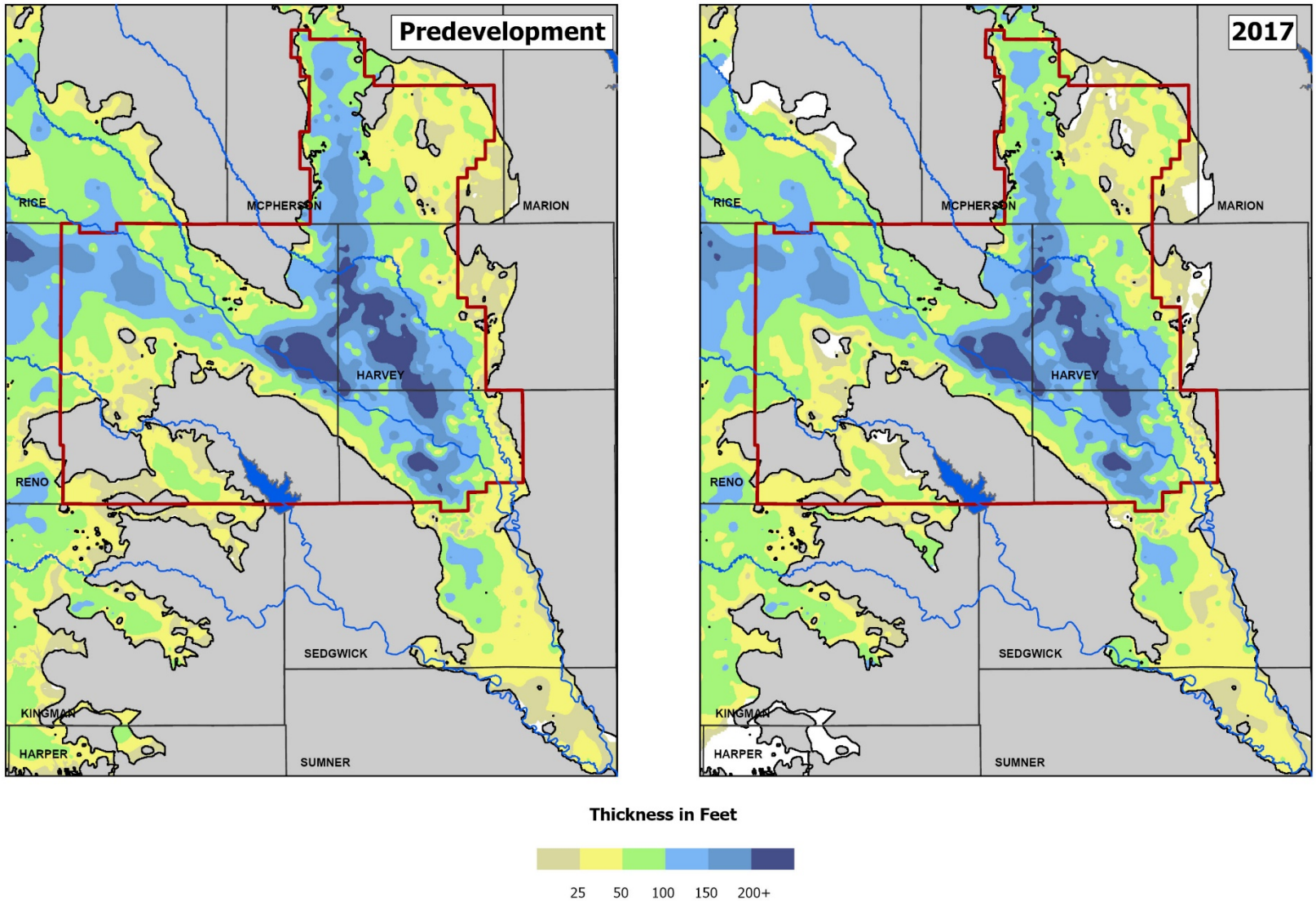

Figure 15. Interpolated predevelopment and 2017 saturated thickness.

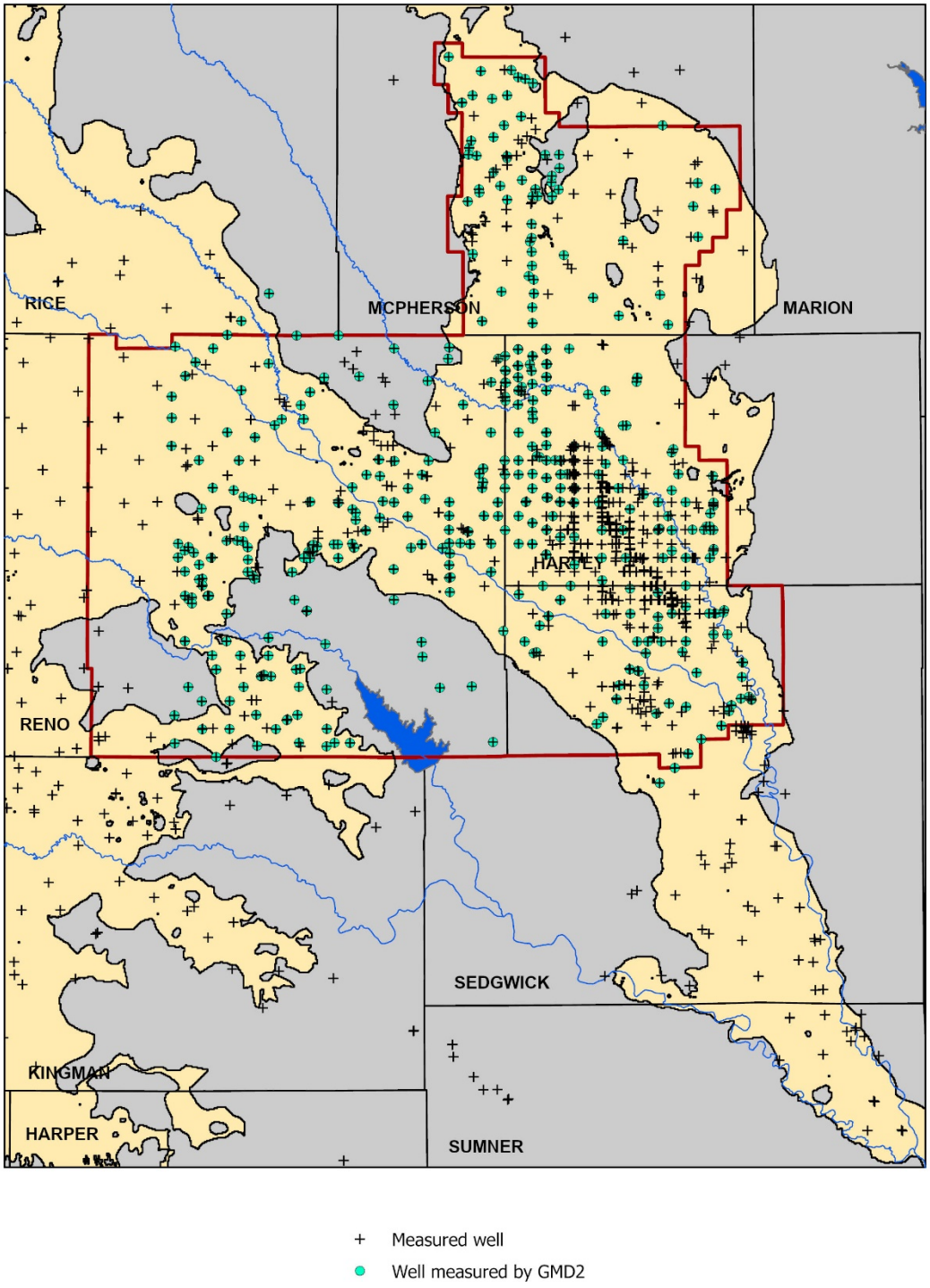

Figure 16. Distribution of water-level measurement wells as of October 2017.

Water-level measurements retrieved from WIZARD that had status codes indicating the value may not reflect normal conditions (e.g., the well was being pumped) were removed from consideration. At any given well, “winter” measurements, those taken between December 1 and April 15, were averaged to represent a single value for the year. The number of wells and their spatial extent across the model area are relatively unchanged until 1975, the year GMD2 was established. Since that time, the number and frequency of measurements has been increasing (fig. 17).

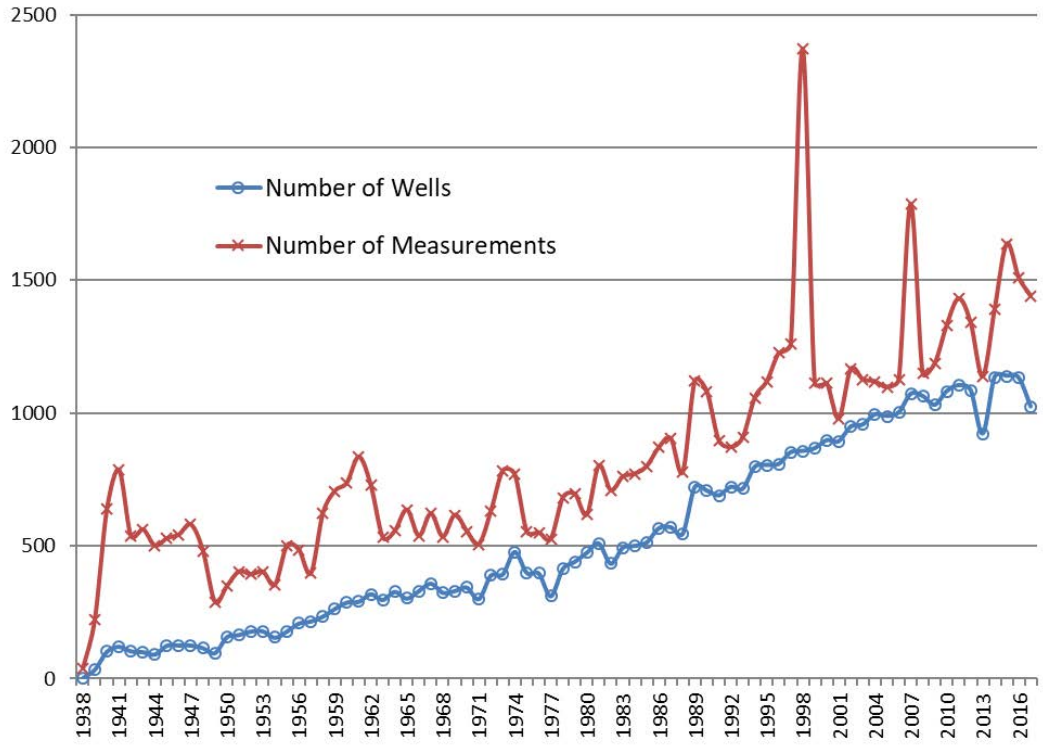

Figure 17. Number of wells and measurements in GMD2 with “winter” (December 1 to April 15) measurements.

Boundary Conditions

The model uses time-varying specified head boundaries along its western edge to represent conditions in the HPA and on its northern edge where the HPA comes into contact with the alluvial deposits of the Smoky Hill River. Given that head boundaries in the model are not necessarily located along natural or known hydrologic boundaries, setting appropriate head values is challenging, especially in areas that lack data. Four different processes were used to set the specified head boundaries and were based on available measurement histories and well distribution.

The western edge of the model extends into Big Bend GMD5, which like GMD2, has an extensive network of wells measured throughout the year. Interpolated water-table elevation surfaces were generated for each year from 1985 to 2017 based on 52 selected GMD5 wells that were measured continuously during this time (fig. 18) and then assigned to the designated specified head model cells. For the missing data gap between predevelopment and 1985, water levels were interpolated assuming a linear transition. A similar interpolation process was used for the specified heads along the northwest corner of the model in Rice County. Here, the number of wells and their associated measurement histories are very sporadic, resulting in spatially interpolated water levels in 1980, 1984, 1990, 1996, 2000, 2005, 2010, 2015, and 2017 (the spatially interpolated values assigned to model cells), with the missing years of water levels being computed based on linear trends.

The model's northern edge extends into the Smoky Hill River alluvium. Here there are numerous measurements from the early 1950s to 1972 during the construction of Kanopolis Reservoir. However, since 1972, the number of wells and available measurements are sporadic. Given the relatively consistent nature of alluvial systems from stream/aquifer interactions, the annual rate of water-level changes from all available wells in the valley were used and applied to the specified head model cells, starting in predevelopment. From 1946 to 2017, the average annual change in water levels in the Smoky Hill River alluvium along the model's edge averages -3.6 inches with a total accumulated change of -2.89 feet.

The southwest corner of the model had the smallest number of available water-level data due primarily to limited groundwater availability. Nine wells were selected in Kingman County, based on their continuous annual measurement history from 1990 to 2017, to interpolate water-table elevations and assign values to the specified head model cells. Water levels were then computed from predevelopment to 1989 based on a linear transition. In the southeast corner, measurements from a few available observation wells suggest relatively stable water levels since 2007 with very small rises and declines. As such, constant heads based on predevelopment estimates were used for the edge of the active area here.

Lastly, constant head cells were set along the edges of the active area in portions within the model domain to prevent nearby cells from drying up (and causing the model to crash) during the transient phase of the model. Most of these are located in thinly saturated sediments along sharp bedrock contacts, specifically along the southern edge of the Arkansas River valley, the western edge of the McPherson Channel, and the northern extent of the Pretty Prairie area west of Cheney Reservoir.

Remaining boundary edges are set to no-flow cells, which prevents flow between active and inactive areas of the model.

.

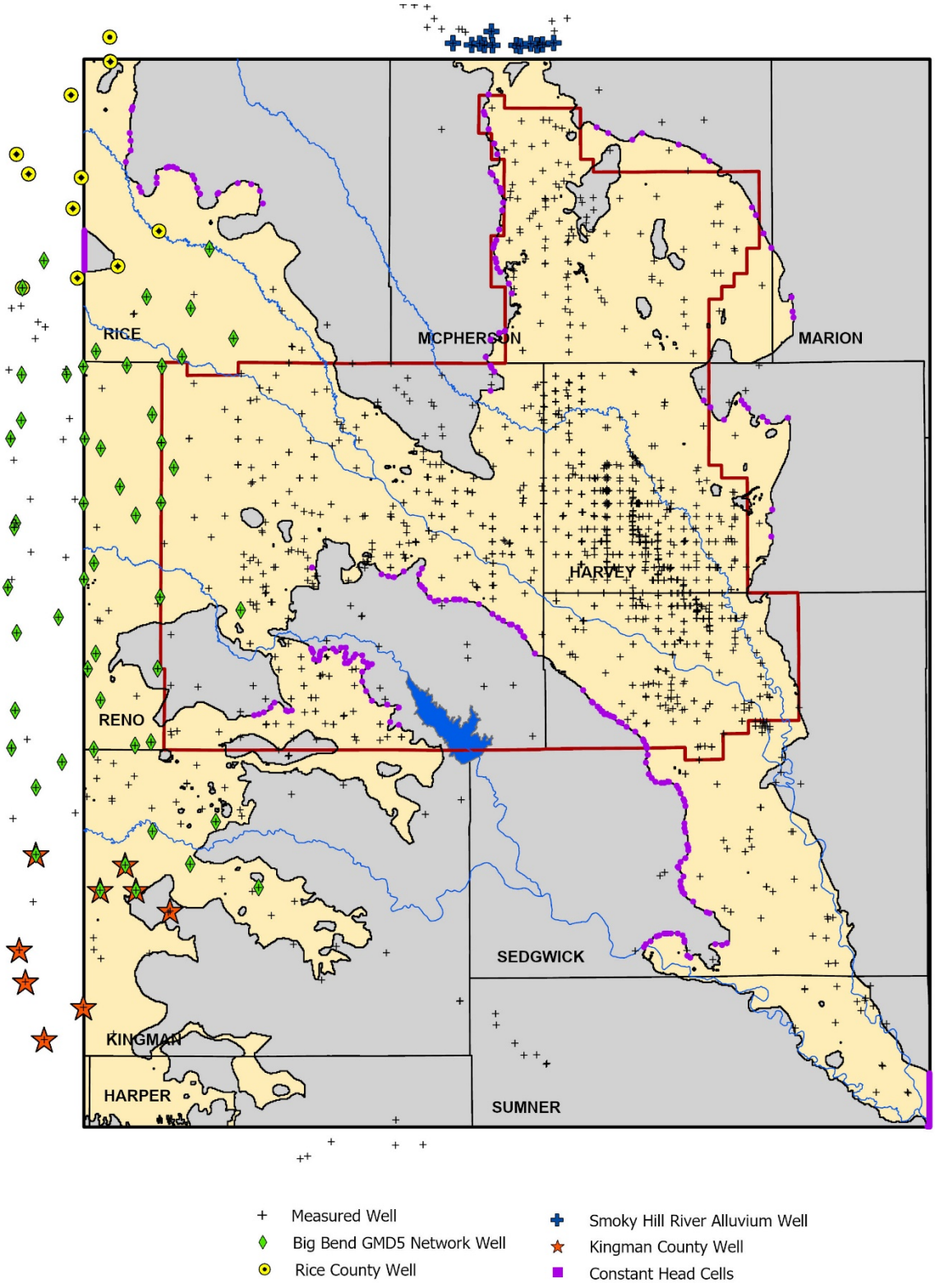

Figure 18. Selected well subsets to establish model boundary conditions.

Stream Characteristics and Flow

The majority of GMD2 is drained by the Arkansas River and the North Fork of the Ninnescah River and their tributaries. Due to the lack of topographic relief, much of the Arkansas River system is poorly drained. This project incorporates the Arkansas River, Cow Creek, Little Arkansas River, North Fork Ninnescah, South Fork Ninnescah, and Ninnescah River in the modeling of stream-aquifer interactions (fig. 19). The stream courses are all classified as perennial.

Mean monthly streamflow records were obtained from the USGS's National Water Information System for all gaging stations in the model area. The model domain has more than 40 gage sites with 18 in operation today. Available data from the gaging stations are used as a measure of the aquifer's baseflow contribution occurring during winter periods of the model. Gaged flow in summer months was not use as streamflow is much more significantly affected by surface runoff from precipitation events.

This project uses the Stream package for MODFLOW, which requires all surface water courses to be broken down into individual segments and reaches. A "segment" is a longer portion of the stream that has identical properties such as width, slope, and streambed hydraulic conductance; a stream segment is in turn further divided into "reaches" that represent each portion of a stream segment within individual model cells. To represent all the streams in fig. 19, the model uses 12 stream segments with more than 8,000 reaches. Figure 20 shows an example of the segment/reach division. Streams were overlain on bare earth LiDAR digital land surface elevation models provided by DASC as a web service, and the average elevation for each stream reach is computed to represent the elevation of the stream channel (i.e., the top of streambed).

The Big Slough creek was simulated using drain cells. As the name implies, drain boundaries allow water to discharge from the aquifer when the water levels are at or above the drain elevations. Unlike stream cells where flow can be into or out of the aquifer, drains allow flow in only one direction, discharge out of the aquifer. If the water tables decline enough, the connection is broken and water will no longer discharge out of the system, rendering the drains effectively inactive. If water levels rise to the level of the creek bed again, the one-way drain connection is reestablished.

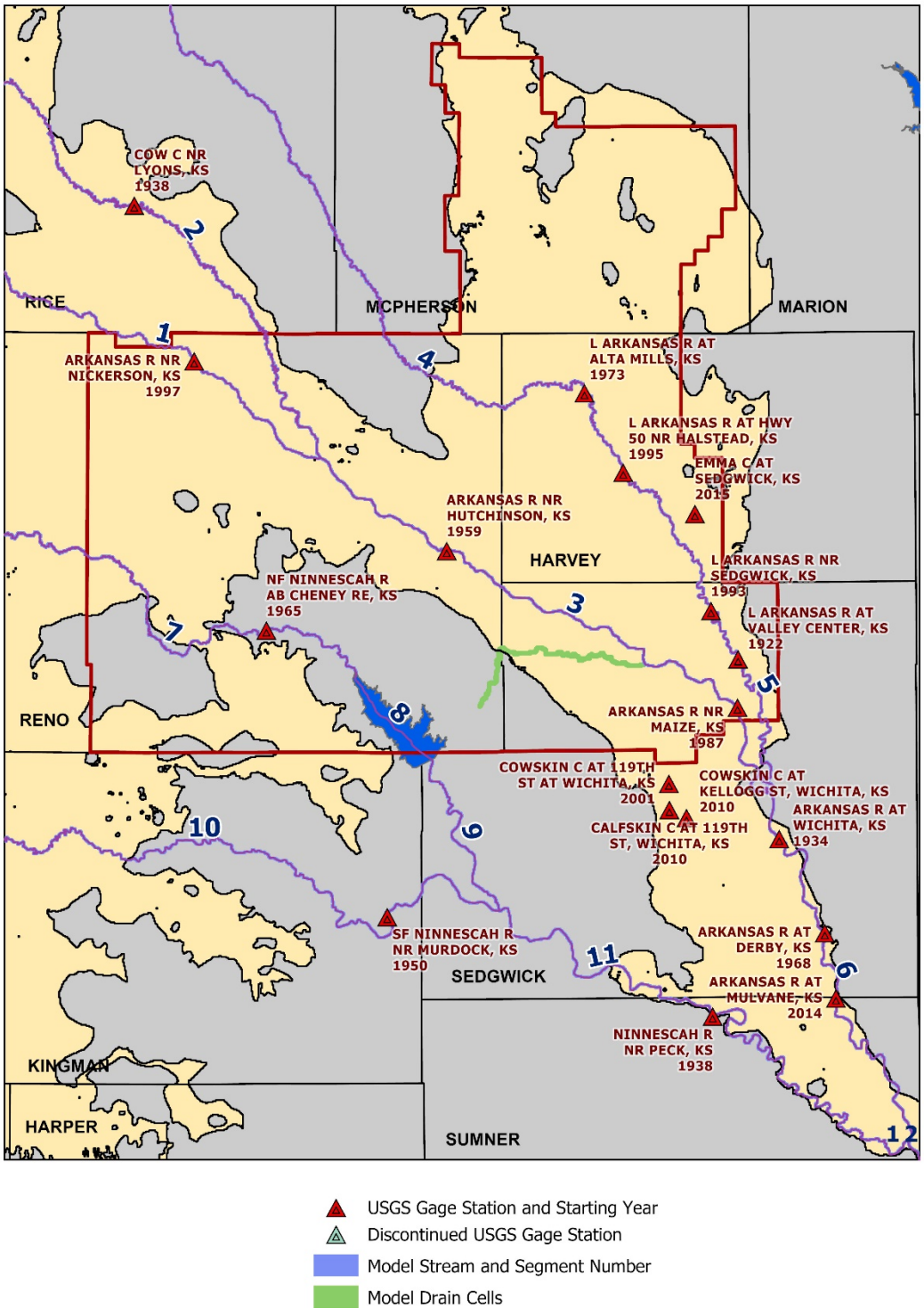

Figure 19. Model stream and drain cells and current USGS stream gaging stations. Gage sites are labeled by their site name and starting year of record.

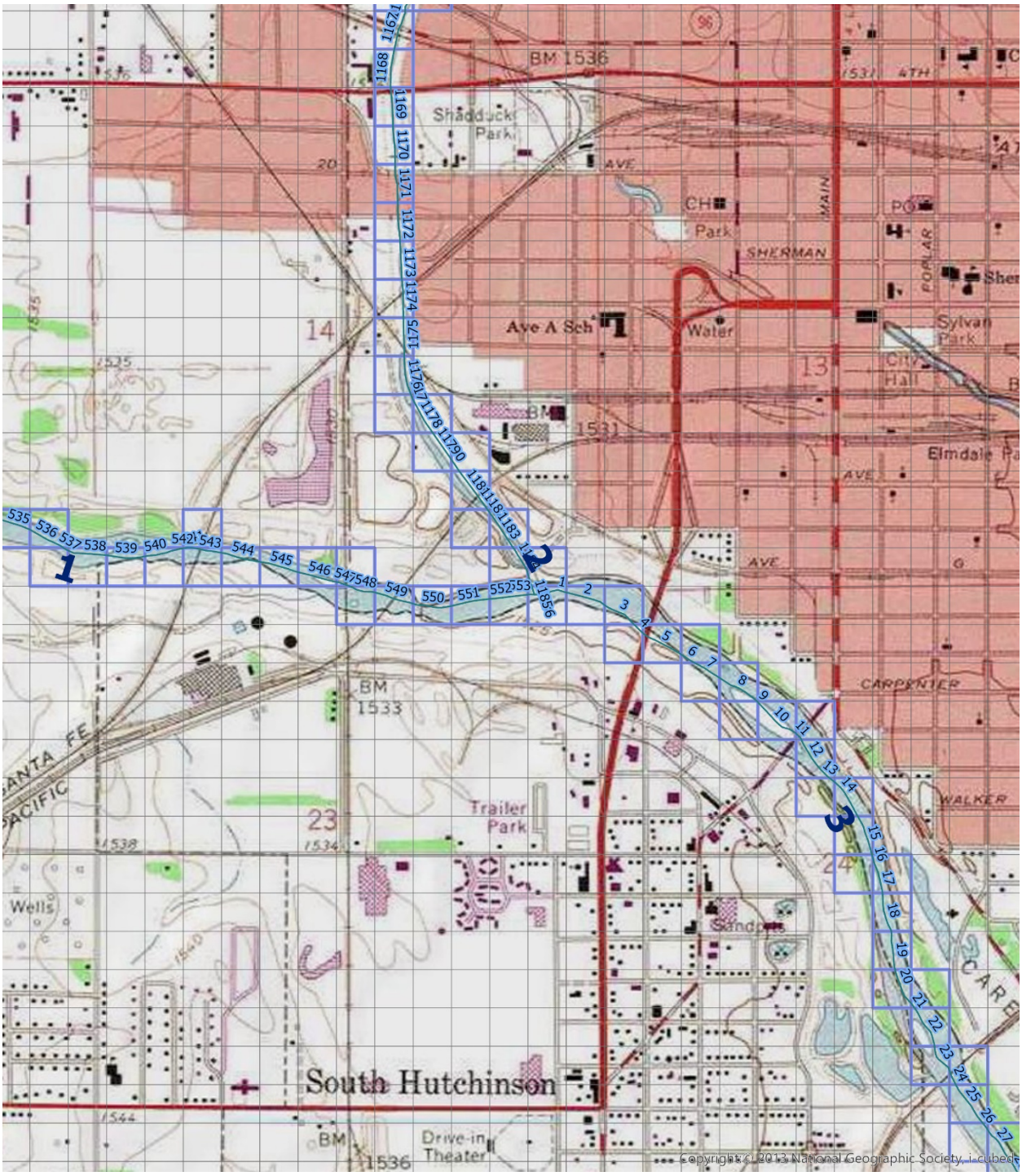

Figure 20. Selected area of the model showing stream segments (larger dark blue numbers) and reach designations (smaller light blue numbers) along the confluence of the Arkansas River and Cow Creek.

Water Right Development

Water rights in Kansas are dynamic entities whose characteristics can change over time. The authorized quantities and water-right locations used in the model represent conditions as of October 30, 2017. Data were accessed from the Water Information Management and Analysis System (WIMAS) (http://hercules.kgs.ku.edu/geohydro/wimas/index.cfm). Within the active area, there are 2,995 unique appropriated and vested water rights and 3,889 active points of diversion. The majority of water rights in the model area are groundwater based (fig. 21), with irrigation making up 68 percent of that total (table 2). Points of diversion (150 in total) that were listed as being screened solely in formations of Cretaceous or Permian age were removed from consideration. Most of these non-Equus Beds points are found in the inactive portions of the model.

The model area also includes a significant amount of municipal development of both ground and surface water resources. The City of Wichita makes up most of the surface water appropriations as its municipal-based permits from Cheney Reservoir and artificial recharge permits (representing the majority of the "Other" category in table 2) along the Little Arkansas River represent 99% of the total. Given that Cheney Reservoir lies outside the active area of the model and the other surface water uses are relatively small, composing only 1 to 2 percent of the total groundwater use each year, surface water diversions are not considered in this model.

Table 2.
Total authorized quantity, in acre-feet, for appropriated and vested water rights, by use made of water and source of supply for GMD2 model active area
Represents conditions as of October 30, 2017

	Domestic	Industrial	Irrigation	Municipal	Recreation	Stockwater	Other
Surface	0.83	0.00	4,040.40	47,728.02	4,361.19	0.00	55,762.22
Ground	93.00	18,241.58	286,466.20	107,345.20	6,993.13	861.31	3358.48
Total	93.83	18,241.58	290,506.60	155,073.20	11,354.32	861.31	59,120.70

The WIMAS database only stores a water right's present authorized quantity. Although quantity values can change as a water right goes through the certification process or by other administration actions (generally becoming less), the historic trends used in the model are based on the appropriated quantity values at the time of the download (10/30/2017) and in relation to the priority date of the water right.

A common complexity with Kansas water-right quantities is that the annual appropriation can be associated with the water right itself (regardless of how many uses or points of diversion it might have), with the water right's uses of water, or with the water right's multiple points of diversion. Because the points of diversion for a particular water right could be located across multiple model cells, the total annual authorized quantities for water rights that had their appropriations stored by the water right or use made of water were divided equally among the water right's point(s) of diversion. Each point of diversion would then have an associated quantity that when added with the other points of diversion under the water right would equal the total quantity authorized. If the quantity was already stored by the point of diversion, it remained unchanged.

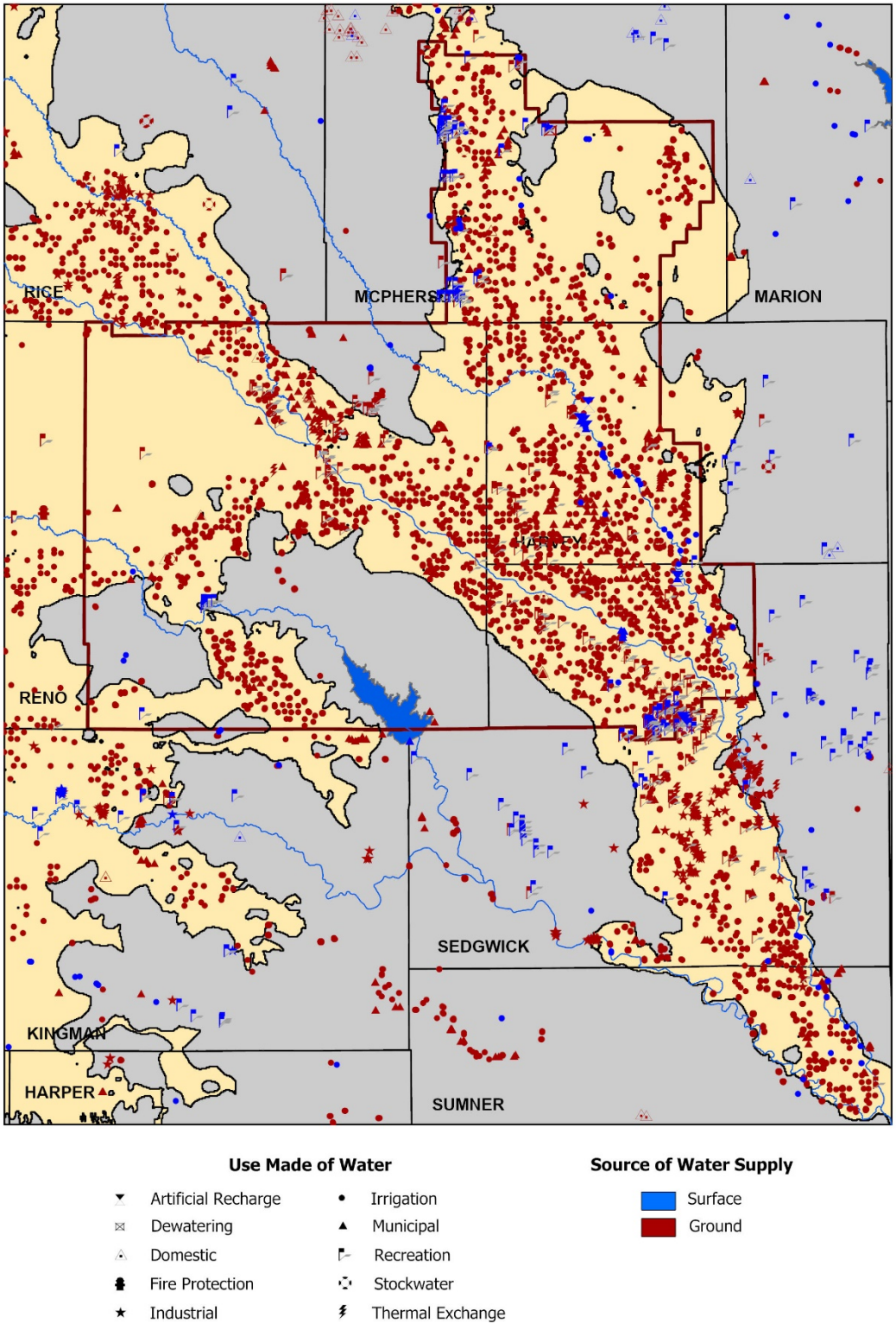

Figure 21. Water-right distribution.

The trend in authorized quantity over time, based on priority dates, in the active portion of the model's area (fig. 22) shows a steady increase. Kansas water law started with the passage of the 1945 Water Appropriation Act. Water users in place before that time could apply for a "vested" water right. Water rights issued after 1945 are referred to as "appropriated" rights. The rate at which water rights were issued accelerates in 1975, again at the same time GMD2 was established.

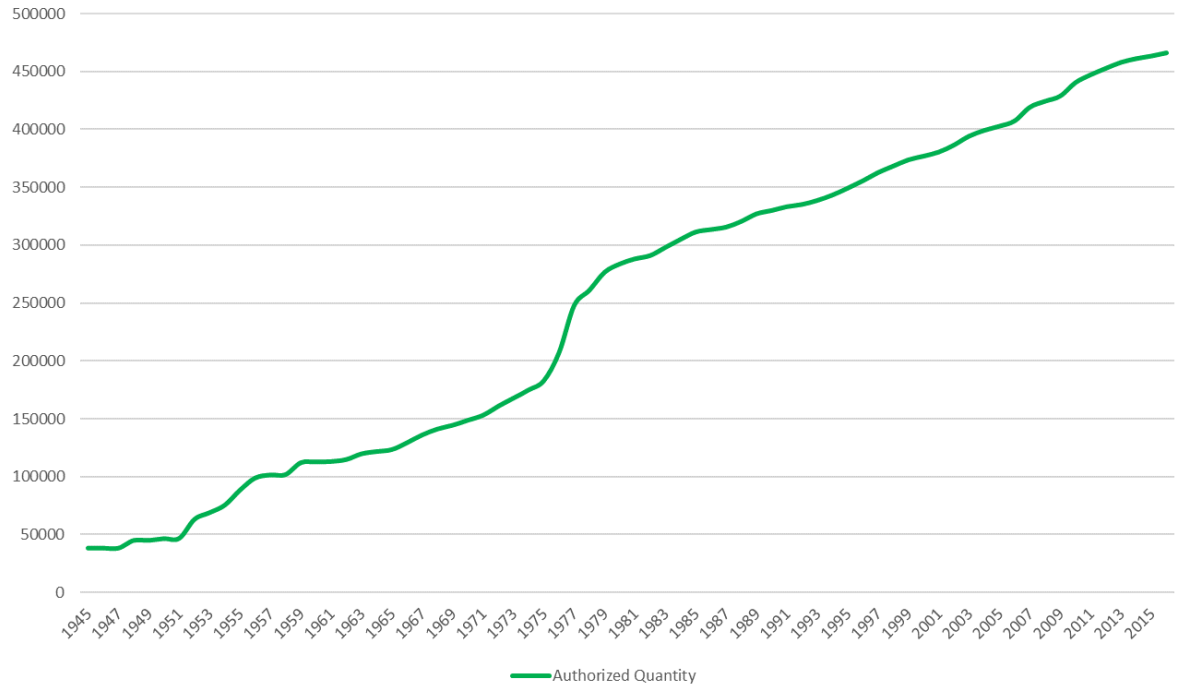

Figure 22. Total authorized quantity (in acre-feet) of groundwater-based water rights in the model's active area.

Estimation of Historic Water Use

Although Kansas water-use reports go back to 1958, actual water usage across large areas was probably much higher than these reports would indicate, since it wasn't until 1978 that water rights were required to be obtained before diverting water for beneficial use. Even then, it wasn't until the early 1980s that water-right holders were required to submit annual water-use reports and not until 1987 that the KDA-DWR had the regulatory authority to fine water-right holders for lack of submission or knowingly falsifying reports. The Water Use Program of the Kansas Water Office was initiated in 1990. Now operated through the KDA-DWR, this program provides quality control and assurance for the submitted water-use reports. As such, reported water-use records were downloaded only from 1990 to 2016 (at the time of the model development, 2016 was the most recent year available for access as the 2017 reports were still under review).

To estimate historical pumping levels before 1990, linear regression equations were determined based on the ratio of water use/authorized quantity versus precipitation between 2002 and 2016, similar to past KGS modeling projects (Wilson et al., 2015; Liu et al., 2010; and Wilson et al.,

2008). Calendar year 2002 marked the first year that more than 50% of the water-use reports in GMD2 were based on metered values.

One challenge with establishing relationships between reported water use and precipitation is that unlike the western GMDs, GMD2 has a significant amount of non-irrigation groundwater usage that is not directly influenced by precipitation patterns. Responses to rainfall events from industrial and, to a lesser degree, municipal applications can be muted to undiscernible. As such, different regressions are employed between groundwater uses for irrigation and those for other uses.

Various iterations found the regression of the water use/authorized quantity ratio against annual precipitation from 2002 to 2016 to be statistically significant and highly correlated for total groundwater use (R-squared value of 0.79) and total irrigated groundwater use (R-squared value of 0.81); however, there were very poor correlations for other uses. A solution was to establish a third equation relating the non-irrigation water use/authorized quantity ratio against the ratio of total irrigated groundwater use/total groundwater use (R-squared = 0.99875).

Figure 23 shows the results of the regression-based water-use estimates against the authorized quantity and the 1990–2016 reported water use for cells in the model's active area. The ratios of water use/authorized quantity for total groundwater use and total irrigation groundwater use are computed for every model cell based on the variations in summer precipitation followed by calculating the non-irrigation groundwater use. The ratios are then multiplied against their respective authorized quantities for a given year to yield an estimate of the actual amount of water used. The transient model uses the regressed water use from predevelopment until 1989, the actual reported water-use data for 1990–2016, and regressed water use for years going forward after 2016 (in future scenarios).

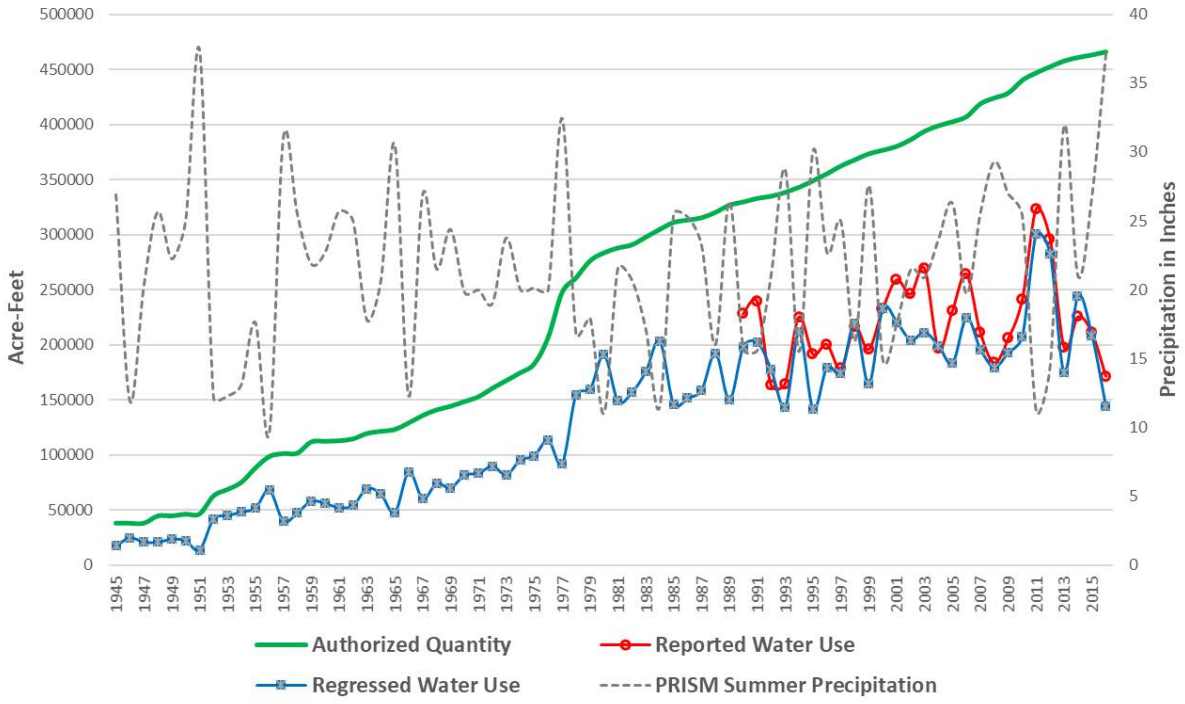

Figure 23. Total authorized quantity, regressed water use, summer precipitation, and reported water use.

Irrigation Return Flow

A certain amount of water applied by irrigation systems makes its way back to the aquifer in the form of irrigation return flow. The rate of this aquifer recharge is determined by a variety of factors, one of which is the efficiency of the irrigation system. Irrigation system types were added to KDA-DWR water-use reports in 1991. County reviews of the reported irrigation systems from 1991 to 2016 across the model area show flood and early pivot systems to be the most common type of system used in the early 1990s. The western counties of Rice and Reno were predominately using early center pivot systems likely because of the sandier soils. All shift to more efficient irrigation systems over time. Figures 24 to 28 show the trends in reported system types for Sedgwick, Harvey, McPherson, Rice, and Reno counties. Figure 29 shows the trends for the counties of Kingman, Harper, and Sumner together as one group. As farming operations have improved with technological advancements, so have irrigation efficiencies, thus reducing the amount of return flow over time.

The irrigation return-flow percentages (relative to the total irrigation water pumped) used in the GMD3 model (Liu et al., 2010) were assigned to the system types reported in the model's water-use data. In order of decreasing return-flow percentages, they are the following: flood irrigation, 25%; center pivot and flood, 17%; center pivot, 9%; sprinkler other than center pivot (Non-CP), 9%; center pivot with low energy precision applicators (LEPA), 7%; and subsurface drip (SDI) in combination with other type, 4%.

The average return-flow percentage was then computed in each county for each year from 1991 to 2016 based on the number of each system type and its assigned return-flow percentage. It was assumed that flood irrigation was the only system type in use before 1955. Between 1955 and 1991, a smooth transition from flood to center pivot types for each county area was then applied. The total return-flow percentage averaged as a whole for each county and the "southern" counties of Sumner, Harper, and Kingman shows a spatial pattern of increasing efficiencies moving from west to east across the model area (fig. 30). Water use occurring within these county areas is multiplied by the average return-flow percentage to determine the total amount of water returning to the aquifer. This return flow is treated separately from precipitation-driven recharge in the model.

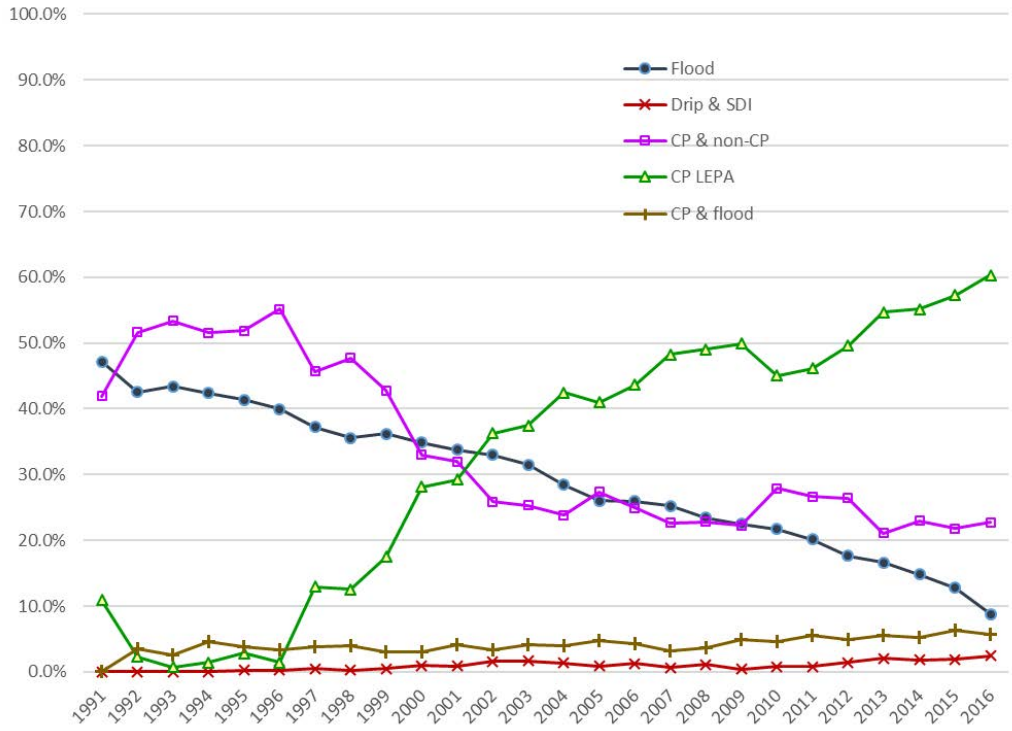

Figure 24. Reported irrigation system types, Sedgwick County GMD2 model area, 1990 to 2016.

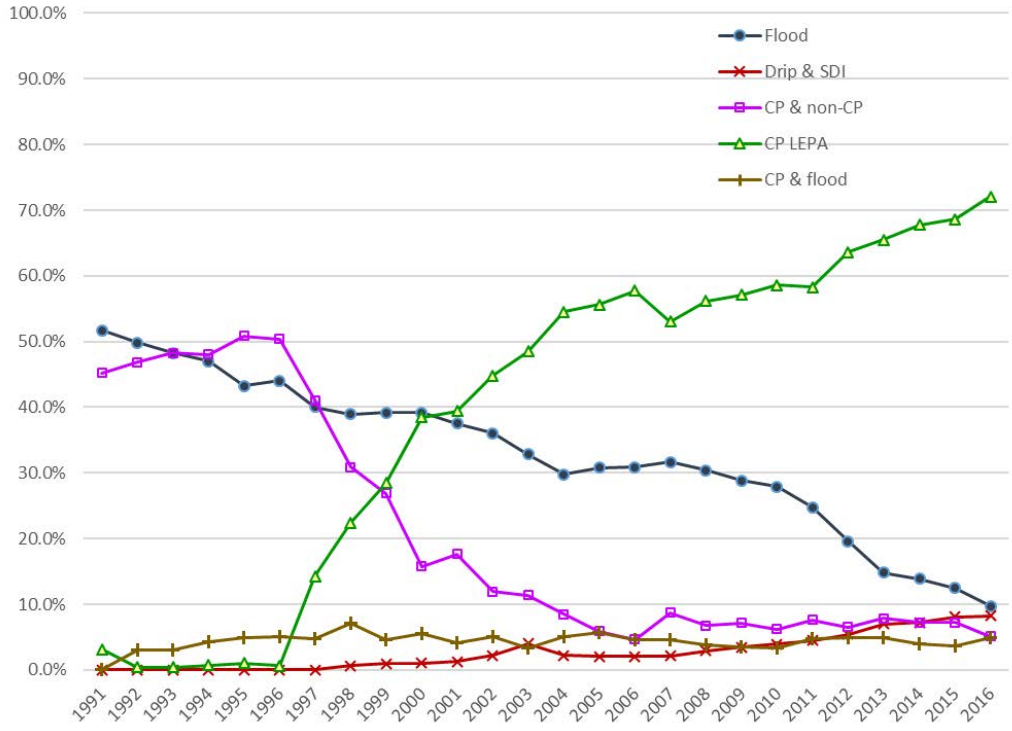

Figure 25. Reported irrigation system types, Harvey County GMD2 model area, 1990 to 2016.

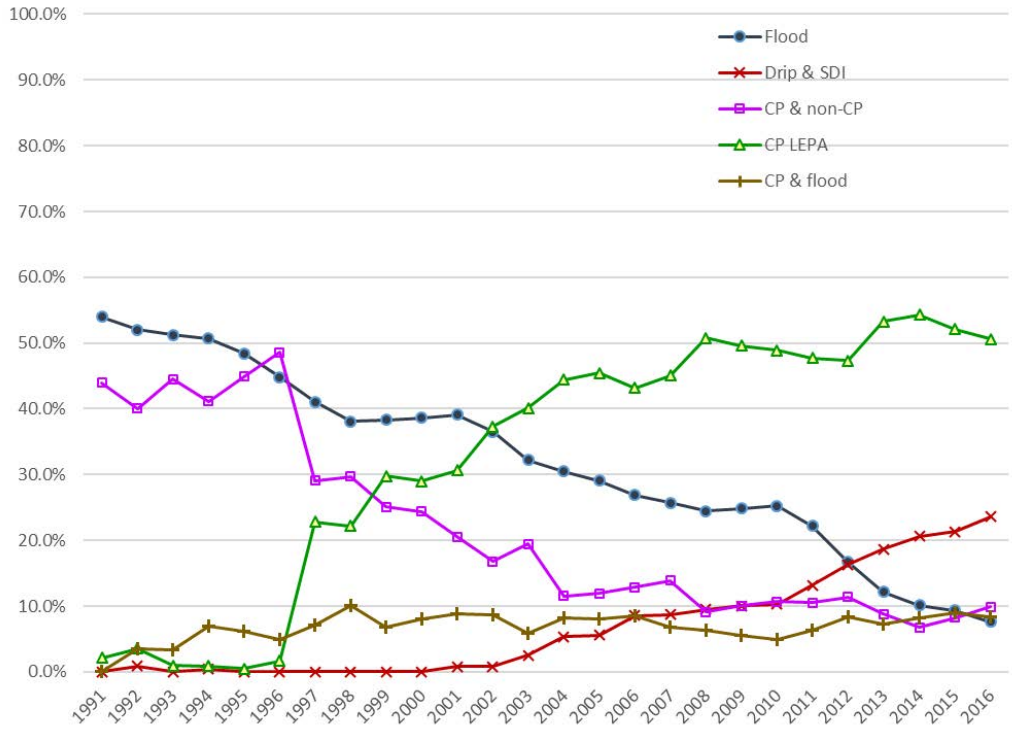

Figure 26. Reported irrigation system types, McPherson County GMD2 model area, 1990 to

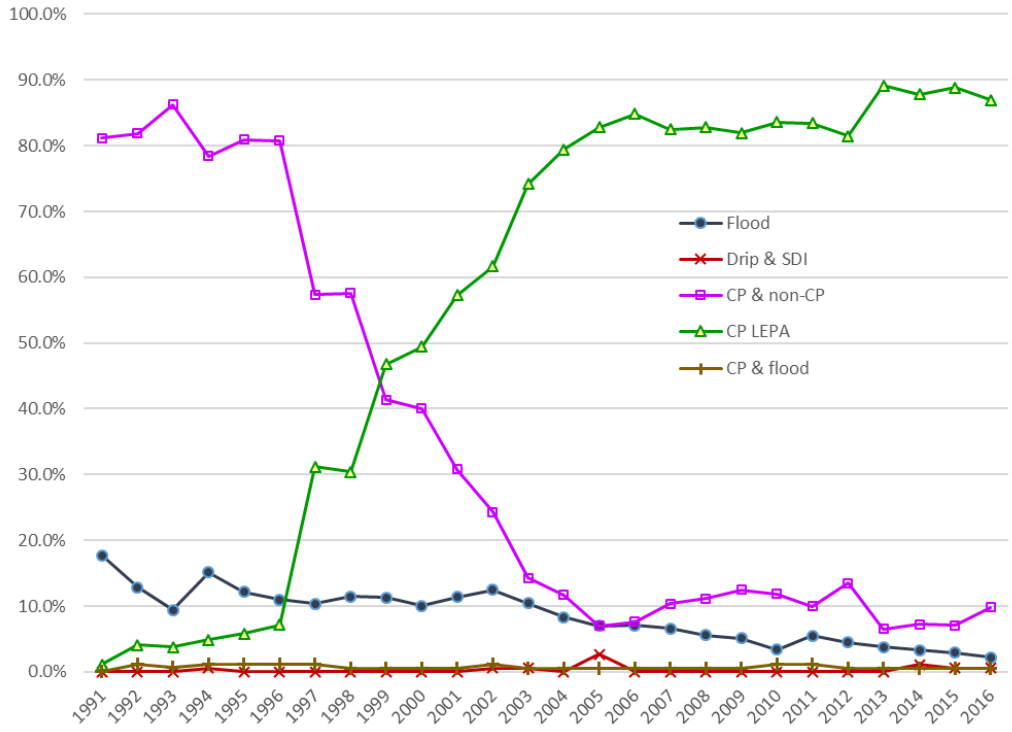

Figure 27. Reported irrigation system types, Rice County GMD2 model area, 1990 to 2016.

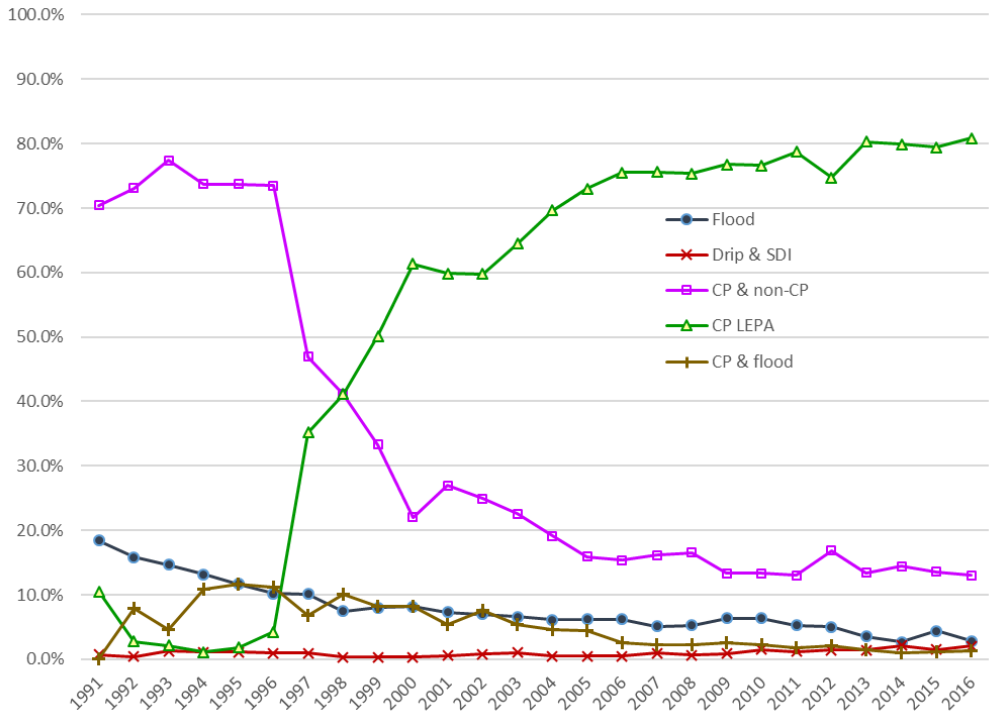

Figure 28. Reported irrigation system types, Reno County GMD2 model area, 1990 to 2016.

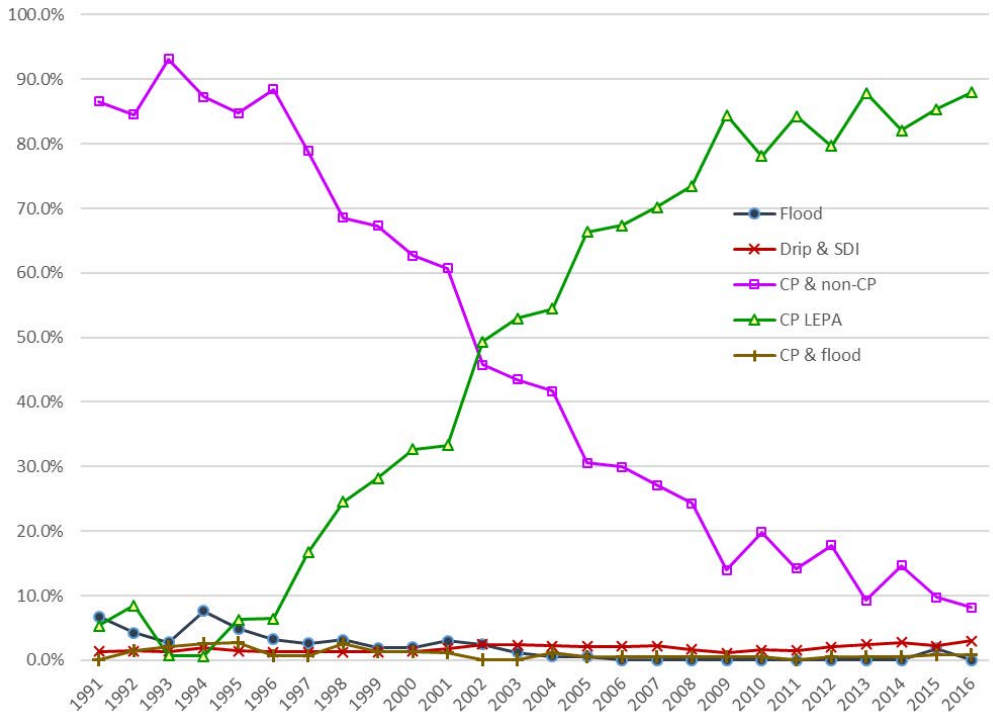

Figure 29. Reported irrigation system types, Kingman, Harper, and Sumner counties GMD2 model area, 1990 to 2016.

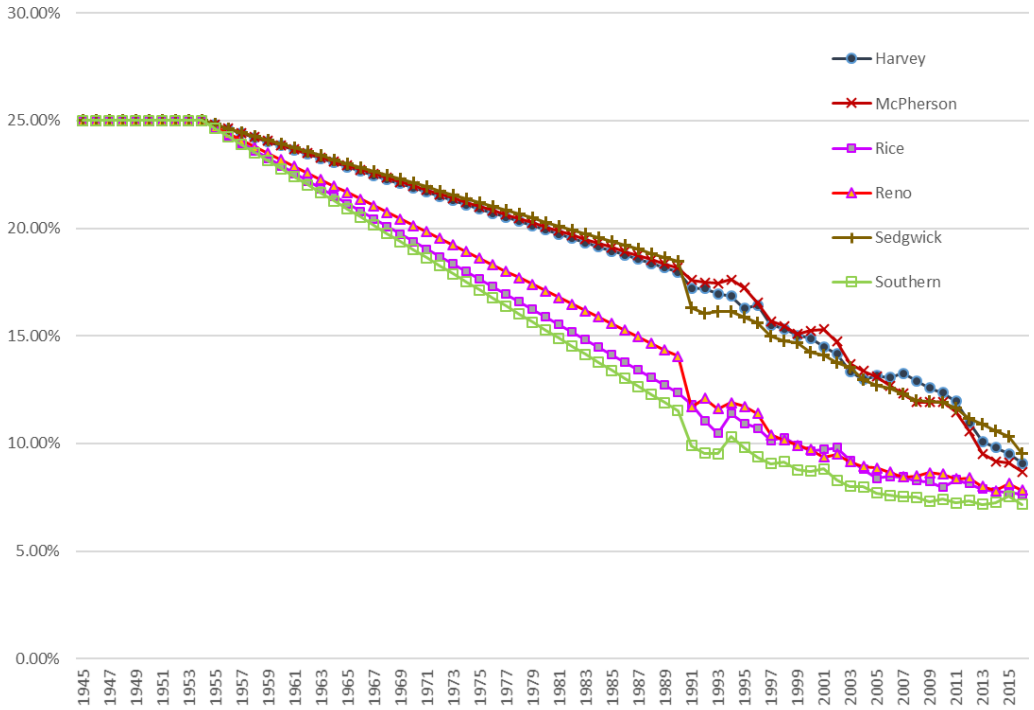

Figure 30. Average percentage of irrigation return flows by county, 1945 to 2016.

MODEL CALIBRATION AND SIMULATION

Like past KGS modeling projects, the GMD2 model is divided into two major simulation periods: a steady-state predevelopment period during which water levels remain relatively stable and a transient period during which groundwater development increases and water levels change over time. The predevelopment simulation establishes the conditions from which the subsequent transient model starts.

The major data sources for the predevelopment period are for the years before 1946, although some of the water-level data extends into the early 1950s. Contrary to the implications of the term "predevelopment" (a period of time representing the aquifer before it was extensively developed), the steady-state GMD2 model includes relatively small but concentrated areas of pumping, with the most significant being around the cities of Wichita and Hutchinson. The transient period simulates groundwater conditions from predevelopment to 2016, during which time groundwater pumping increased. The transient period is based on six-month time steps—a "summer," or growing, season from April to September and a "winter" period representing the months of October to March.

Model Characteristics

Predevelopment pumping

Williams and Lohman (1949) described groundwater usage in the area primarily focusing on industrial and municipal diversions since irrigation development at the time was for the most part insignificant. To create a steady-state or predevelopment pumping file, both present-day active and inactive vested water rights (those permitted water rights that had verified water uses in place before the 1945 Kansas Water Appropriation Act) were queried from the WIMAS data. Vested water-right wells that were known to have been re-drilled since 1945 were removed from consideration. Point density functions show a large concentration of municipal-based rights around Wichita and Hutchinson along with primarily industrial-based rights in and around Hutchinson and McPherson (fig. 31).

Two-thirds of the vested water rights' present-day authorized quantity was assumed to represent predevelopment pumping. Given the lack of any over-riding state or local water law and the readily accessible water supply, it was thought historic pumping would be higher than for most water rights, where reported use is typically between 50 and 60 percent of the allocation. For the vested rights that today are listed as inactive, the model used the average authorized quantity of other active vested rights of similar uses of water to represent a past quantity (authorized quantity in WIMAS is only valid as of the date of the download and historic quantity values are not maintained).

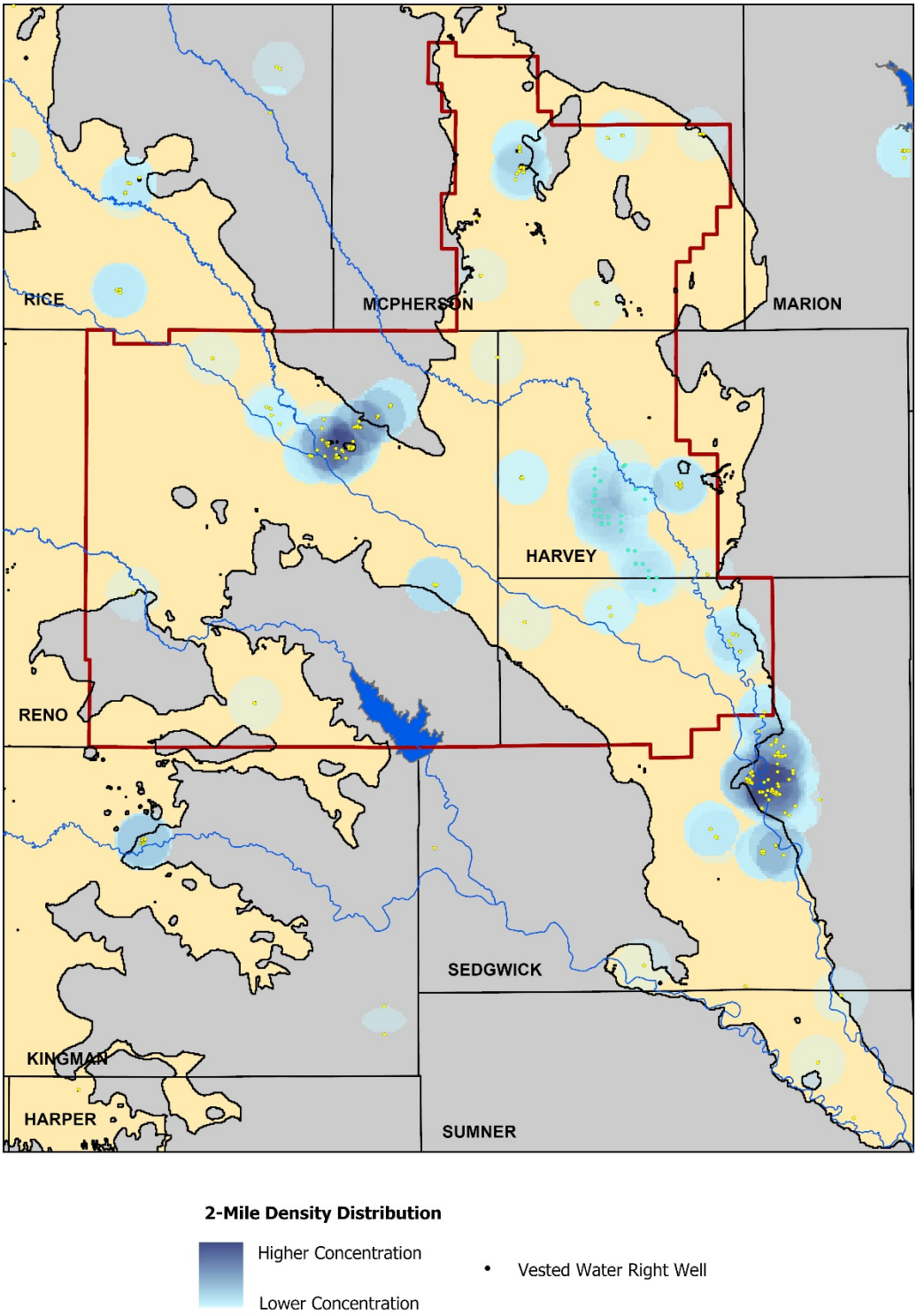

Figure 31. Distribution of vested water rights.

Transient Pumping and Irrigation Return Flows

The “Water Right Development” section of this report describes how groundwater pumping is determined. The reported and regressed water usages are annual values. For the model’s six-month time steps, all irrigation usage was assigned to the “summer” period, representing conditions from April to September. All other groundwater usage was proportioned with 60 percent occurring in the summer period and 40 percent occurring during the winter period. Irrigation return flows were added to the overall recharge input file used by the model for the summer period.

Stream Characteristics

The Arkansas River, Cow Creek, Little Arkansas River, North Fork Ninnescah, South Fork Ninnescah, and Ninnescah River are simulated in this project as rectangular channels with an underlying streambed. The streambed widths were assigned a value of 15 ft throughout the model area. The streambed thickness is assumed to be 1 ft with a streambed conductivity of 0.01 ft/day. Streamflow data available from the USGS were used in calibrating the stream-aquifer interactions.

Drains

Drains, which allow water to discharge from the aquifer to the creek based on water-table elevations relative to the drain cell’s elevation, are used only along Big Slough Creek. The drain elevation for each drain cell was set to the land surface.

Evapotranspiration

Evapotranspiration (ET) from groundwater is an important part of the groundwater system as the water table is relatively shallow through much of the district. The maximum ET rate at the land surface was set to 1 ft/yr. The extinction depth was set to 10 ft below land surface, at which point the ET rate becomes zero. When the depth to water is between the land surface and extinction depth, the ET rate is linearly interpolated based on the depth to water relative to the extinction depth.

Time-Varying Specified-Head Boundaries

Time-varying specified-head boundaries are used for active model cells along the model edges. Time-varying specified heads were determined based on a time- and labor-intensive process of reviewing each model cell in relation to any surrounding water-level measurement. Water-level trends shown in the measurement history of nearby wells were applied to the head-boundary cells.

Precipitation Recharge

Precipitation-based recharge was calculated based on the power-function used in the GMD3 model (Liu et al., 2010),

$$R = \begin{cases} 0, & P < P_0 \\ a\left(P - P_0\right)^b, & P \geq P_0 \end{cases}, \quad (1)$$

where R is precipitation recharge to groundwater, P is precipitation at a given model cell in a six-month time step, P_0 is threshold precipitation above which groundwater recharge occurs, and *a* and *b* are the coefficients of the power function.

The model divides the recharge-precipitation power functions into four zones. Three zones (alluvium, McPherson Channel and regional HPA; and fringe aquifer area with thin saturated thickness [fig. 32]) were initially based on HyDRA lithology classifications from table 1, vertically averaged from the predevelopment water-table surface to bedrock. During the construction of the model, a fourth area was manually added to represent the sand hills north and northeast of Hutchinson. The parameters in the power function are adjusted between different recharge zones. In each recharge zone, between the summer and winter periods, the recharge parameters are assumed to be the same for the summer and winter periods except for the threshold precipitation (lower P_0 in winter steps).

The Arkansas River valley and the sand hills have the highest recharge rates relative to the McPherson Channel/High Plains aquifer and the other fringe areas. The actual recharge rate varies for each model cell as the precipitation amounts change between cells and time steps. For the same precipitation, the recharge rate is higher in the non-growing season than in the growing season as surface evapotranspiration is much more significant in the growing season (higher temperature and more consumptive use by plants). The power-function parameters P_0, *a*, and *b*, along with some other model parameters, are calibrated by matching observed water levels and streamflows to simulated values.

.

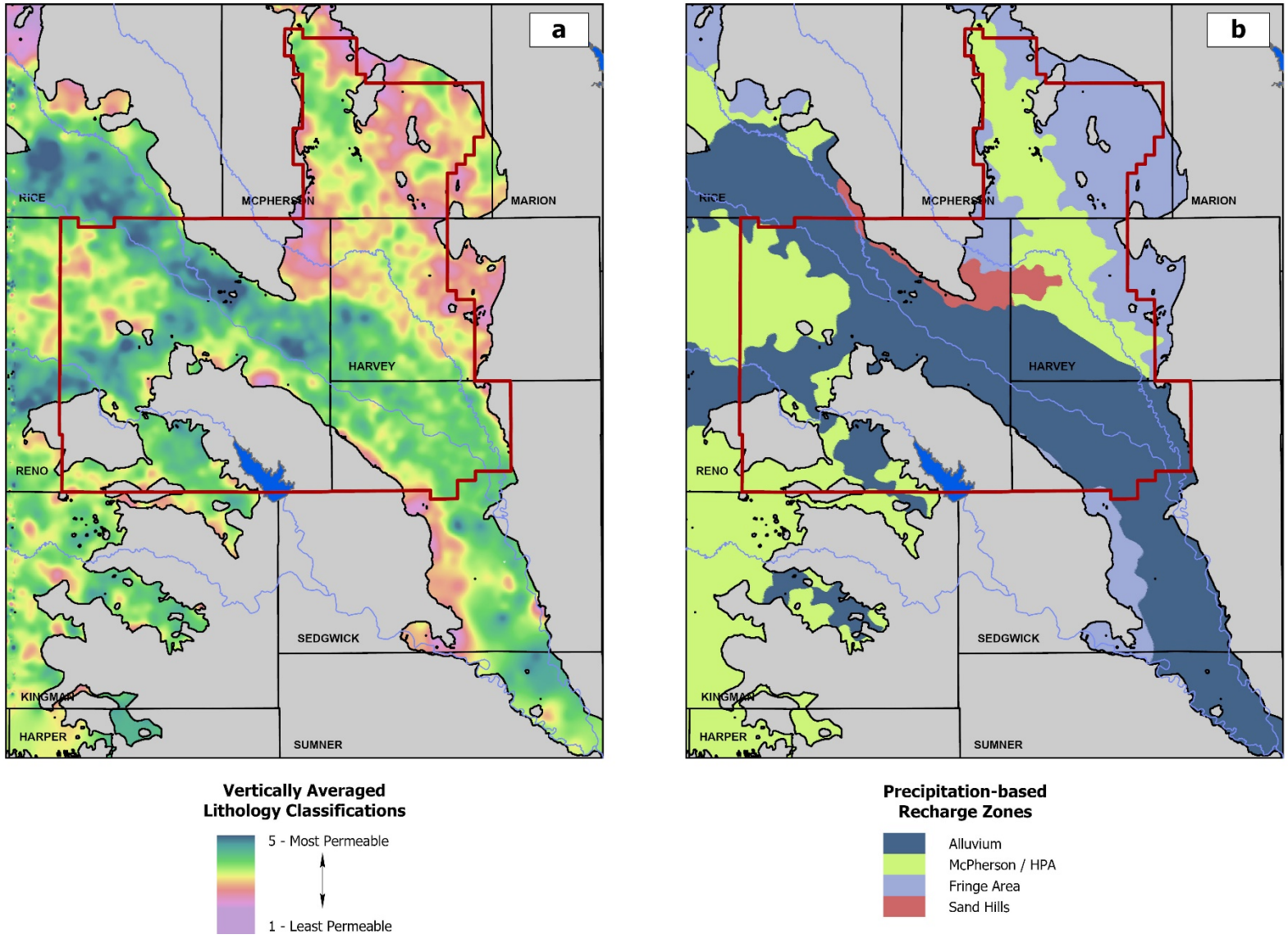

Figure 32. Classified standardized lithologies (a) and zones for precipitation-based recharge calculation (b).

Hydraulic Conductivity and Specific Yield

As described earlier, the code developed for the HyDRA project was used to develop a three-dimensional grid describing the proportional distribution of five different categories of the material composing the aquifer throughout the model domain, based on drillers' logs contained in the WWC5 database and other sources. A special program was then used to compute K and SY based on the selected values for each lithological category and the predevelopment water level (materials above the predevelopment water level did not affect the calculation of K or SY).

Figure 33 shows the HyDRA lithology-based estimated K for the interval between the predevelopment water levels and the bedrock surface based on the estimates of K for each of the lithology categories listed in table 1. The average K across the active area in GMD2 was approximately 129 ft/day with the highest estimates originating from the coarse gravel deposits found mostly in the upper extent of the active area of the model of the Arkansas River valley. Similarly, fig. 34 illustrates the HyDRA-estimated SY from the predevelopment water table to the bedrock surface based on the estimates of SY for each of the lithology categories listed in table 1. The average SY across the active area in GMD2 was 5.8 percent. This is substantially less than traditional estimates of SY for numerical models but within ranges established through the water-balance relationships computed for the GMD2 sustainability assessment (Butler et al., 2017).

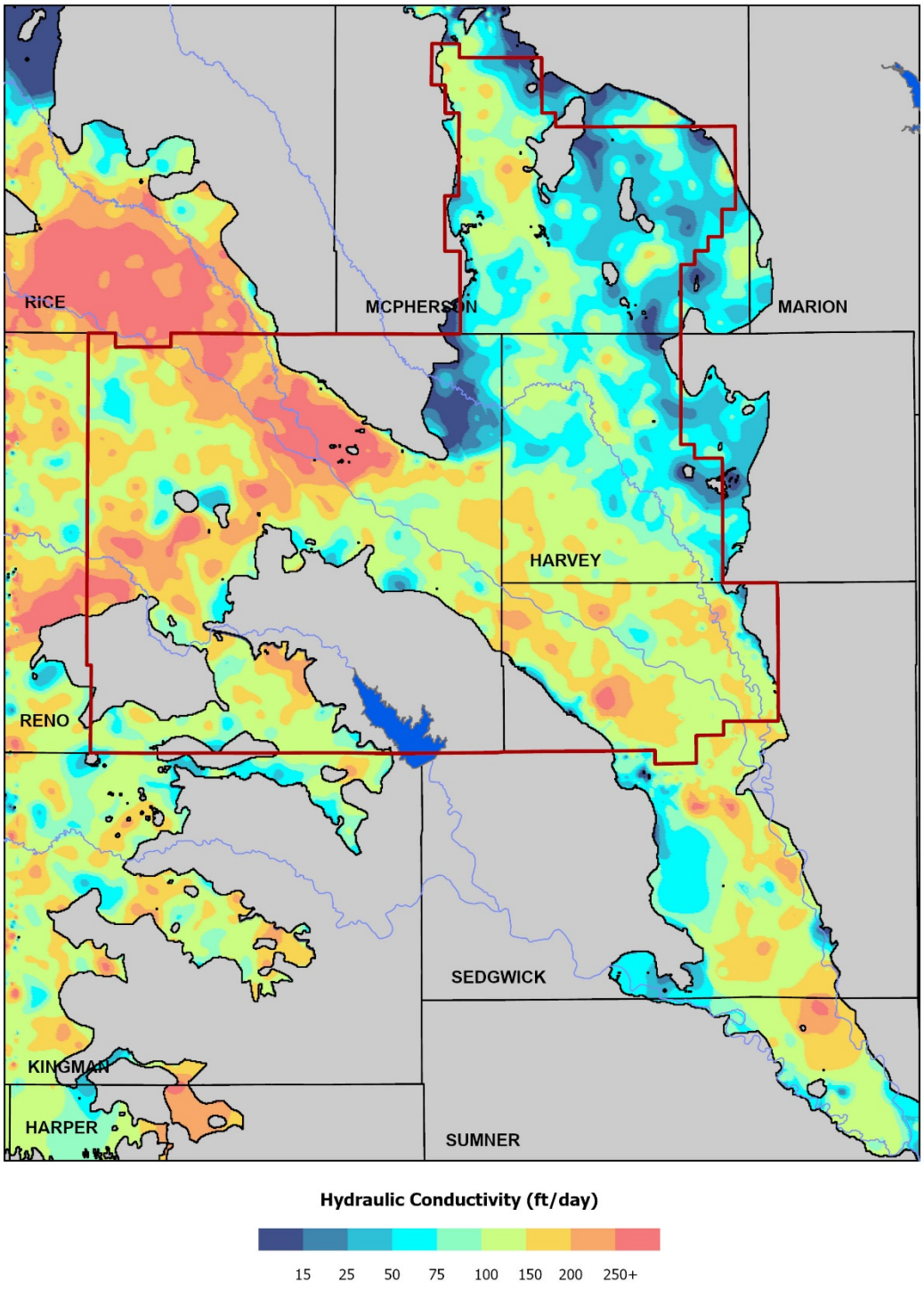

Figure 33. Vertically averaged K between the predevelopment water level and bedrock based on the calibrated K values for the five lithology categories shown in table 1.

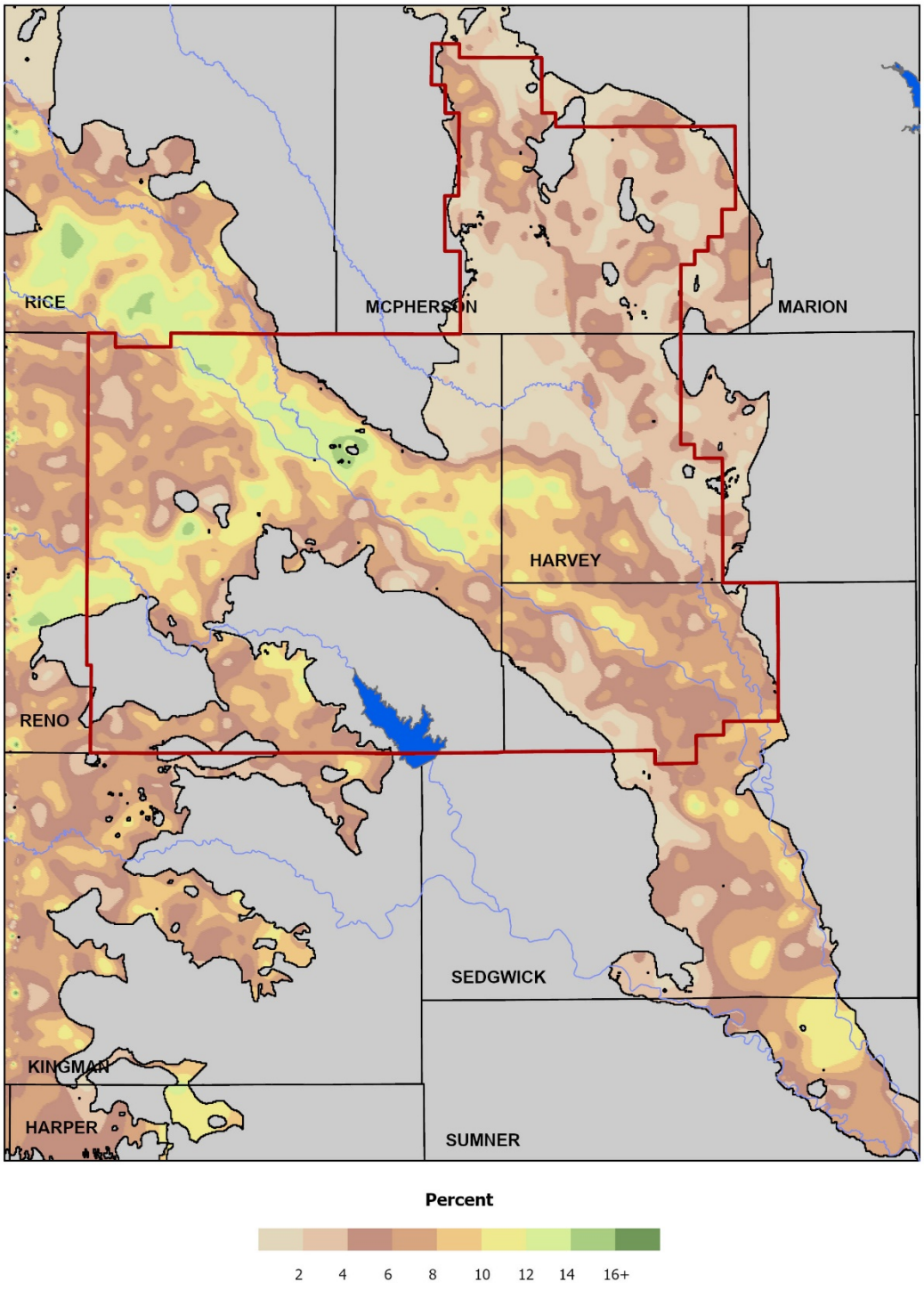

Figure 34. Vertically averaged SY between the predevelopment water level and bedrock based on the calibrated SY values for the five lithology categories shown in table 1.

Model Calibration

Because of our imperfect understanding of the hydrologic conditions in the field, some model parameters, especially those that are key contributors to aquifer budget calculations (e.g., aquifer K and SY, recharge rate), need to be adjusted so that the simulated results match with observed data to the best extent possible. This process is generally referred to as model calibration. For the GMD2 model calibration, data for comparison with the simulated results include 1) water levels for a number of wells in the active model area from predevelopment to January 2017 and 2) streamflows for the Arkansas River, Cow Creek, Little Arkansas River, North Fork Ninnescah, South Fork Ninnescah, and Ninnescah River. The water levels for the predevelopment period are used directly. In the transient period, the changes between consecutive water-level measurements are used rather than the water levels themselves. The water-level change provides a more sensitive indicator of aquifer response to different hydrologic processes during the transient simulation.

Different weights were assigned to different data sets to ensure model calibration is balanced between different components. For predevelopment heads, a weight of 5 was used. For transient water-level change, a weight of 10 was used as the temporal change in water levels was considered more important for water resources management purposes. For streamflow, because the focus was the stream-aquifer interaction (i.e., the baseflow component), streamflow values were log-transformed before they were used in the calibration. A weight of 500 was used for the log-transformed streamflow to ensure stream-aquifer interaction was adequately taken into account during calibration.

The model parameters that were adjusted during calibration are 1) the threshold precipitation P_0 for recharge during the summer and winter periods and the power function coefficients *a* and *b* for all four recharge zones; 2) the hydraulic conductivity and specific yield for five lithological categories, and the averaging power in K calculation (the averaging power is between 0.5 to represent the geometric mean and 1 for arithmetic mean); and 3) the streambed hydraulic conductivity. As a result, there are 28 parameters in total: 16 for precipitation recharge, 5 for lithology category K, 5 for lithology category SY, 1 for the K averaging power between categories, and 1 for streambed K. The calibration process was performed with the parameter estimation program PEST (Doherty, 2004).

Figure 35 shows the calibrated precipitation recharge curves for the recharge zones. Note that in the non-growing season, the threshold precipitation at which water starts to infiltrate through the top soil (i.e., recharge starts) is lower, resulting in a larger recharge rate than that in the growing season for the same precipitation amount. For a given precipitation amount, precipitation recharge is the lowest in the fringe areas followed by the McPherson channel/High Plains aquifer, whereas the Alluvium and Sand Hill zones have higher simulated values.

Figure 36 shows the simulated versus observed predevelopment heads from the PEST calibration. As the figure illustrates, the simulated heads align very well with the observed values during predevelopment time. Figure 37 shows there is little correlation between the simulated versus observed transient water-level changes from the PEST calibration, especially with large changes. Water-level changes were computed by subtracting the later water levels from their corresponding earlier values, so that positive values indicate a decline of the water table with time. Figure 38 shows the simulated versus observed streamflows for the Arkansas River, Cow Creek, Little Arkansas River, North Fork Ninnescah, South Fork Ninnescah, and Ninnescah River.

The simulated values are generally smaller than the observed values, especially during the high-flow periods, because the model does not simulate surface runoff into the streams during rainfall events.

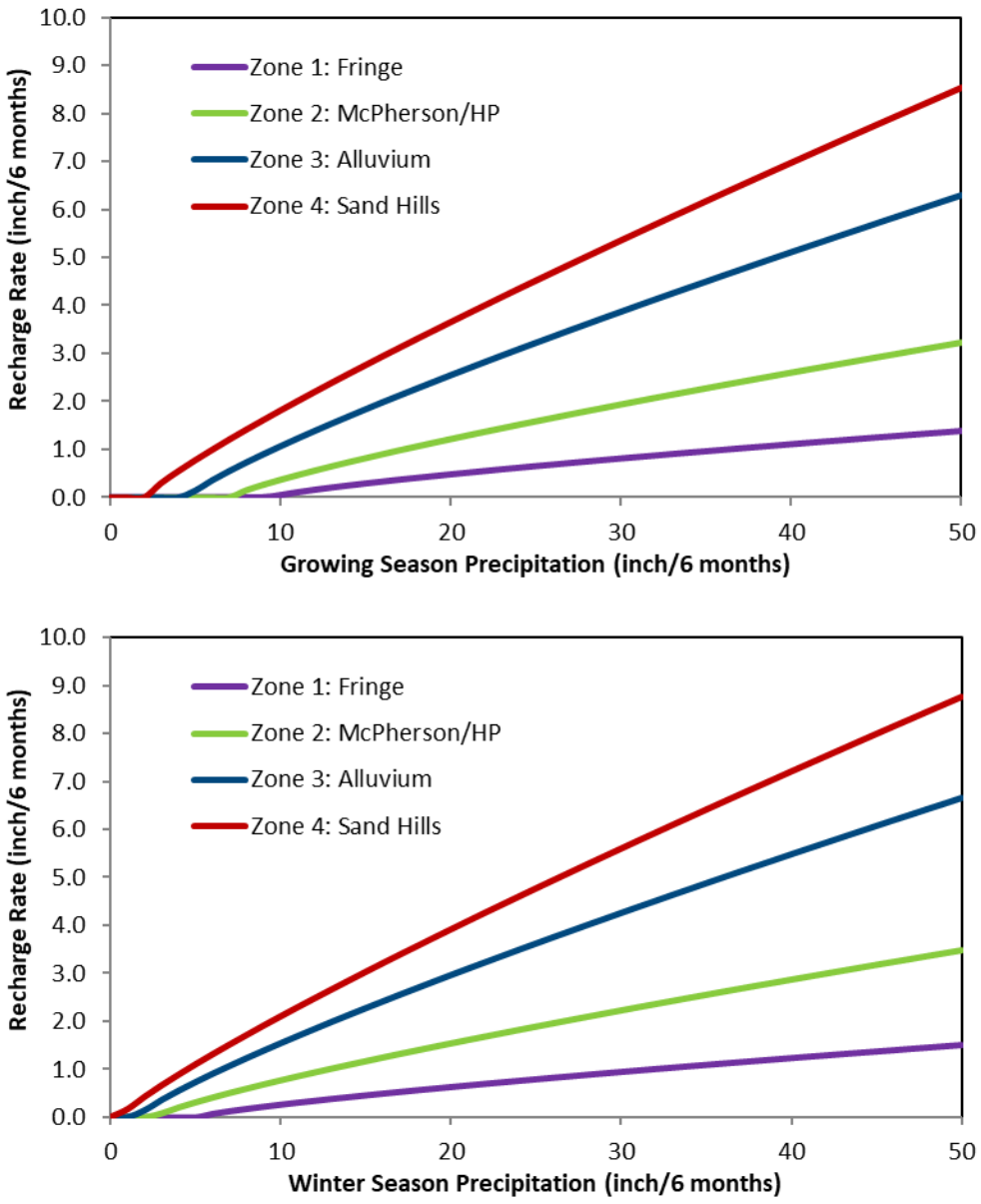

Figure 35. The calibrated precipitation recharge curves for different recharge zones in the growing (top chart) and non-growing (bottom chart) seasons.

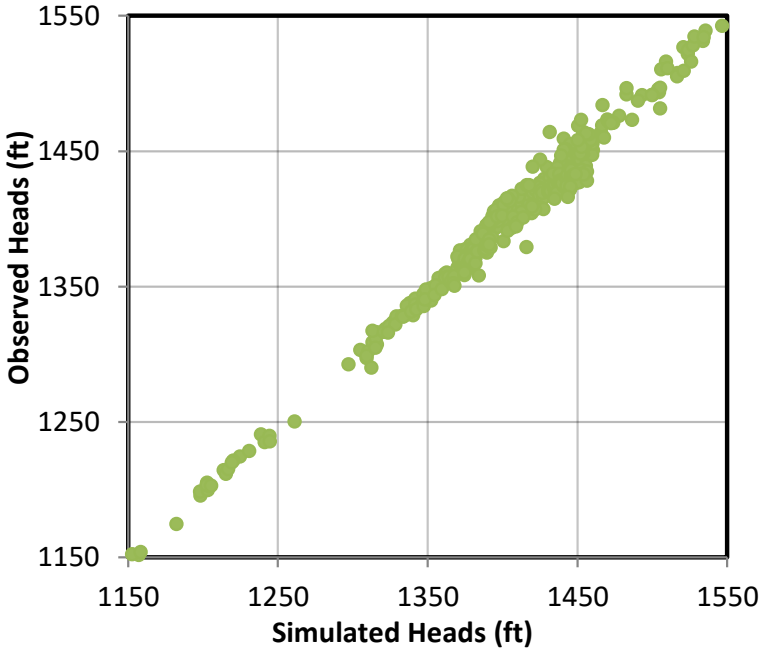

Figure 36. Observed versus simulated predevelopment heads from the calibrated model. These are the water levels used in PEST calibration.

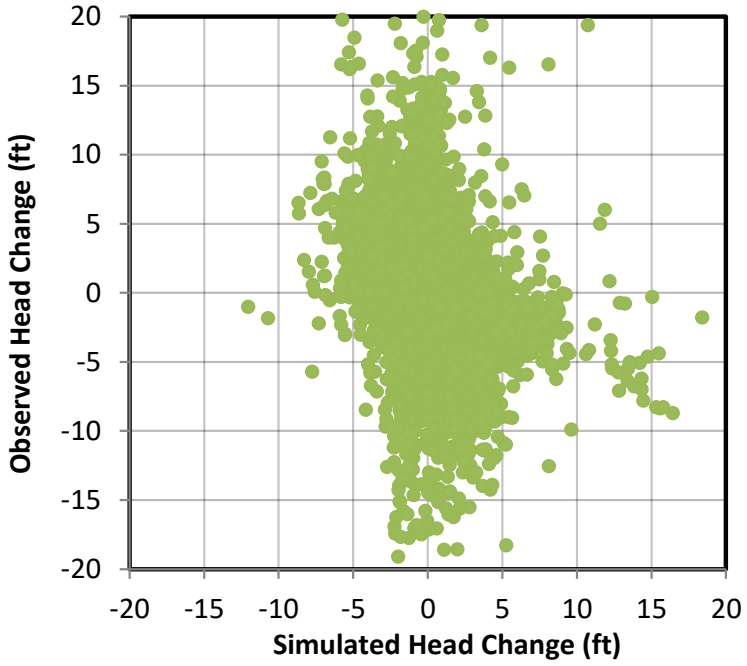

Figure 37. Observed versus simulated water-level changes from the calibrated transient model. Water-level changes are computed between two adjacent winter water-level measurements (separated by one or more years for each well).

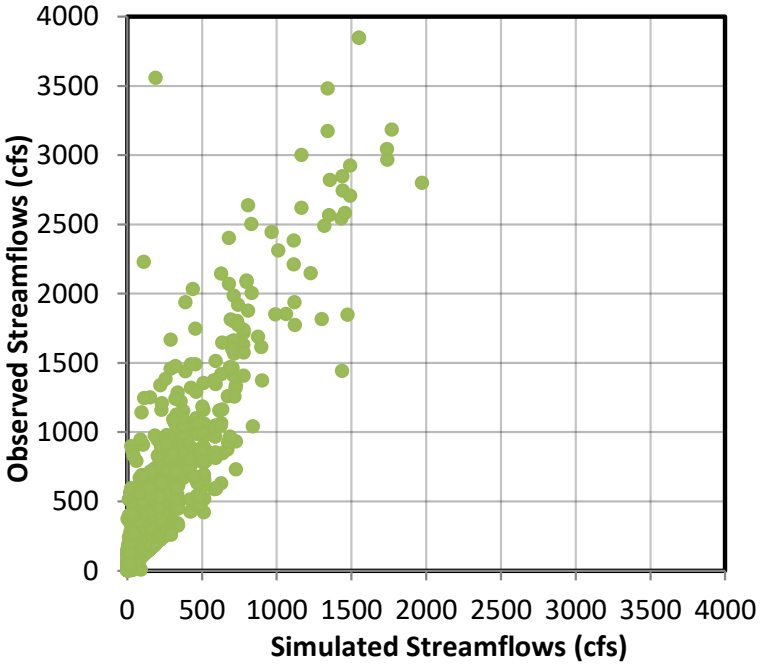

Figure 38. Observed versus simulated streamflows from the calibrated model. The flows are six-month averages during the growing (April–September) and non-growing (October–March) seasons.

Table 3 lists the mean residual, mean absolute residual, and root mean square of residuals of the PEST calibration data targets. The mean residual is given as the mean of observed minus simulated values, whereas the mean absolute residual is the mean of the absolute values of observed minus simulated values. The statistics for both predevelopment heads and transient water-level change are similar to those in the previous models developed for other HPA regions in Kansas (Wilson et al., 2015; Liu et al., 2010).

Table 3. Mean residuals, mean absolute residuals, and root mean square of residuals for model calibration targets.

	Number of data	Mean residual	Mean absolute residual	Root Mean Square of residuals (RMS)
Predevelopment head (ft)	449	5.38	8.24	10.38
Transient water-level change (ft)	25,739	0.11	2.83	3.88
Streamflow (ft^3/sec)	924	-298.41	299.79	509.72

Sensitivity Analysis

Table 4 lists the sensitivities of different model parameters during calibration. The relative sensitivity of a parameter *p* (RS_p) is computed as (Liu et al., 2010)

$$RS_p = \sqrt{\frac{1}{N}\sum_{i=1}^{N}\left(\frac{\partial d_i}{\partial p/\acute{p}}\right)^2} \quad (2)$$

where ∂p is the small perturbation around the calibrated parameter value $\acute{p}$; ∂d_i is the change in the model-simulated groundwater level or streamflow at observation *i,* and *N* is the total number of observation data points used in the sensitivity calculation. In table 4, p11 and p12 are the initial precipitation amount of recharge to start during the growing and non-growing seasons in recharge zone 1 (fringe area), respectively, and p13 and p14 are the precipitation recharge power function coefficients for recharge zone 1. Similarly, p21 through p24, p31 through p34, and p41 through p44 are the precipitation recharge parameters defined for the second, third and fourth recharge zones, respectively. The parameters hy1 through hy5 and sy1 through sy5 are the hydraulic conductivity and specific yield for the first through fifth lithological categories, respectively. Parameter hyw is the averaging power for computing K between different lithological categories, and stk is the hydraulic conductivity for the streambed. Based on table 4, p13, p14, hy4, hy5, and sy1 have the highest sensitivities, indicating that they have the most significant influence on the statistical agreement between the model-simulated water levels and streamflows and the observed values.

Table 4. Relative sensitivities of different model parameters during the PEST calibration.

Parameter	Relative Sensitivity	Parameter	Relative Sensitivity	Parameter	Relative Sensitivity
p11	0.036	p12	0.052	p13	18.81
p14	33.12	p21	0.011	p22	0.005
p23	0.041	p24	0.090	p31	0.015
p32	0.005	p33	0.082	p34	0.225
p41	0.001	p42	0.001	p43	0.027
p44	0.117	hy1	0.000	hy2	0.000
hy3	0.266	hy4	35.68	hy5	51.60
sy1	5.35	sy2	0.000	sy3	0.005
sy4	0.065	sy5	0.053	hyw	0.105
stk	0.001				

Transient Model Results

Water Levels

Figures 39 to 41 show a series of comparisons of the simulated groundwater elevations in relation to interpolated observed data for the years of predevelopment, 1972, 1982, 1992, 1997, 2002, 2007, 2012, and 2017. The contour maps (top) are an indication of flow directions and water-level gradients while the cell-based shaded maps (bottom) show absolute differences between the simulated and within 5 miles of observed water levels. In general, the model estimates water levels relatively well within the Arkansas River valley, underestimates water levels along the western edge of GMD2 in Reno County, and overestimates water levels in the McPherson Channel. The areas of local mismatches between simulated and observed data tend to improve later in the transient period, when reported water uses are used. Figures 42 and 43 compare the model's simulated water-level change maps (top) and interpolated (bottom) between 1972 and 1982, 1982 and 1992, 1992 and 2002, 2002 and 2007, 2007 and 2012, and 2012 and 2017. The model captures regional changes in the water levels with some local mismatches.

Figure 44 plots monitoring well locations, labeled by the row and column of the model cell in which each well is located, that were used in the model calibration. The wells were selected based on measurement history and spatial distribution across the model. In cases of well nests of adjacent wells with various depths and screening intervals, the deepest well in the collection was chosen. Hydrographs for these wells are plotted in figs. 45 to 55 and are all at the same 50 foot vertical scale (y axis) except for a few with larger vertical ranges, indicated by red axis labels.

The model matches the simulated and observed water levels well throughout most of GMD2. At most of the well sites, the water levels are within 5 feet of each other and mimic the same long-term trends and annual variations. There are examples of wells where the matches are poor. The greatest disagreements occur in the McPherson Channel area, where the model tends to overestimate the water levels, and the Pretty Prairie area (just west of Cheney Reservoir), where the model underestimates water levels.

In some cases, the areas of disagreement between simulated and observed water levels are likely a result of wells being close to boundaries where inactive cells restrict lateral inflows. In other cases, the mismatch is caused by vertical head gradients, which are not accounted for in the two-dimensional model, combined with a limited screened interval in the selected observation well. For example, the well located in row 460, column 81, along the western boundary of GMD2 in Reno County (fig. 46, top right) is the deepest of four wells in a nested well site measured by GMD5. At this location, the head difference between the deepest well and the shallowest in the nest is roughly 40 feet, indicating a significant vertical gradient at this location. In contrast, the one-layer model represents vertically averaged heads with the simulated water levels between the two wells.

Streamflow

The transient model was also calibrated to streamflow data available for gages along the Arkansas River, Cow Creek, and Little Arkansas River. The model simulates only the stream-aquifer interactions and does not take into account surface runoff from precipitation events (i.e. emphasis is on match at low flows). Gaged flow at the Little Arkansas River near Alta Vista was directly inputted into the model to assist with calibration. Figure 56 plots the model-simulated versus observed streamflows at various gages.

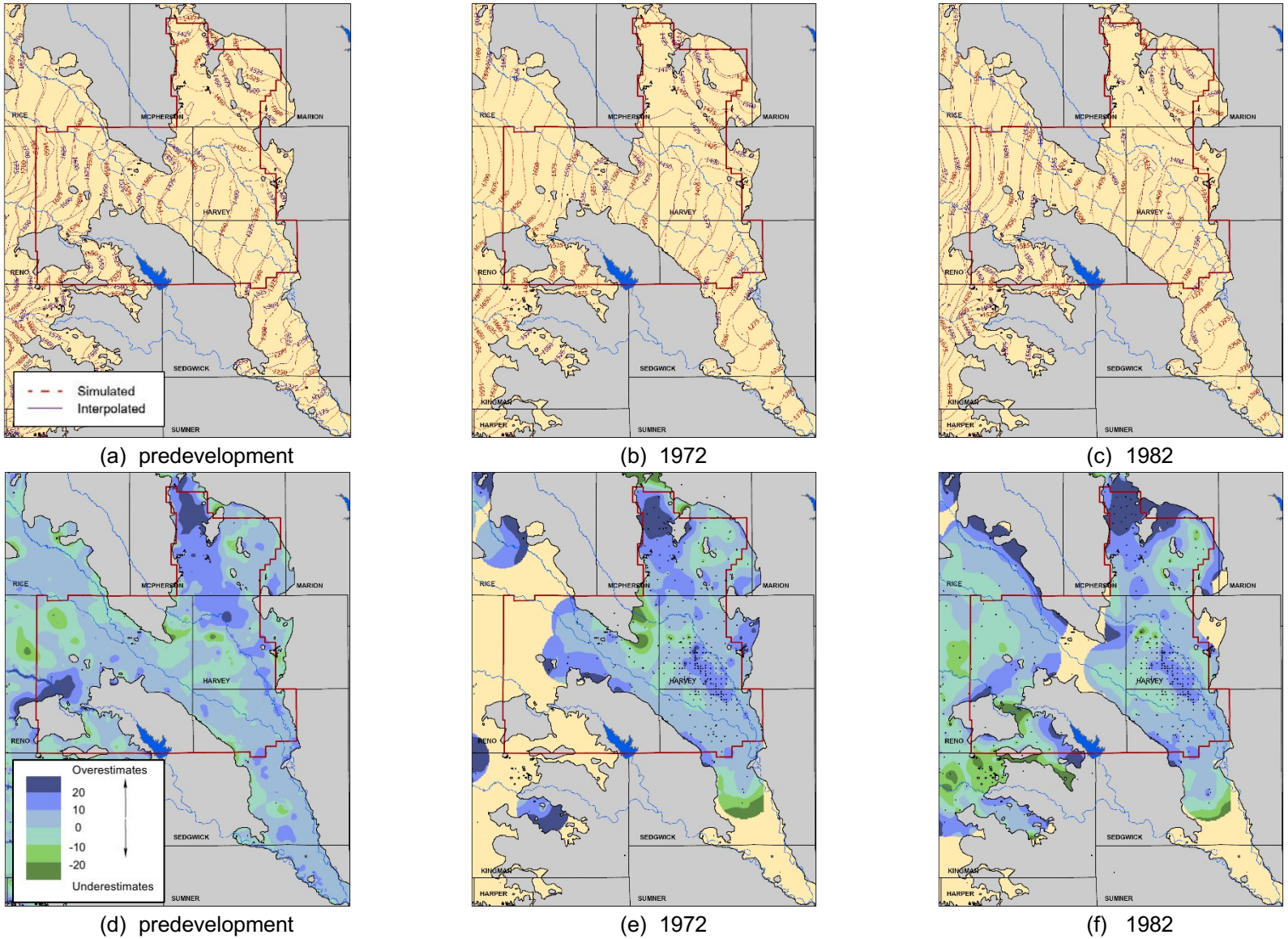

(a) predevelopment (b) 1972 (c) 1982

(d) predevelopment (e) 1972 (f) 1982

Figure 39. Comparison of simulated versus observed water levels, predevelopment, 1972, and 1982. Active area shown in yellow.

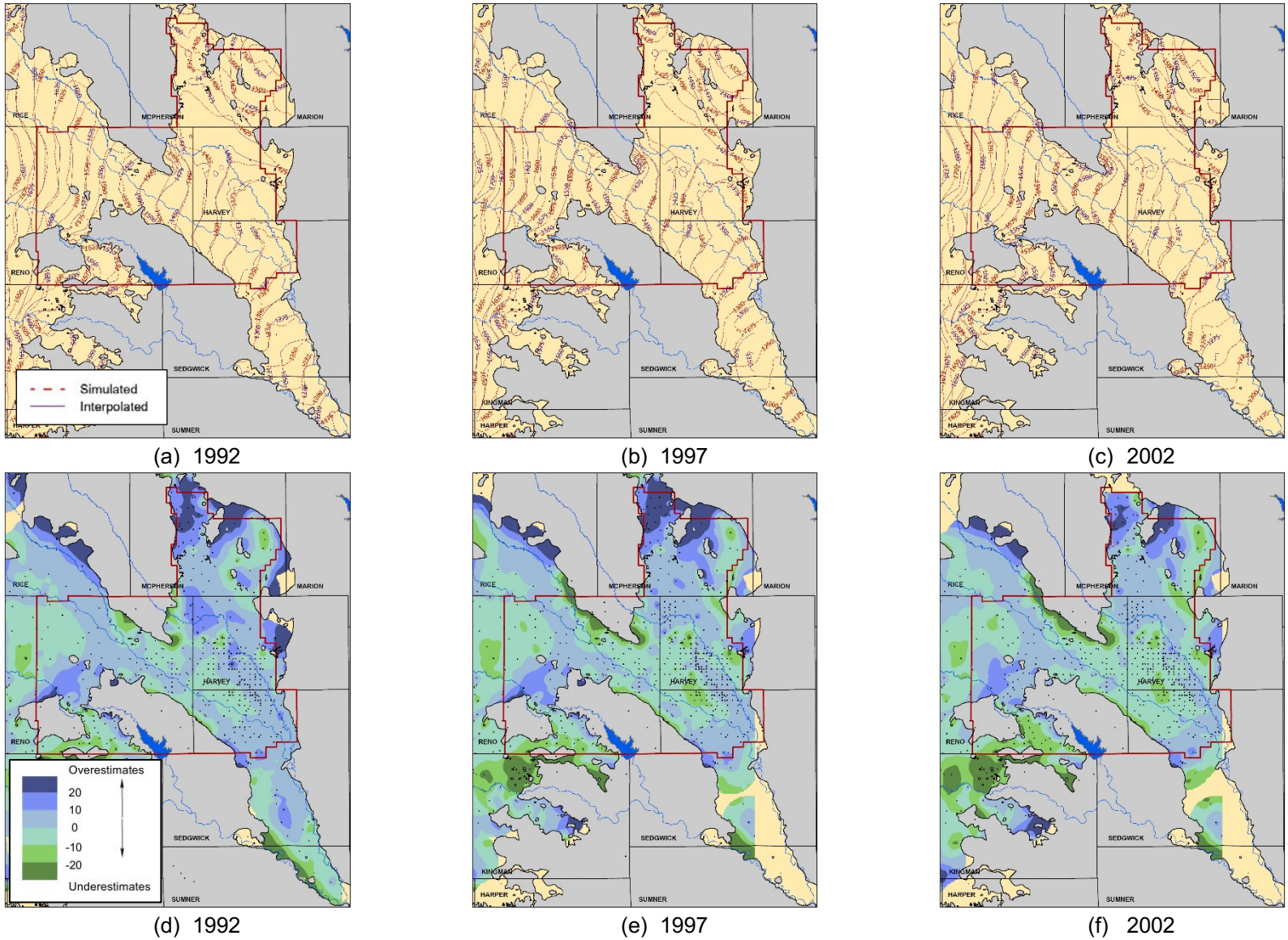

(a) 1992 (b) 1997 (c) 2002

(d) 1992 (e) 1997 (f) 2002

Figure 40. Comparison of simulated versus observed water levels, 1992, 1997, 2002.

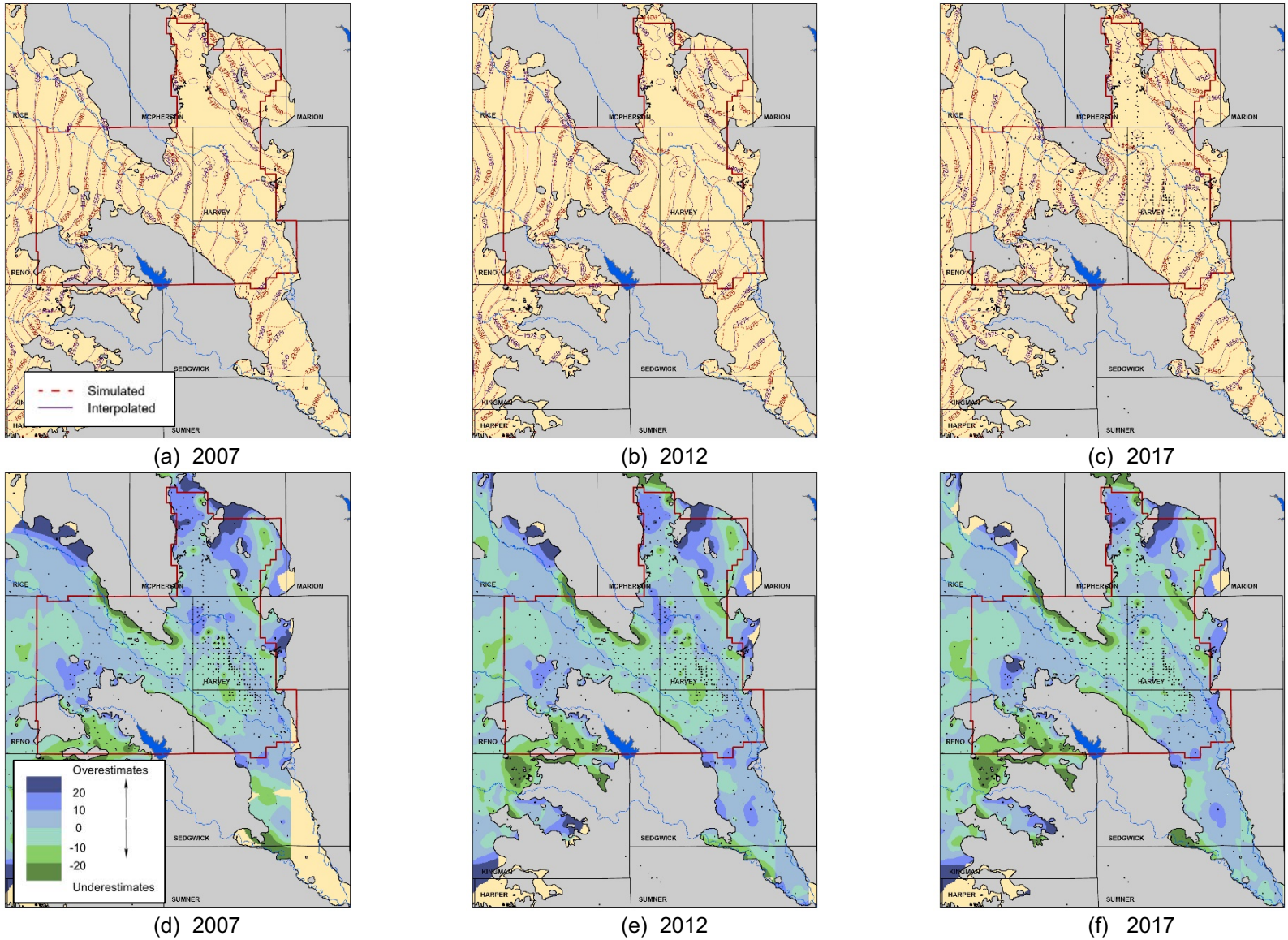

(a) 2007 (b) 2012 (c) 2017

(d) 2007 (e) 2012 (f) 2017

Figure 41. Comparison of simulated versus observed water levels, 2007, 2012, 2017.

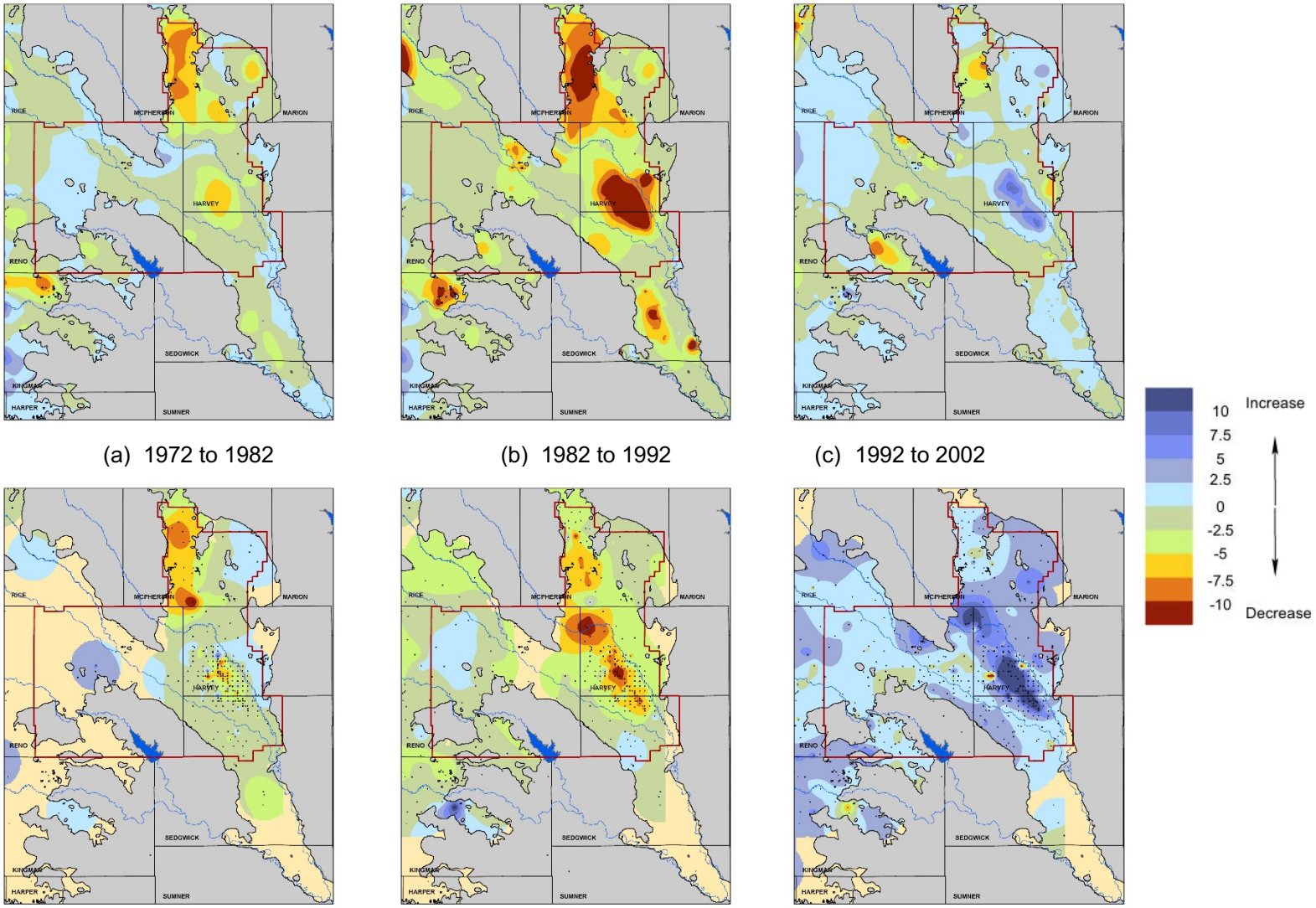

(a) 1972 to 1982 (b) 1982 to 1992 (c) 1992 to 2002

(d) 1972 to 1982 (e) 1982 to 1992 (f) 1992 to 2002

Figure 42. Simulated (top) versus observed (bottom) water-level changes, in feet, for the intervals 1972-1982, 1982-1992, and 1992-2002.

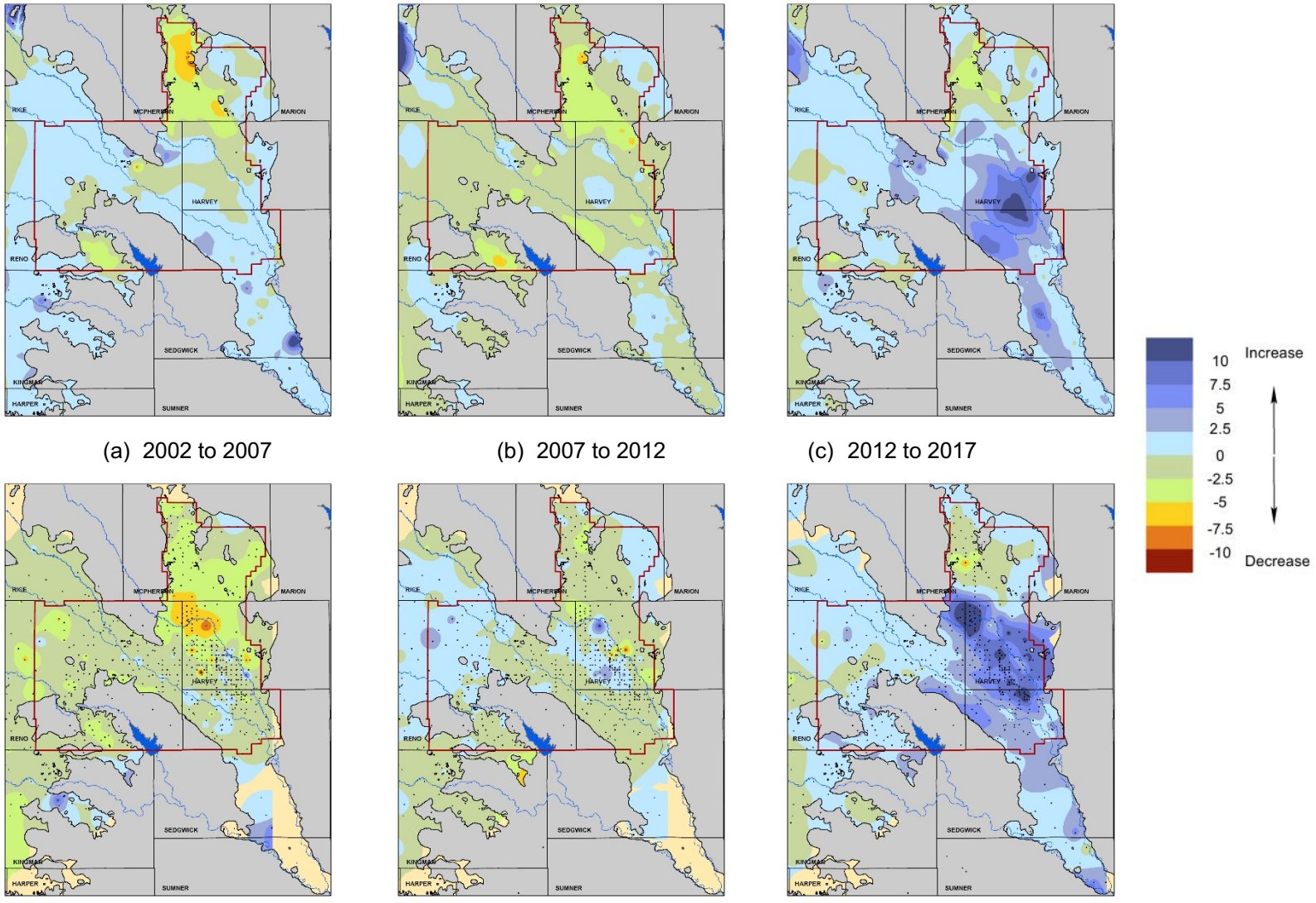

(a) 2002 to 2007 (b) 2007 to 2012 (c) 2012 to 2017

(d) 2002 to 2007 (e) 2007 to 2012 (f) 2012 to 2017

Figure 43. Simulated (top) versus observed (bottom) water-level changes, in feet, for the intervals 2002-2007, 2007-2012, and 2012-2017.

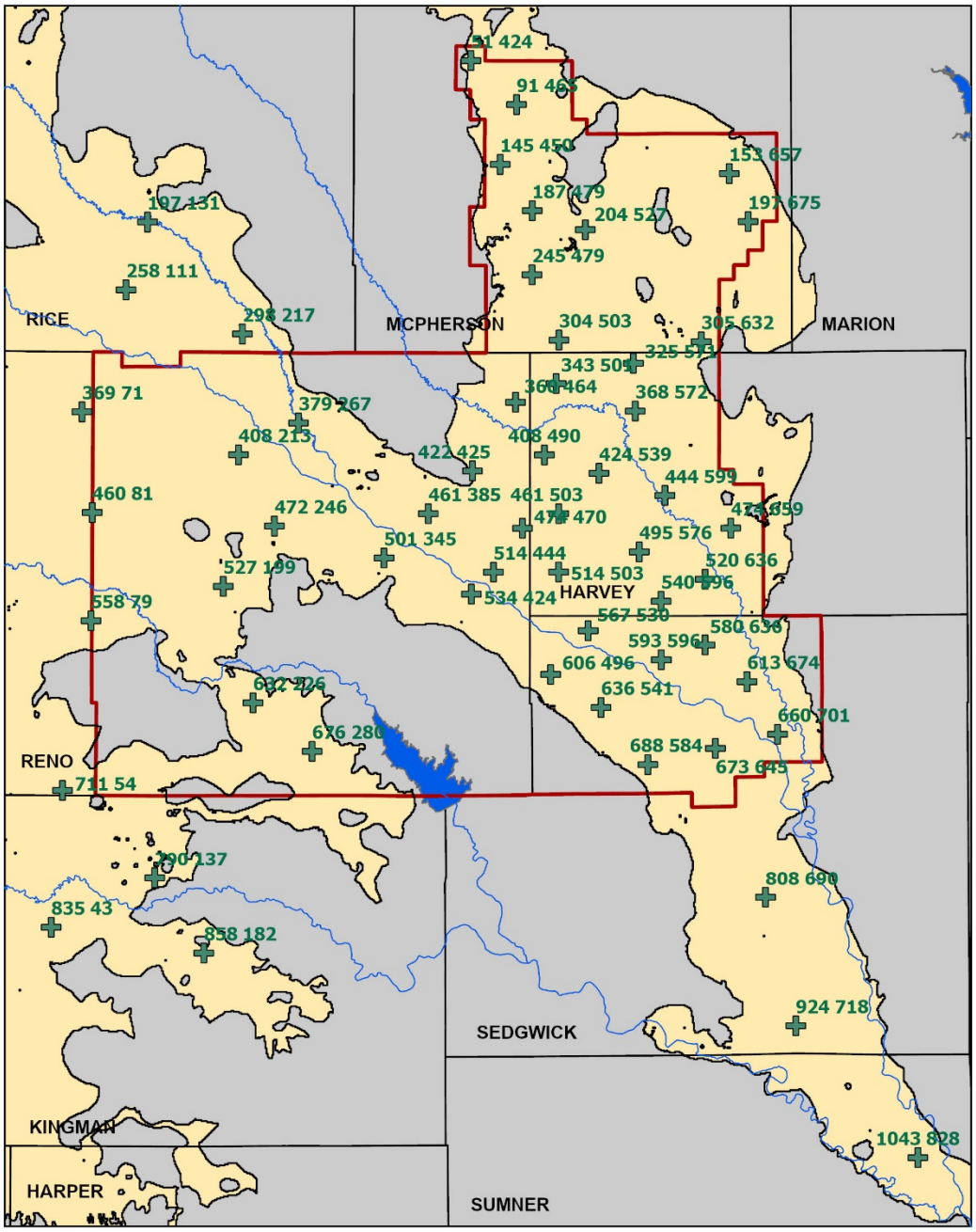

Figure 44. Wells with long-term measurement histories used for model calibration, labeled by row and column of the model cell in which the well is located.

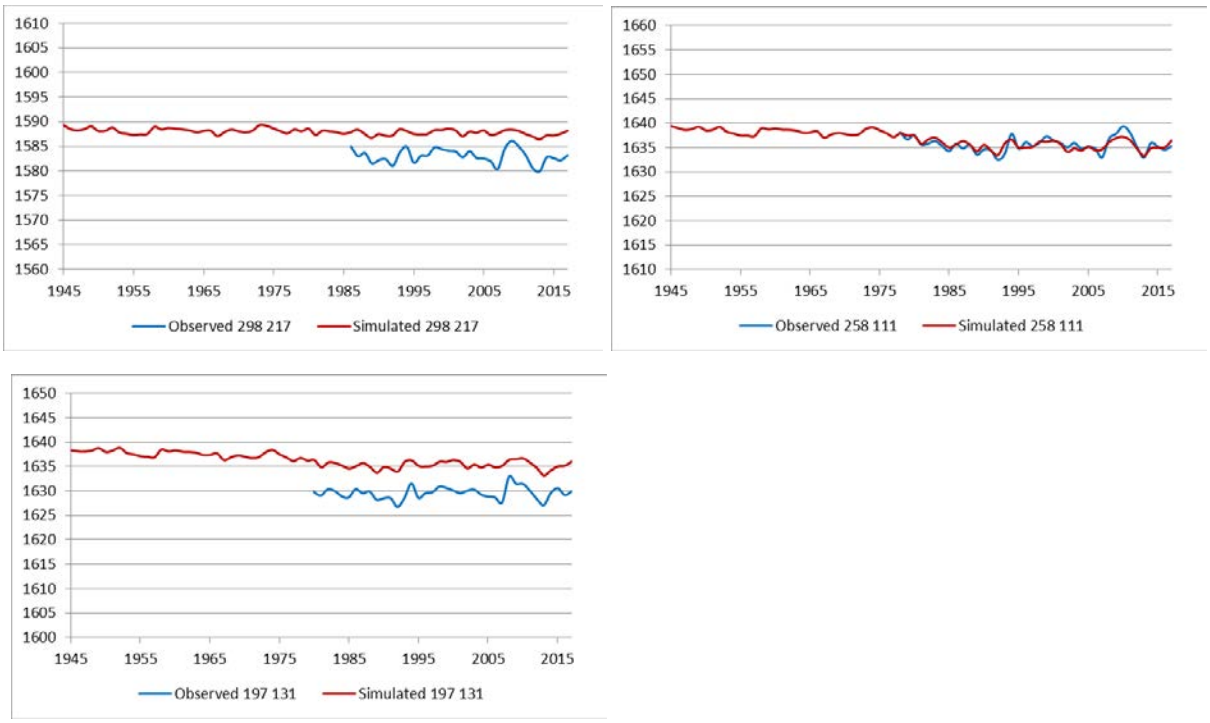

Figure 45. Simulated versus observed well hydrographs, Rice County.

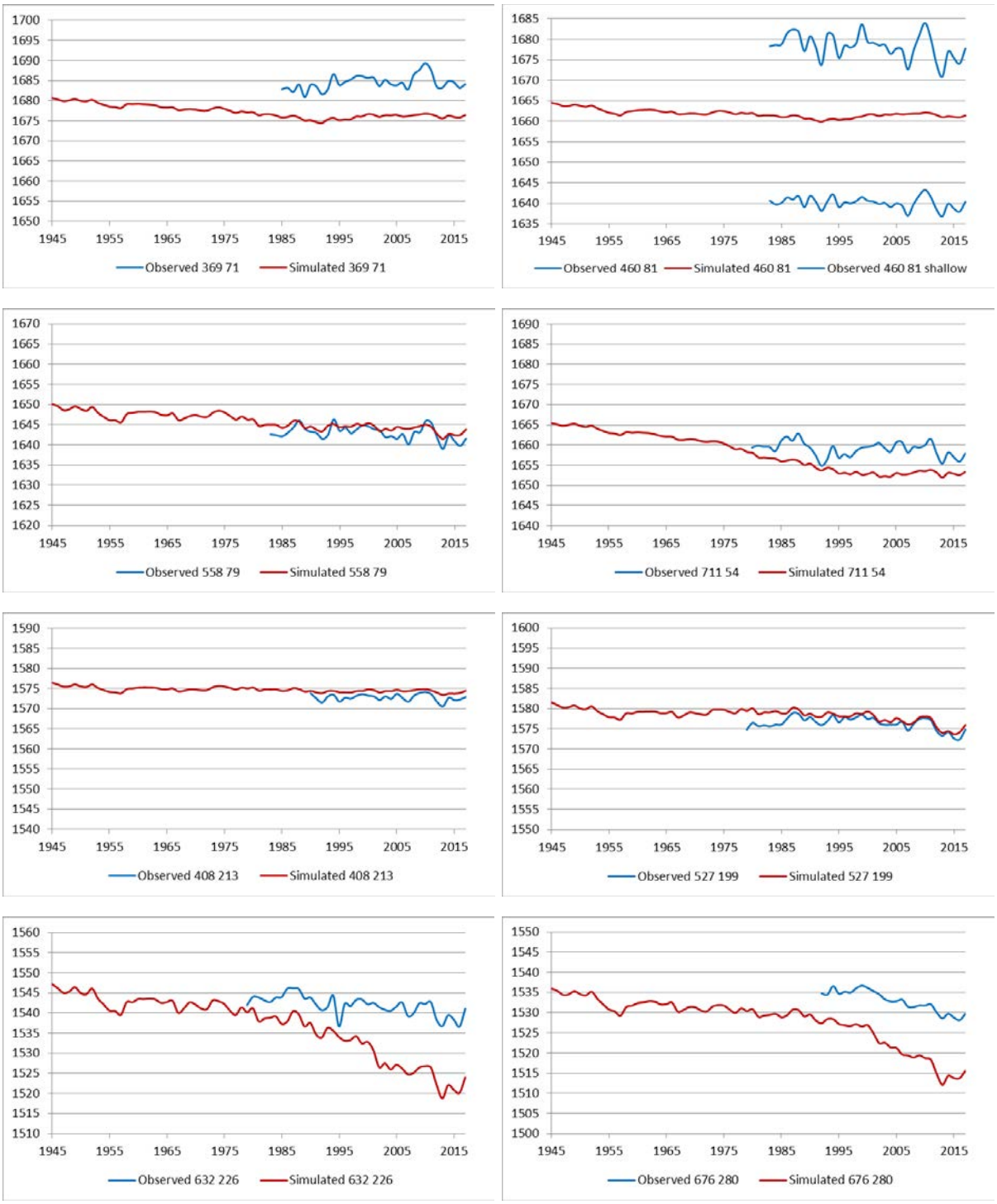

Figure 46. Simulated versus observed well hydrographs, western Reno County. See text for explanation of dual "observed" results for well 460 81 (top right).

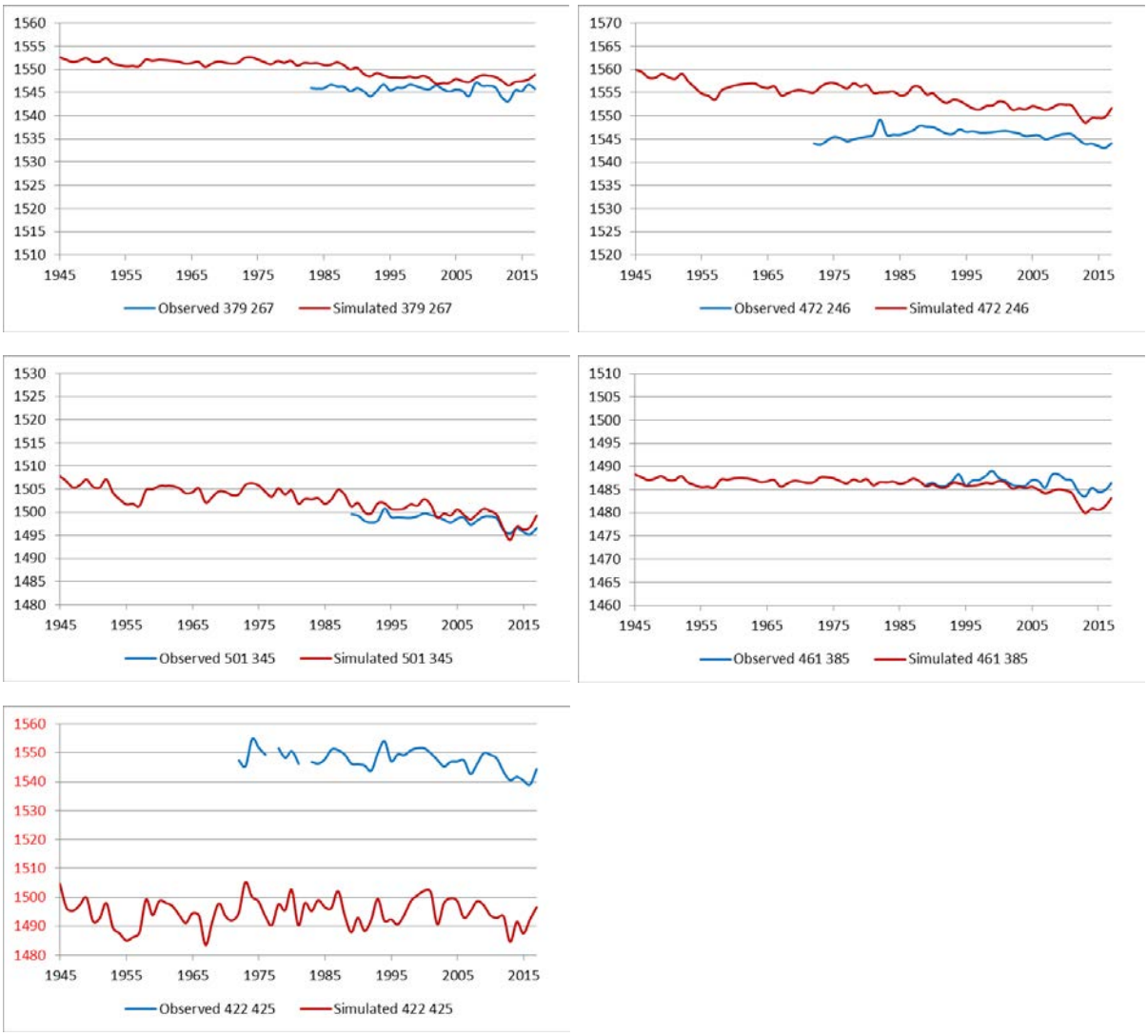

Figure 47. Simulated versus observed well hydrographs, north-central Reno County.

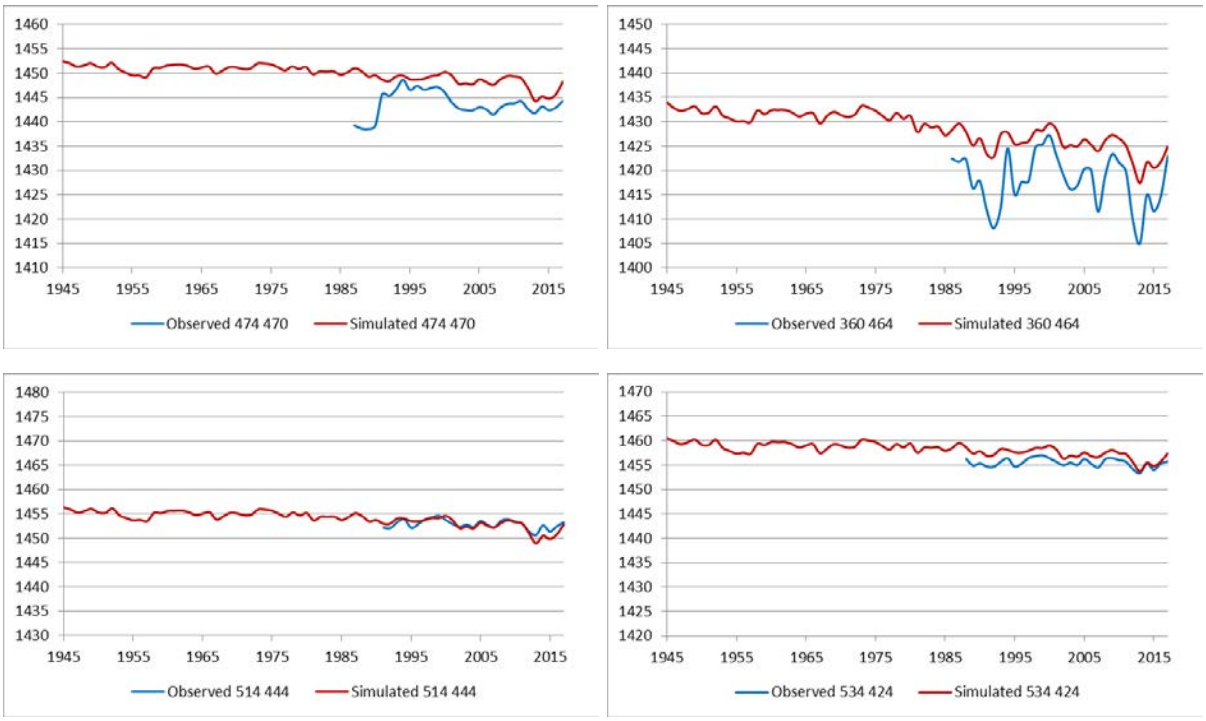

Figure 48. Simulated versus observed well hydrographs, eastern Reno County.

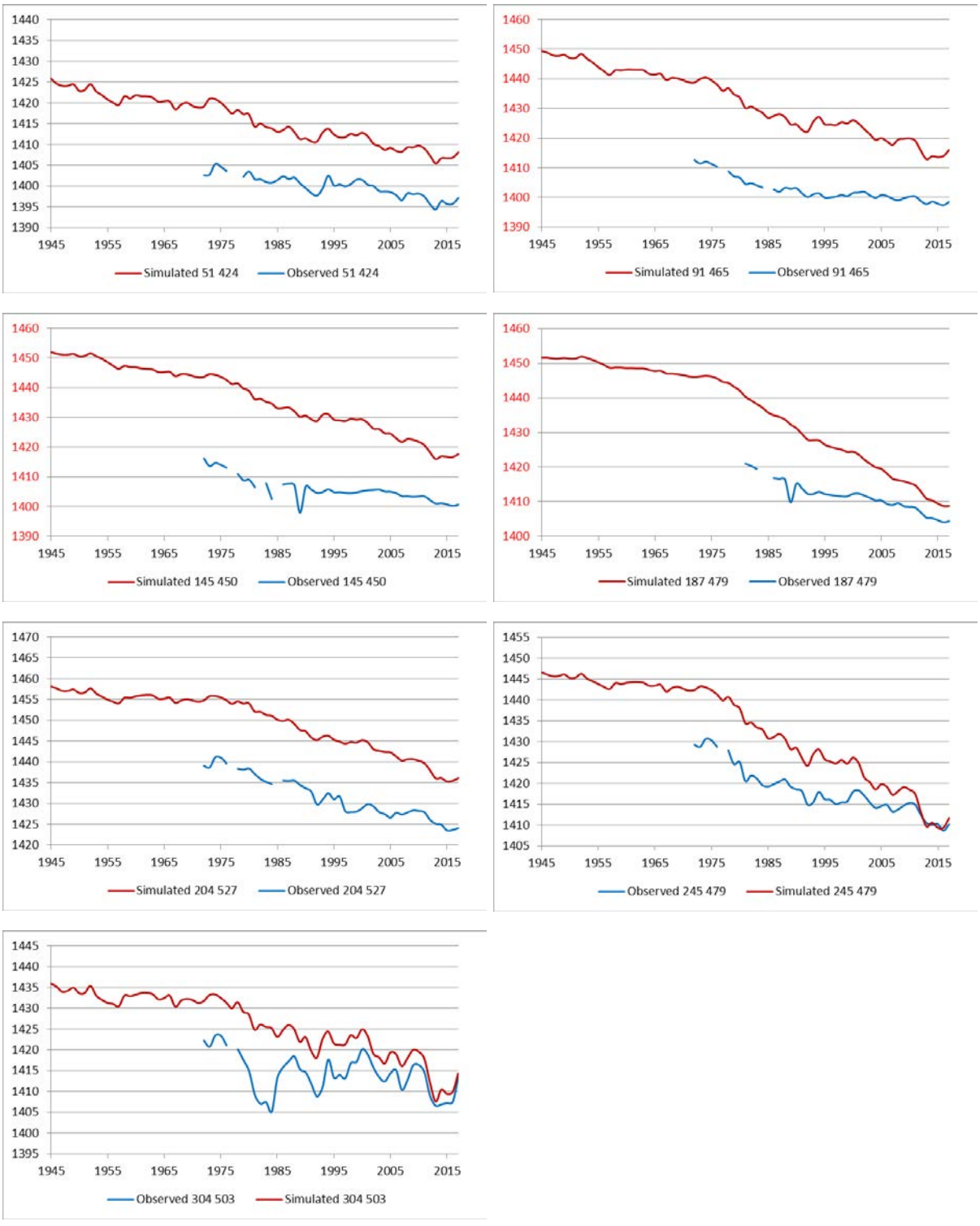

Figure 49. Simulated versus observed well hydrographs, central McPherson County.

Figure 50. Simulated versus observed well hydrographs, eastern McPherson County.

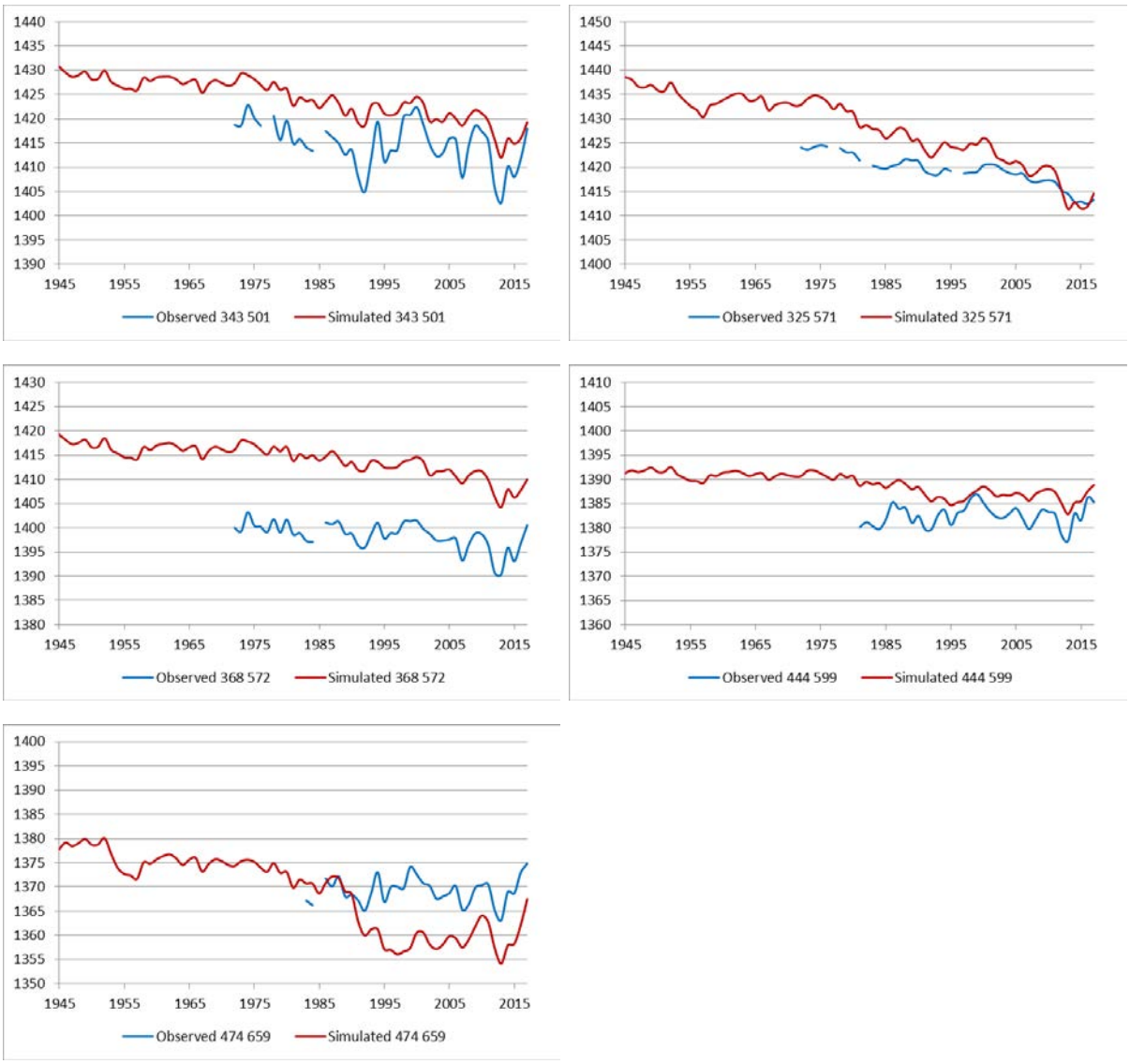

Figure 51. Simulated versus observed well hydrographs, Harvey County, north of the Little Arkansas River.

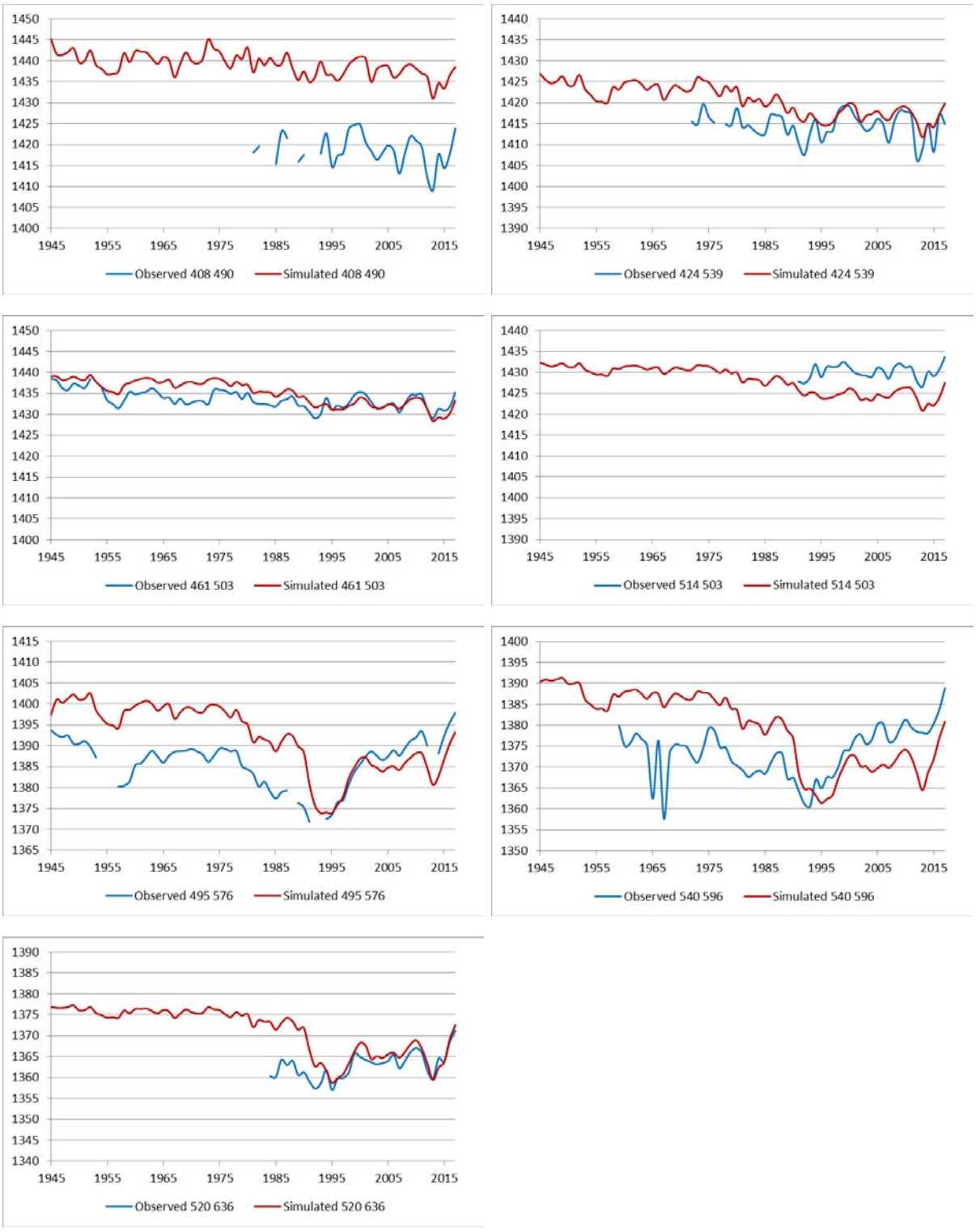

Figure 52. Simulated versus observed well hydrographs, Harvey County, south of the Little Arkansas River.

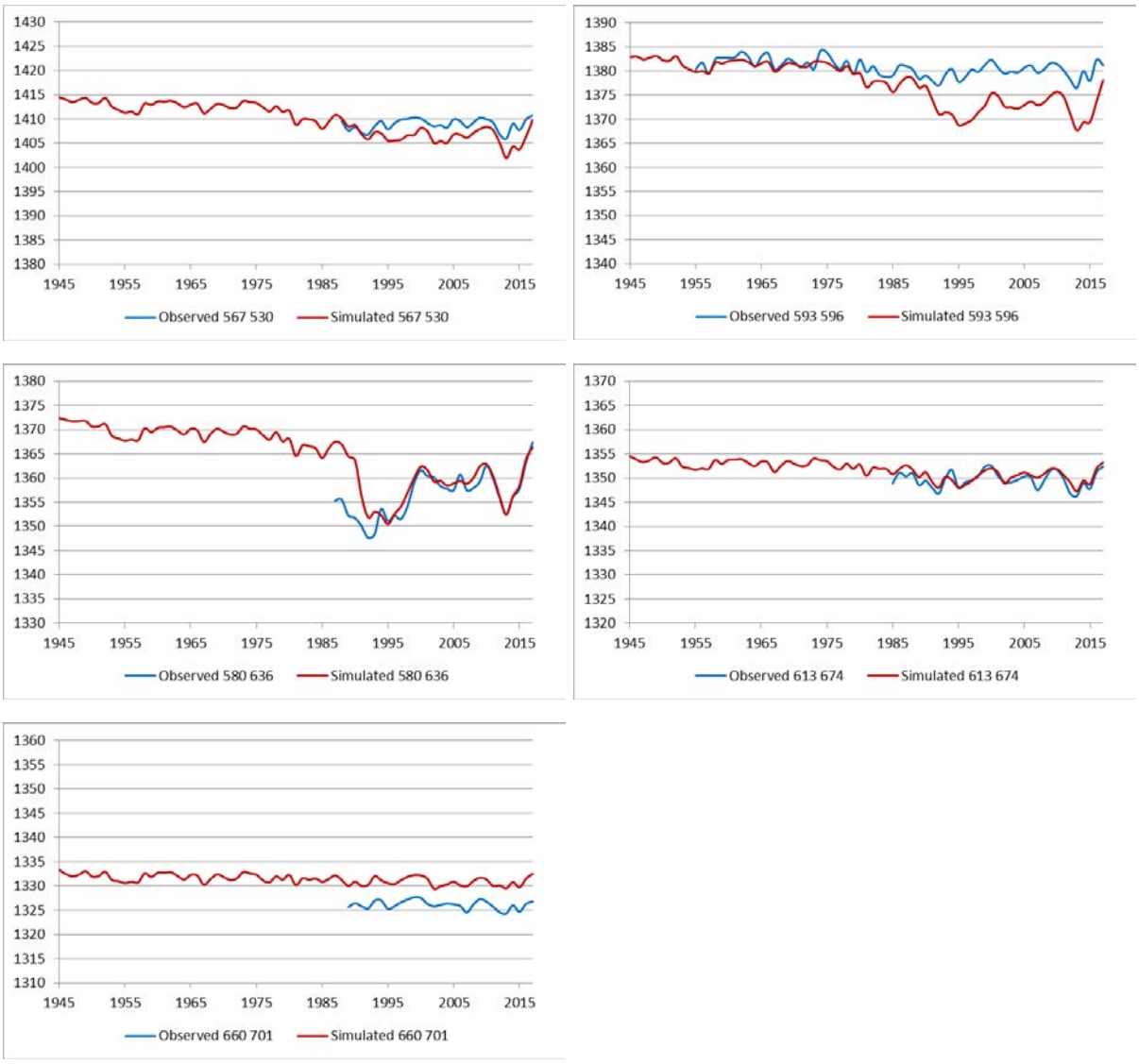

Figure 53. Simulated versus observed well hydrographs, Sedgwick County, north of the Arkansas River.

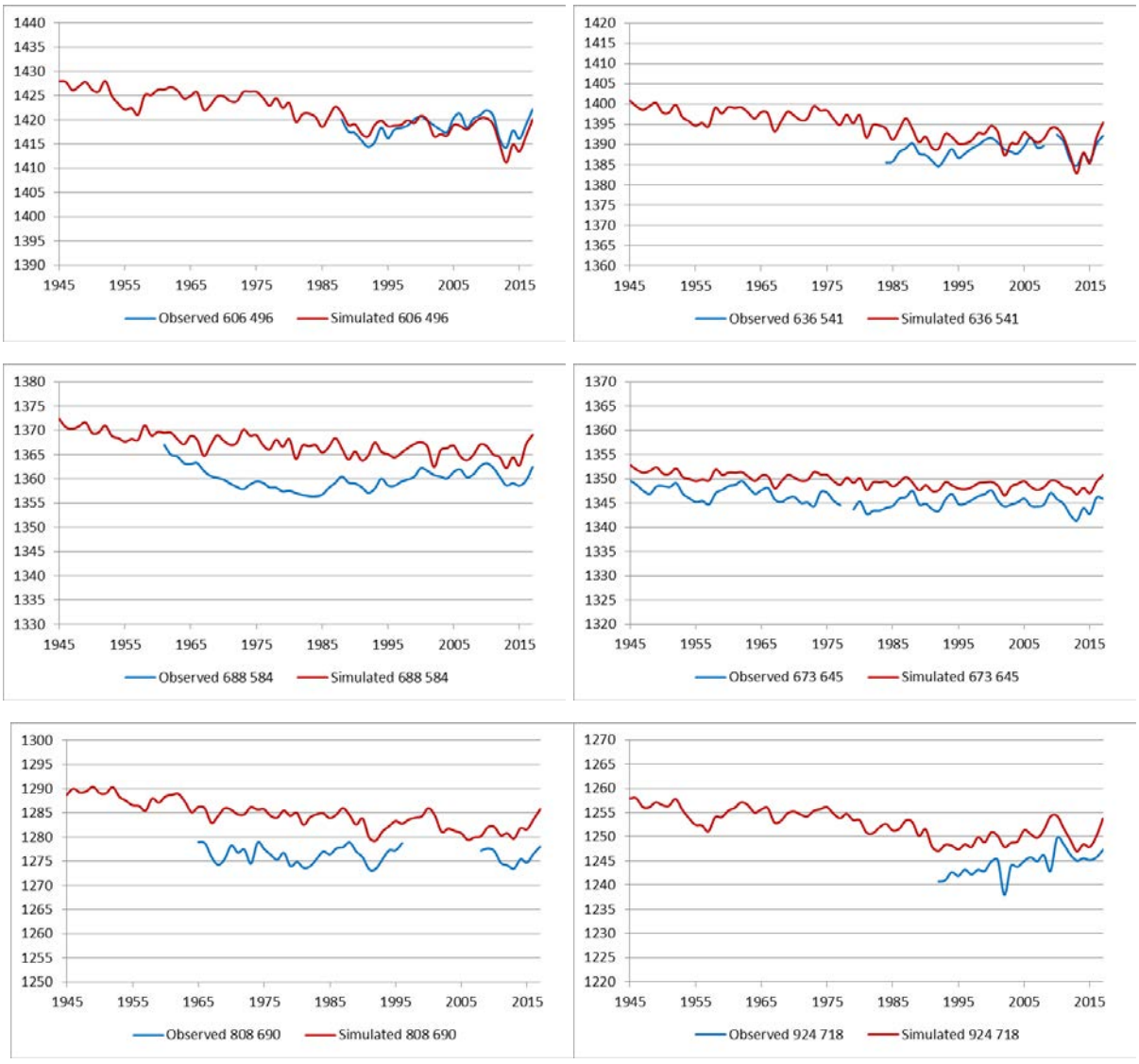

Figure 54. Simulated versus observed well hydrographs, Sedgwick County, south of the Arkansas River.

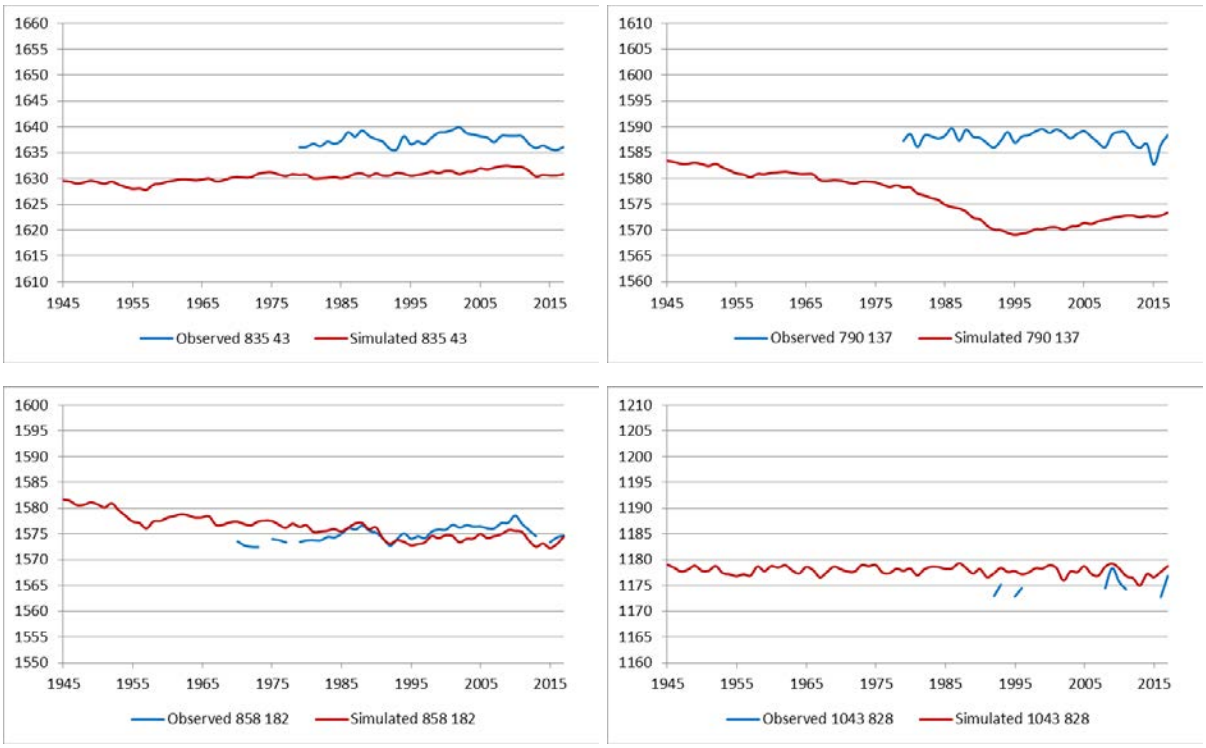

Figure 55. Simulated versus observed well hydrographs, Kingman and Sumner counties.

Figure 56. Simulated versus observed streamflows.

Model Budgets

Figure 57 shows the groundwater budget for the entire model over the transient period, including the net storage, flow across head boundaries, well pumping, evapotranspiration loss, total areal recharge, drain cell loss, and stream leakage. Positive values indicate inflows of water to the aquifer system (recharge and lateral flow from the head boundaries), and negative values indicate outflows from the aquifer.

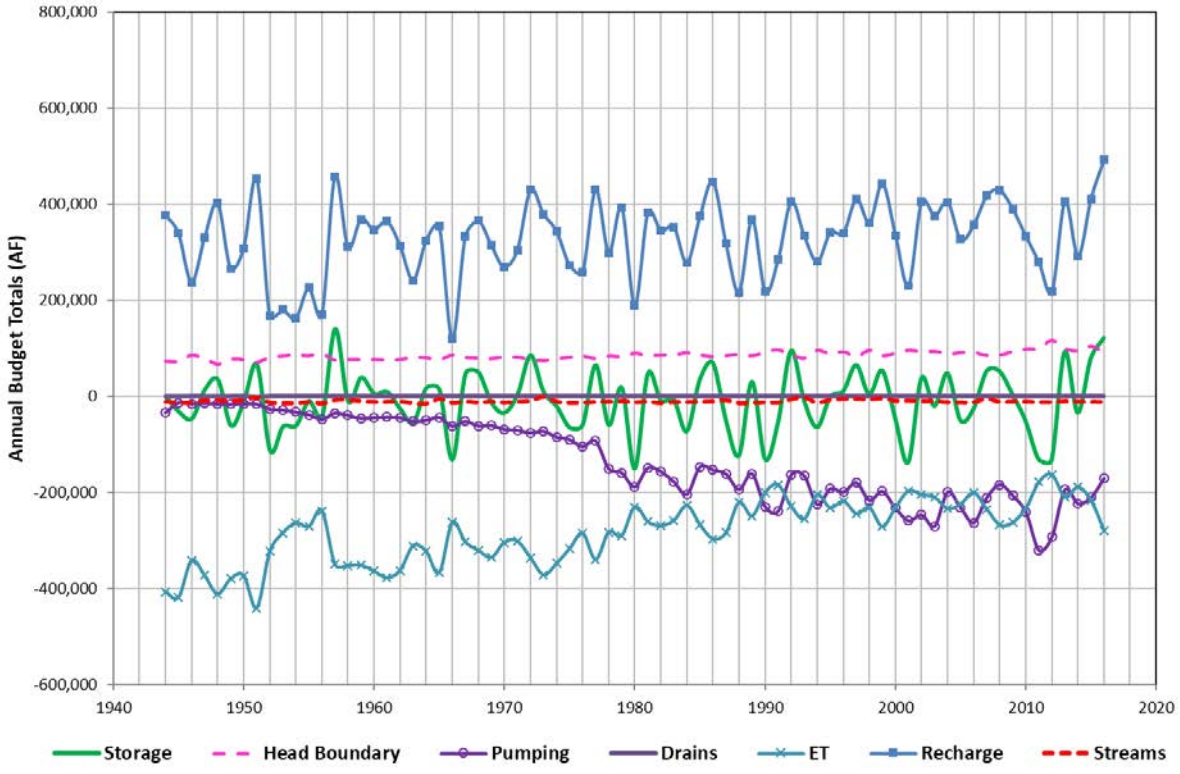

Figure 57. Annual aquifer budget components from the calibrated model.

Recharge is the largest component of inflows to the aquifer and represents the sum of precipitation-based recharge and irrigation return flows. Precipitation recharge is generated by the recharge curves described earlier in this report (fig. 35) and represents the amount of new water entering the aquifer. Recharge from irrigation return flows represents the amount of pumped irrigation water that infiltrates past the root zone of the irrigated crops, eventually reaching the water table. Groundwater pumping and evapotranspiration represent the largest outflows from the aquifer. Lateral flow of groundwater in and out of the model (head boundary component of the budget) is positive, indicating that more groundwater has been flowing into the model area than flowing out. The largest volume of water enters the model through the western head boundaries. Water flows laterally following the general northwest-to-southeast gradient of the Arkansas River valley. In McPherson County, groundwater generally flows to the south except in the very northern area of GMD2, where it flows to the north. The negative values of stream-aquifer interactions indicate that the aquifer is discharging water into the streams, although the amount of the discharge is small. Very little water leaves the aquifer via drains.

Comparison with Sustainability Assessment, KGS OFR 2017-3

Figure 58 shows the model-simulated net inflow for selected townships, and fig. 59 shows the net inflows for the same townships calculated by Butler et al. (2017) based on water-level and water-use data. As discussed in Butler et al. (2017), net inflow is defined by the summation of all aquifer budget components except pumping and represents the maximum amount of pumping the aquifer can sustain without any water-level decline. Overall, the simulated net inflows show a good agreement with the data-based calculations. The most significant differences are found in T. 20 S., R. 03 W. in McPherson County, where the net inflow of the data-based approach is 5,785 AF/yr while the simulated value is 3,517 AF/yr, and in T. 26 S., R. 06 W. in Reno County, where the net inflow from the data-based approach is 4,907 AF/yr while the simulated value is 2,767 AF/yr. In both cases, the proximity to assumed no-flow boundaries is likely the reason for the smaller simulated values. The overall consistency between the model results and the data-based net inflow calculations shows that the model provides a good representation of aquifer conditions and can be used as an effective tool for resources management by the district.

Figure 60 shows the model's average annual precipitation recharge over 2005–2014 for different townships. In the core aquifer area through the Arkansas River valley, recharge is the highest due to large precipitation rates and high infiltration capacity of the soils above the water table (the recharge curves for the sand hills and alluvium zones are above those for other areas shown in fig. 35).

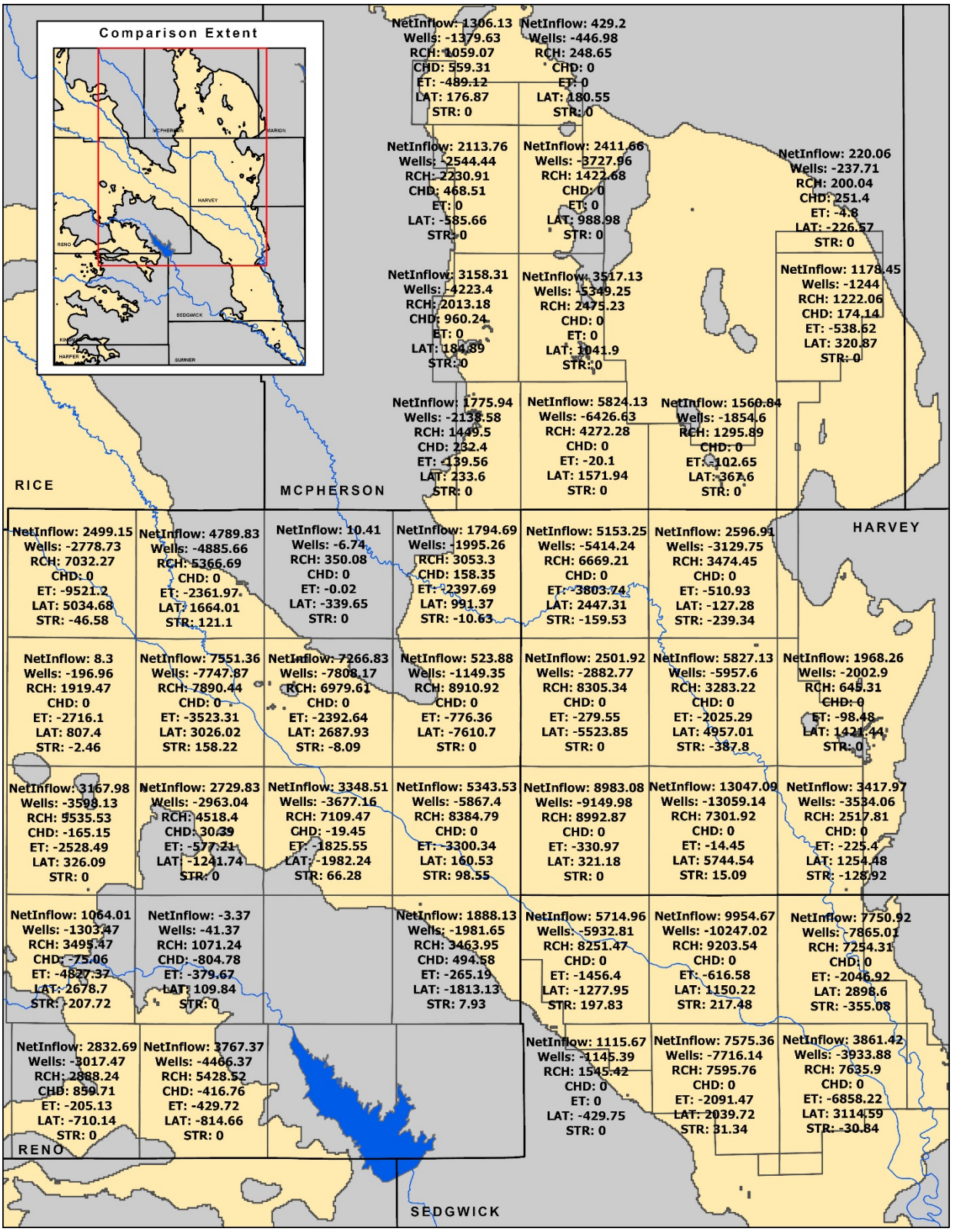

Figure 58. Model-simulated net inflow and other aquifer budget components for selected townships. RCH = surface recharge, CHD = specified head boundaries, ET = Evapotranspiration, LAT = lateral flow, and STR = stream/aquifer interactions.

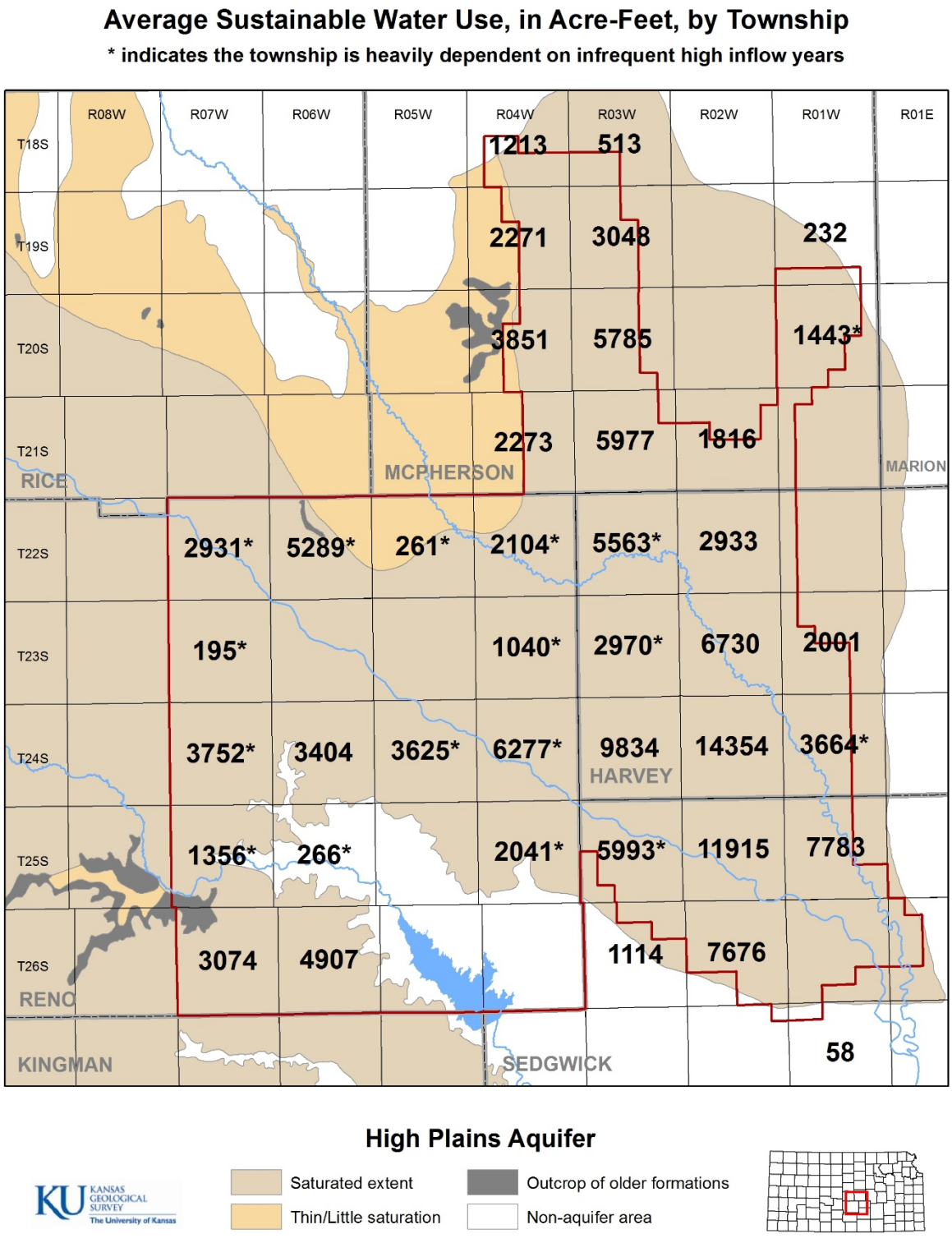

Figure 59. Net inflow computed for different GMD2 townships by Butler et al. (2017). Results are based on 2005–2014 water-level and water-use data.

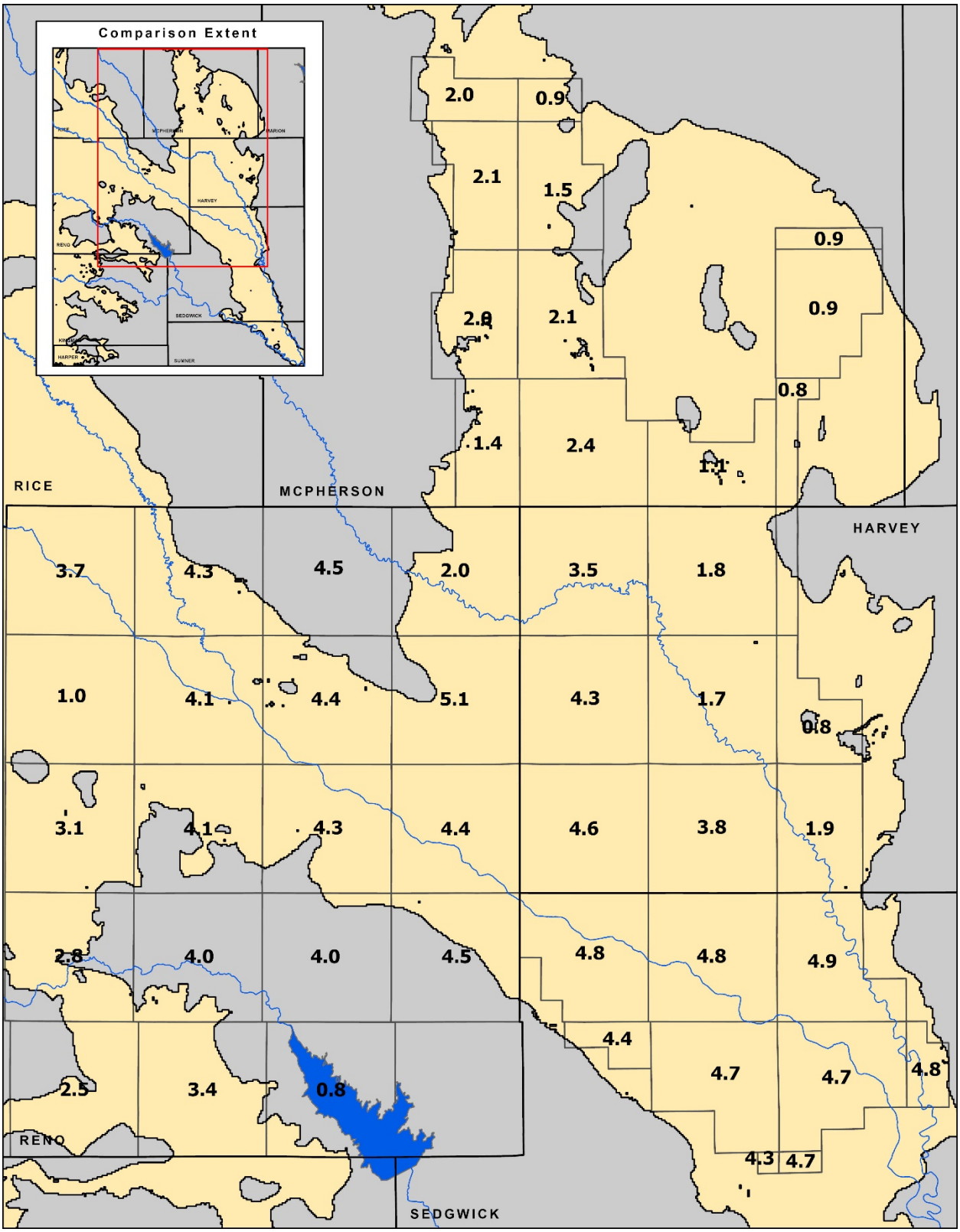

Figure 60. The annual precipitation recharge averaged over 2005-2014 from the calibrated model.

MODEL SCENARIOS

One of the important uses of a calibrated groundwater model is to assess the future responses of an aquifer to different water resources management and climatic scenarios. Three basic scenarios were considered in this study:

1) No change in water-use policy
2) Enhancing extreme wet and dry climatic events
3) Reoccurring droughts

In all three scenarios, the calibrated model is run from 2017 to 2088 with some type of repeat or modification of the 1945 to 2016 climatic conditions. Irrigation system types are assumed to be the same as for 2016. For the specified head boundaries, the water level for 2016 is used for all different future years as there has been no significant change in the boundary heads between predevelopment and 2016.

The first scenario assumes there is no change in the water-use policy and future pumping is driven by current (2016) water-right demands. In the second scenario, extreme climatic events, defined here as those precipitation events that are one standard deviation away from the mean over the model's transient period, are enhanced by 20 percent, dryer or wetter. In the third scenario, reoccurring droughts are simulated by repeating the climatic conditions from 1951 to 1960 continuously through the future simulation.

Scenario 1: No Change in Water-Use Policy

This scenario uses the regression equation determined in the transient model calibration to compute the ratio of water use/authorized quantity, assuming there is no change in future water-use policy. For a given future year, the ratio, which is dependent on summer precipitation, is converted into the actual water-use demand by multiplying it by the present day (2016) authorized quantity.

Figure 61 shows the annual aquifer budget for scenario 1. Groundwater pumping and evapotranspiration are the two largest discharges from the aquifer and remain relatively constant with annual variations dictated by the summer precipitation patterns. As in the transient phase, recharge continues to be the largest component of inflows to the aquifer and represents the sum of precipitation-based recharge and irrigation return flows. The modeled areas also gain water from lateral flow across head boundaries with most of that coming in along the western edge of the model domain. Baseflow contributions from the aquifer to streams through stream/aquifer interactions account for a small portion of the budget. The overall annual changes in aquifer storage fluctuate between a losing and gaining system and are highly dependent on precipitation patterns, which, in turn, determine the pumping demands, ET, and recharge.

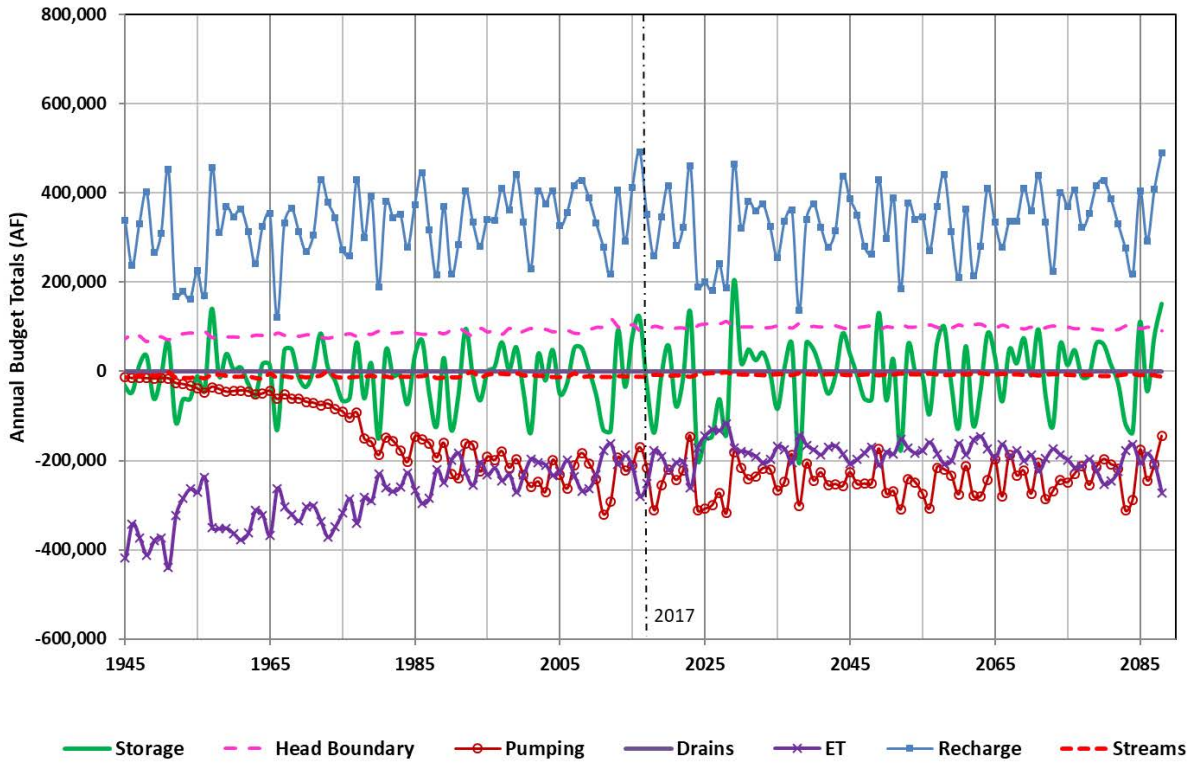

Figure 61. Annual aquifer budget for the scenario 1 (no change in future water use). The calibrated model budget (1945 to 2016) is also plotted for comparison.

Figure 62 shows simulated head changes for selected intervals for the no change in future water use scenario. The effect of a repeat of the 1950s drought can clearly be seen as water levels drop significantly across the core areas of GMD2 from 2020 to 2030. The average simulated water-level change for GMD2 during that period is a decline of 6.35 feet with much of southwest Harvey and southern McPherson counties averaging declines of 10 to 20 feet. As shown by the changes in storage from fig. 61, future water levels fluctuate up and down in response to ever-changing precipitation patterns.

.

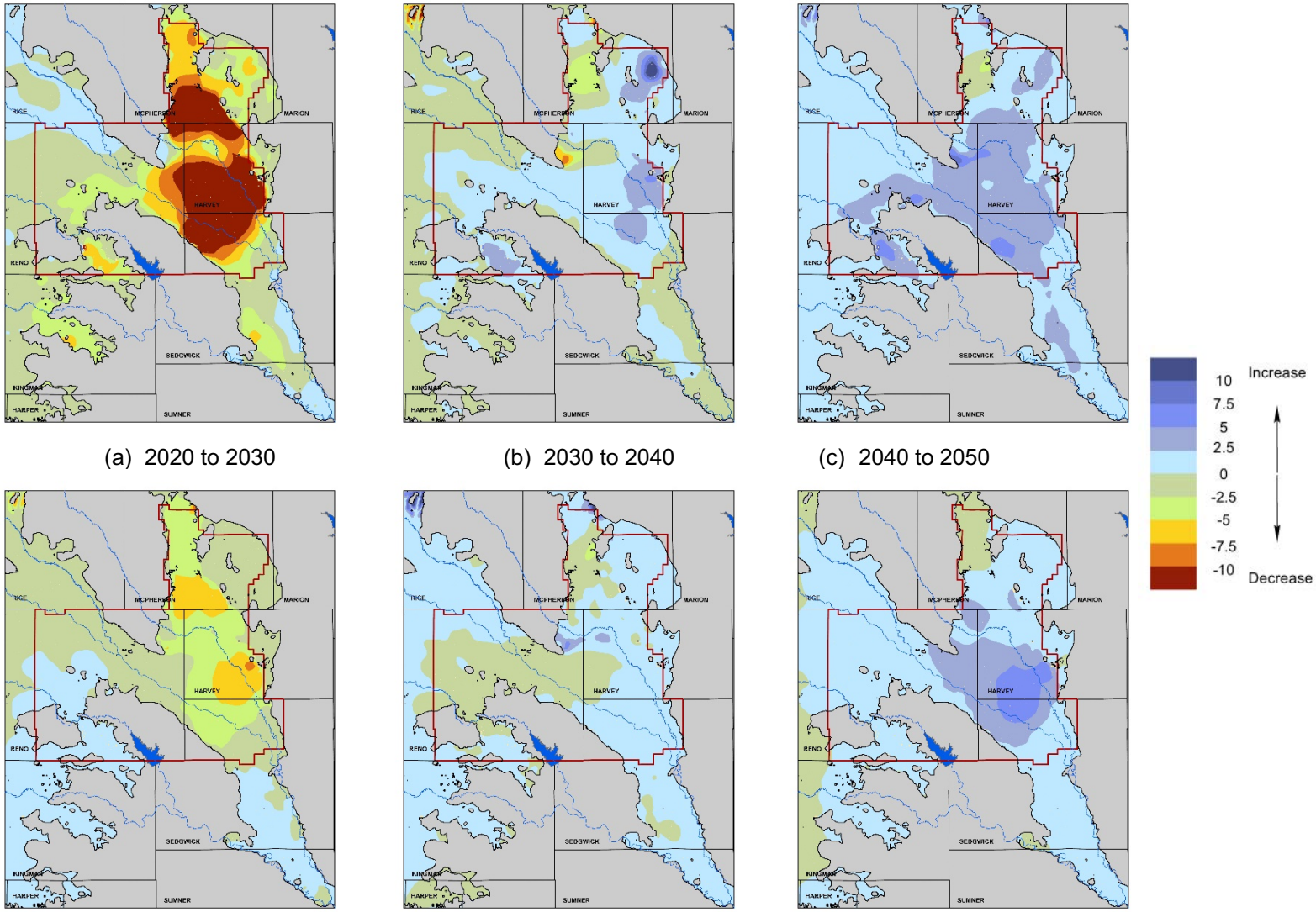

(a) 2020 to 2030 (b) 2030 to 2040 (c) 2040 to 2050

(d) 2050 to 2060 (e) 2060 to 2070 (f) 2070 to 2080

Figure 62. Simulated water-level change, in feet, for scenario 1.

Scenario 2: Enhancing Extreme Wet and Dry Climatic Events

In this scenario, extreme precipitation events, both wet and dry, are further enhanced while keeping the overall average precipitation the same. Extreme events are defined as those summer precipitation totals that are more than one standard deviation away from the mean. For this simulation, summer precipitation totals are increased or decreased by 20% if they are plus or minus 6.53 inches from 21.71 inches, which is the mean summer precipitation for pumping cells from 1945 to 2016.

Figure 63 shows the annual aquifer budget for the enhanced extreme wet and dry climatic events scenario. The subtle changes in the precipitation totals during significant wet and dry events are reflective in both the annual pumping and recharge totals. Under the driest conditions, pumping totals are slightly greater and recharge slightly less in comparison to scenario 1, while the reverse is true during exceptionally high precipitation events.

Figure 64 displays the simulated water-level changes at selected year intervals for the extreme wet and dry climatic events scenario. In comparison to scenario 1, the effects of significant wet and dry events illustrate that, overall, the aquifer gains more water from the additional aquifer recharge that occurs from enhanced wet conditions than it loses from the additional pumping that occurs from the enhanced dry conditions. Even the average groundwater declines in GMD2 during the 2020 to 2030 period (5.93 ft), which replicates the 1950 drought conditions, are less than in the no-change scenario (6.35 ft).

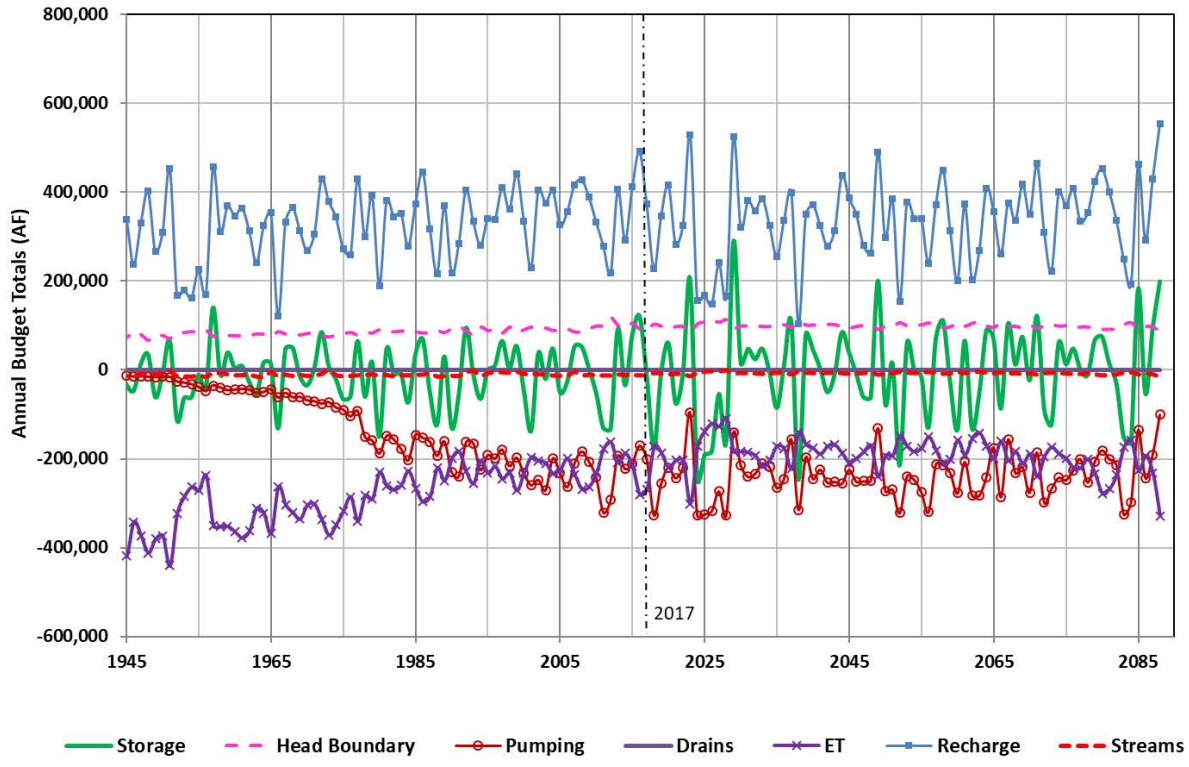

Figure 63. Annual aquifer budget for scenario 2 (extreme wet and dry climatic events). The calibrated model budget (1945 to 2016) is also plotted for comparison.

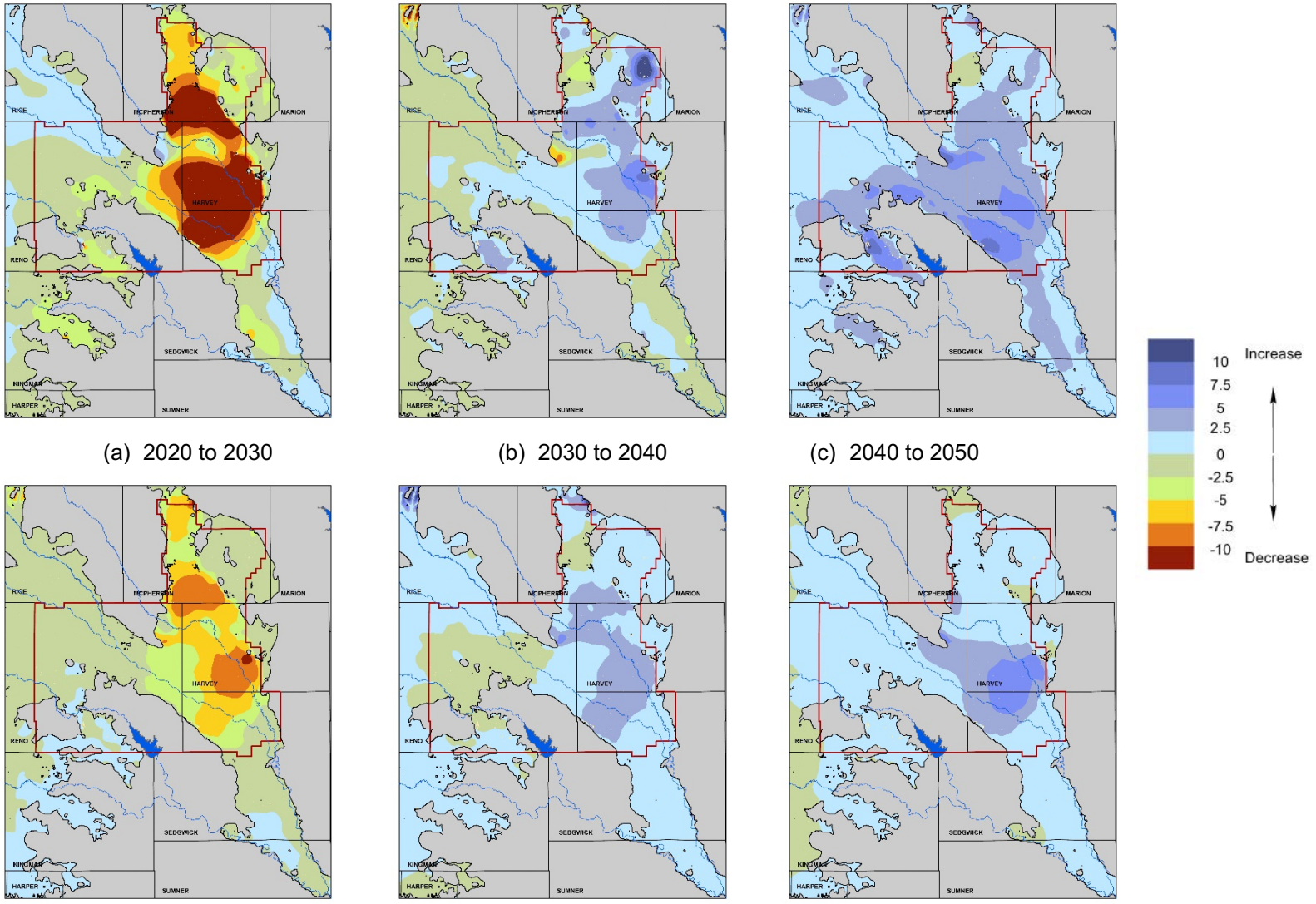

(a) 2020 to 2030 (b) 2030 to 2040 (c) 2040 to 2050

(d) 2050 to 2060 (e) 2060 to 2070 (f) 2070 to 2080

Figure 64. Simulated water-level change, in feet, for scenario 2

Scenario 3: Reoccurring Droughts

The multi-year drought that dominated the 1950s is considered the drought of record for several Kansas water-management policies and programs. This scenario continuously repeats the precipitation patterns from 1951 to 1960 into the future to simulate reoccurring drought conditions. As can be seen by the annual aquifer budget (fig. 65), the prolonged dry conditions keep pumping demands near maximum levels while aquifer recharge is consistently low relative to the two other scenarios. The repeated above-normal precipitation events that happen in 1951 and again in 1958 serve to recharge the aquifer. Despite that, however, the aquifer loses much more water than it gains over the entire simulated period. This is reflected in fig. 66, which shows the simulated head changes at selected intervals for the reoccurring drought scenario. Even though the timing of the drought in the first 2020–2030 interval results in less drawdown than in scenario 1, the higher pumping demands combined with lower recharge volumes keep most of the aquifer in a state of decline across all periods.

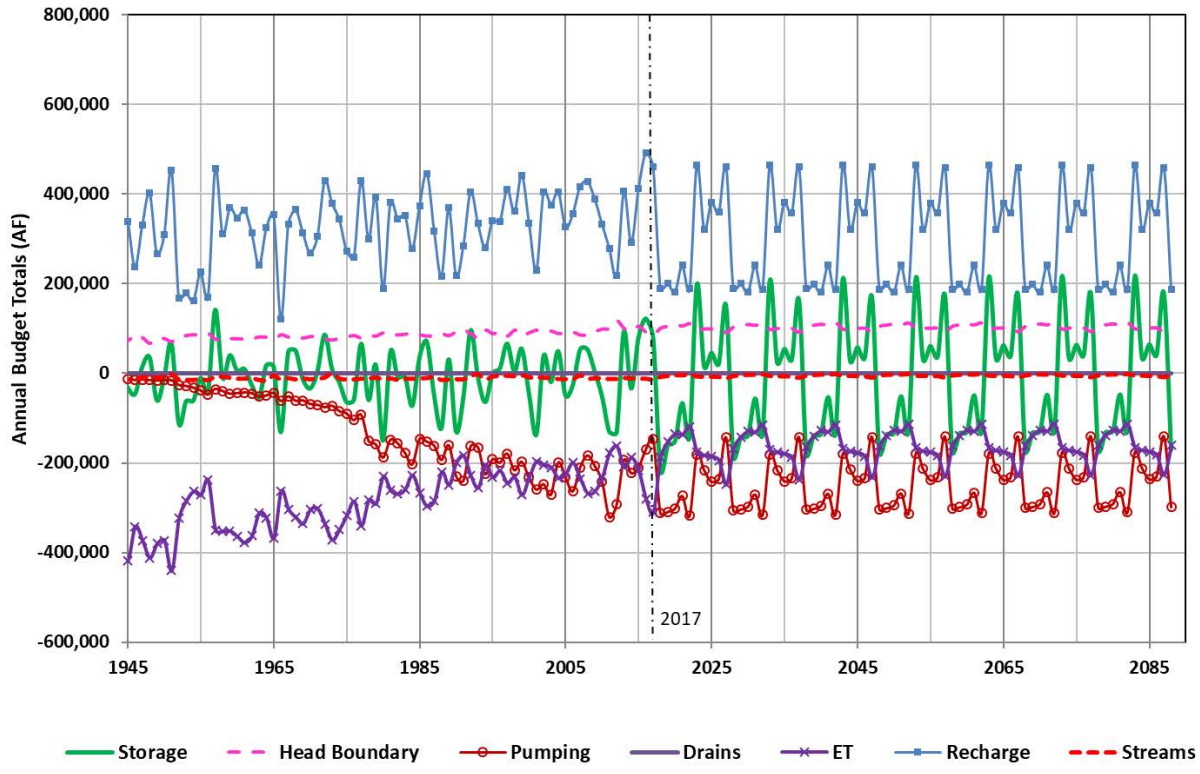

Figure 65. Annual aquifer budget for scenario 3 (reoccurring droughts). The calibrated model budget (1945 to 2016) is also plotted for comparison.

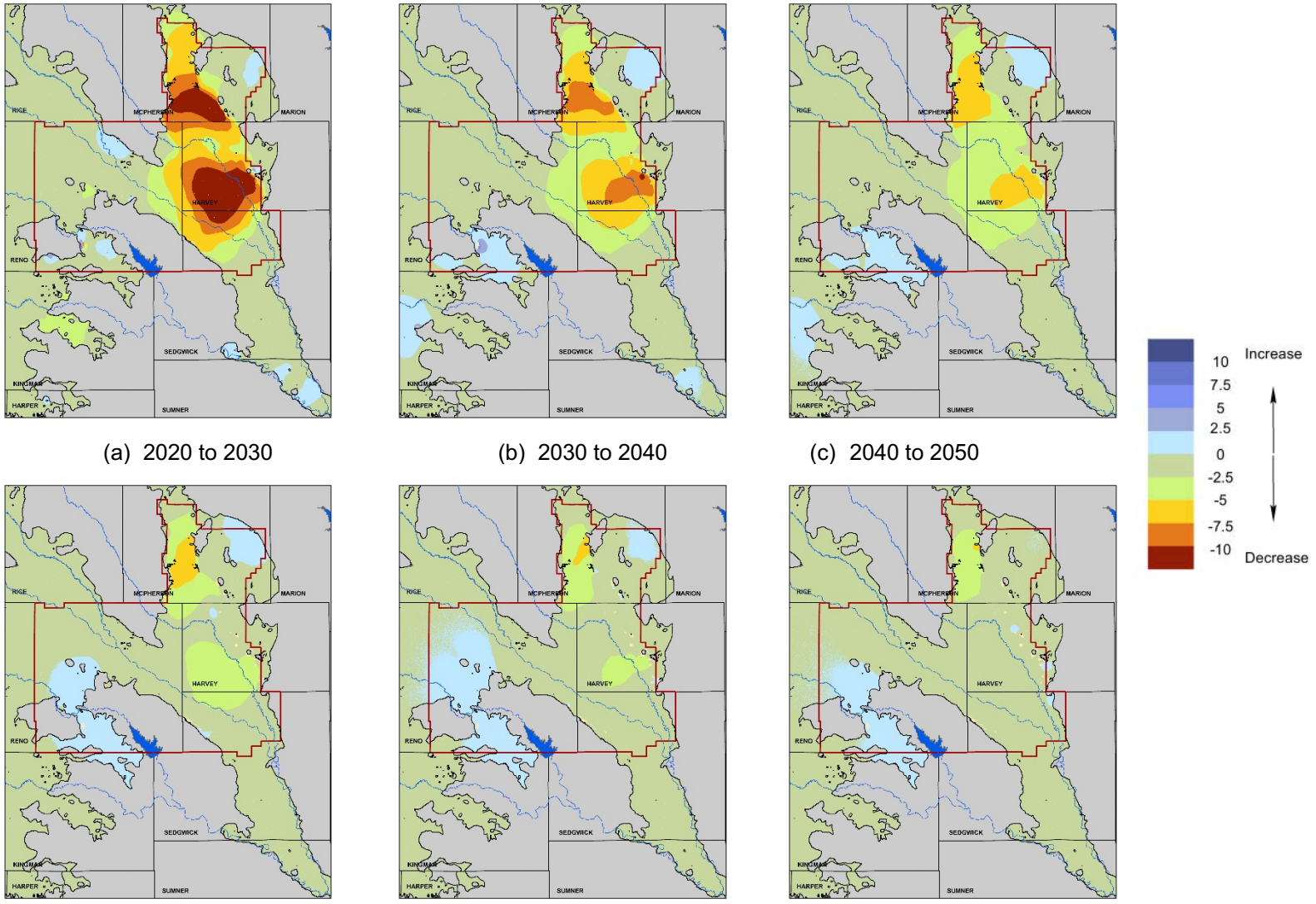

(a) 2020 to 2030 (b) 2030 to 2040 (c) 2040 to 2050

(d) 2050 to 2060 (e) 2060 to 2070 (f) 2070 to 2080

Figure 66. Simulated water-level change, in feet, for scenario 3.

Comparison of All Scenarios

Figure 67 shows the accumulated simulated change in storage among the three scenarios. The most drastic effect on the aquifer occurs in scenario 3 (reoccurring 1950 drought conditions), where, overall, water levels are clearly trending down. However, even under these simulated harsh conditions, the aquifer has periods of recharge. The importance of these recharge events are further illustrated in scenario 2, where the extreme precipitation events are enhanced by 20%. The aquifer still gains more water over the simulated period in comparison to scenario 1 (no change in water-use policy). This echoes findings from Butler et al. (2017) on the importance of periodic large recharge events to recharge and stabilize the Equus Beds. Without those events, the aquifer will struggle to recover from significant drought conditions under present-day water-right demands.

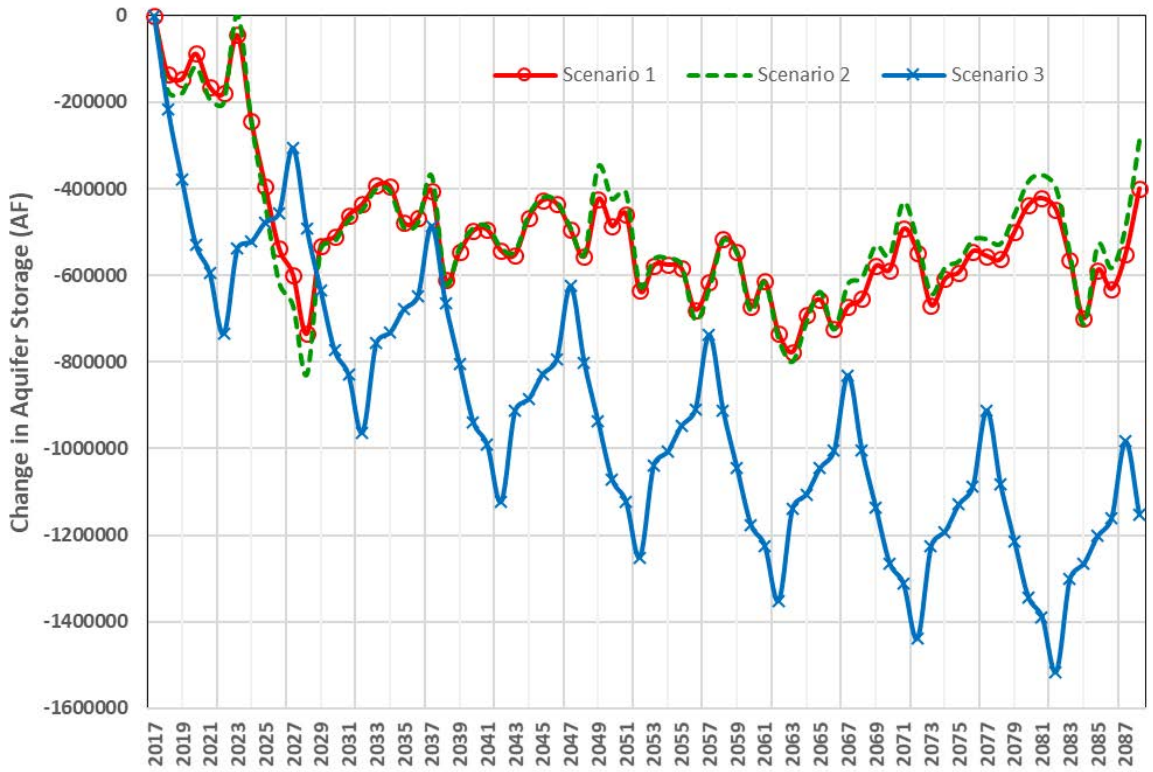

Figure 67. Accumulated change in GMD2 aquifer storage for all three future scenarios.

Figures 68 and 69 compare the simulated, accumulated water-level change, in feet, from 2020 to 2080 for the three scenarios. The effect of repeating the 1950s drought at the start of each scenario is significant. However, for scenarios 1 and 2, most of the aquifer is within 10 feet of the original water table by the end of the simulation period. The exception to that is the McPherson Channel area and southwest Harvey County, where the combination of relatively lower recharge rates (McPherson Channel) or higher pumping rates (Harvey County) caused notable water-level declines that are never fully recovered in any of the scenarios.

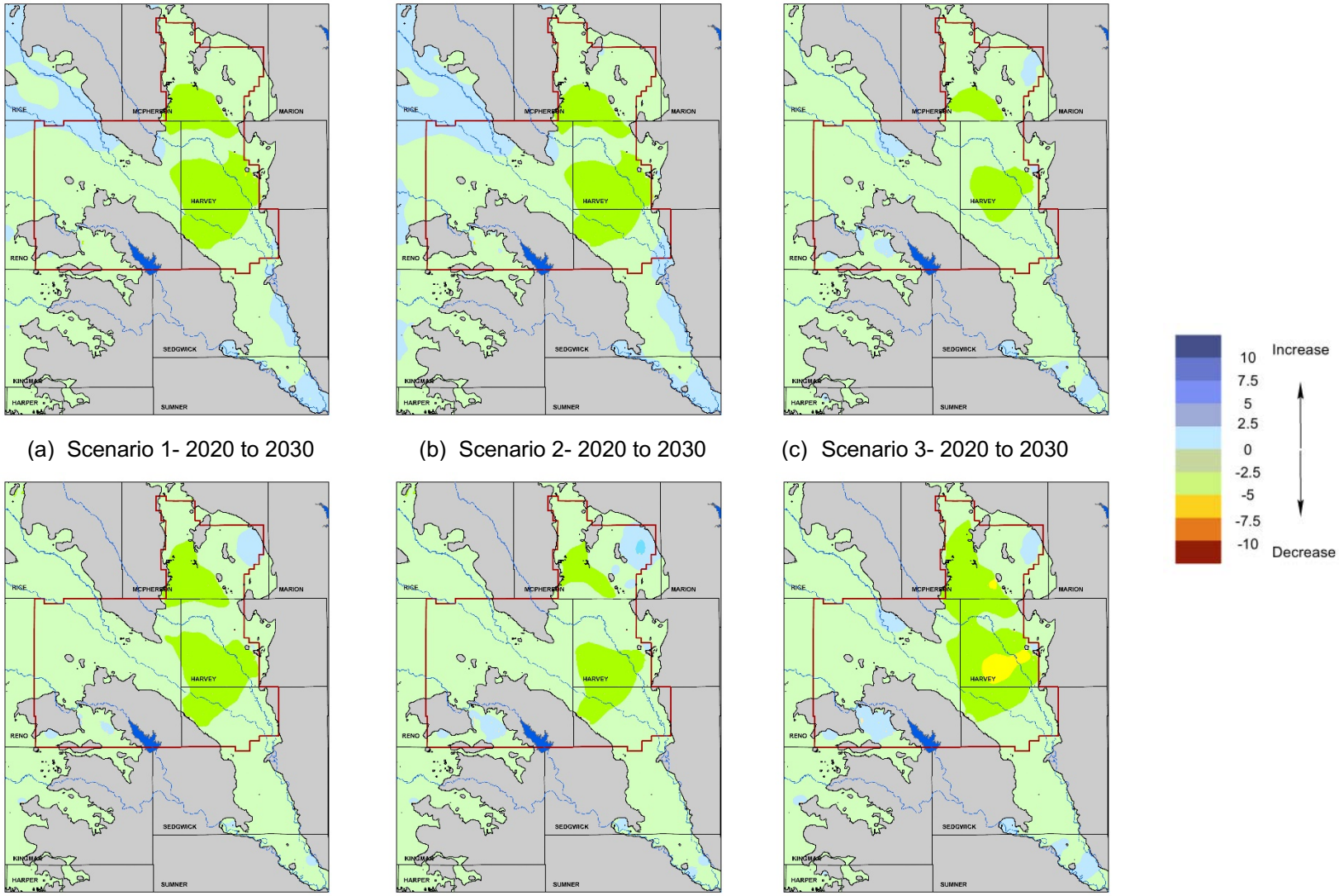

(a) Scenario 1- 2020 to 2030 (b) Scenario 2- 2020 to 2030 (c) Scenario 3- 2020 to 2030

(d) Scenario 1- 2020 to 2040 (e) Scenario 2- 2020 to 2040 (f) Scenario 3- 2020 to 2040

Figure 68. Simulated water-level change, in feet, for all three scenarios.

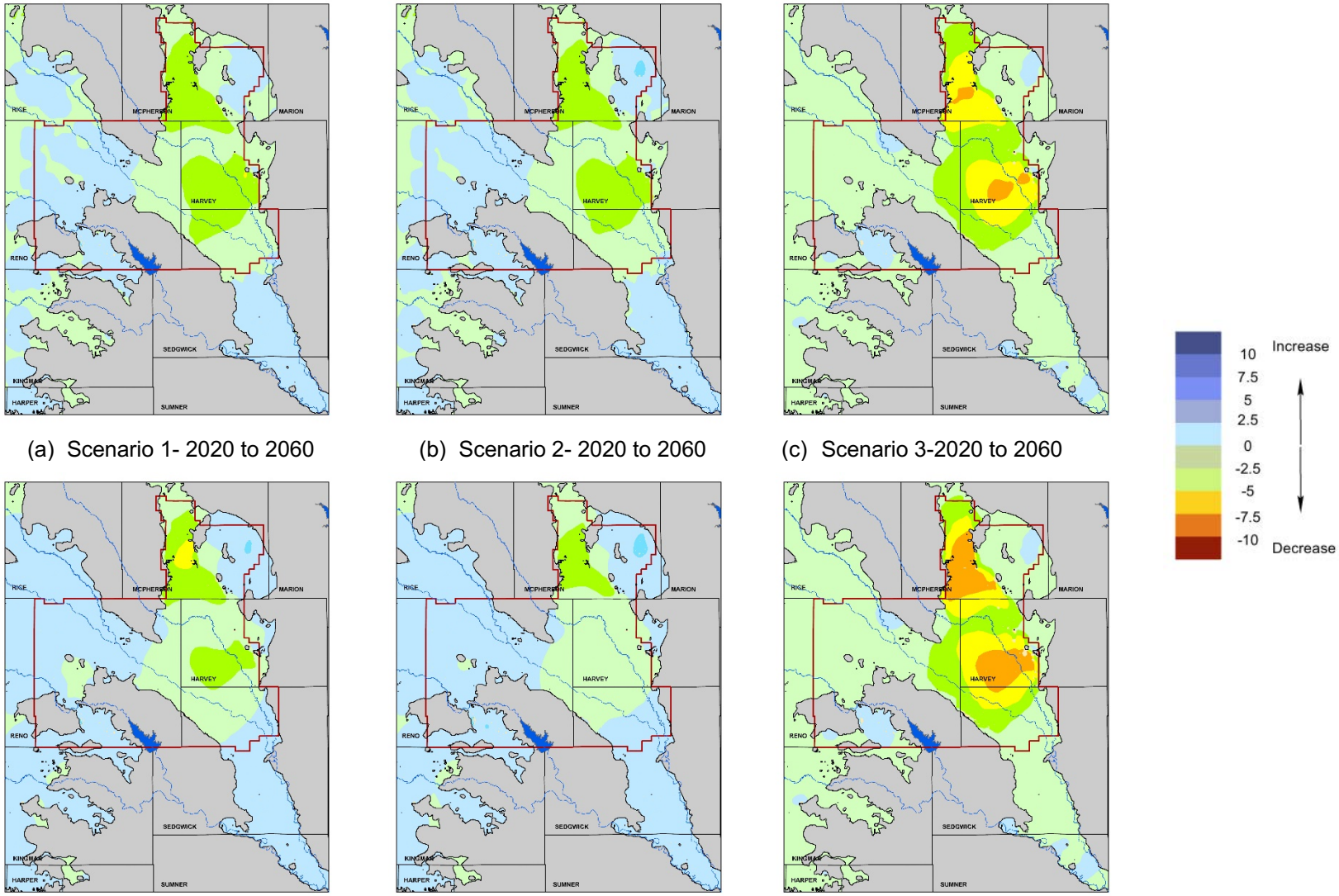

(a) Scenario 1- 2020 to 2060 (b) Scenario 2- 2020 to 2060 (c) Scenario 3-2020 to 2060

(d) Scenario 1-2020 to 2080 (e) Scenario 2-2020 to 2080 (f) Scenario 3-2020 to 2080

Figure 69. Simulated water-level change, in feet, for all three scenarios.

Acknowledgments

The KGS modeling team acknowledges the funding support of the Kansas Water Office (and the State Water Plan fund) and Equus Beds GMD2 for this project. The authors thank Matt Unruh and Josh Olson of the KWO and Tim Boese of GMD2, who served as the primary contacts. In addition, we thank Steve Flautery, formerly of GMD2, who helped review the model's initial development. We also acknowledge KGS staff who contributed to this report. Andrea Brookfield, formerly of the KGS, provided reviews of other similar modeling efforts. John Woods spent a substantial amount of time identifying stream elevations along the selected stream courses used in the project. We also thank Julie Tollefson, KGS editor, who reviewed the final report.

Appendix A

Lithologic-Based Model Layers

The five lithologic categories listed in table A-1 and shown in fig. A-1 were aggregated and proportioned to explore approaches for establishing continuous and relatively smooth surfaces that divide the model into naturally occurring vertical layers. Two approaches were pursued. The first was to maximize the percentage contrast between fine (categories 1 and 2 from table 1) and coarse (categories 3, 4, and 5) materials occurring between successive layers. The second method was to establish layers that are composed of the largest percentage from a single category by minimizing mixing of the categories within the same layer.

Table A-1. Standardized Lithologies Categories.

Category 1	Category 2	Category 3	Category 4	Category 5
shale clay bedrock red bed siltstone	fine silty clay fine to medium silty clay silty clay medium silty clay fine to coarse silty clay medium to coarse silty clay fine sandy clay fine to medium sandy clay medium sandy clay sandy clay fine to coarse sandy clay medium to coarse sandy clay coarse sandy clay clayey silt fine silt silt top soil overburden marl calcified material (limestone/caliche)	fine sandy silt fine to medium sandy silt medium sandy silt sandy silt fine to coarse sandy silt medium to coarse sandy silt coarse sandy silt gravelly clay sandstone	clayey sand fine silty sand fine to medium silty sand silty sand medium silty sand fine to coarse silty sand medium to coarse sandy silt coarse silty sand unknown cemented sand and/or gravel fine sand fine to medium sand	sand medium sand fine to coarse sand fine to medium coarse sand medium to coarse sand coarse sand clayey gravel silty gravel

All defined layers lie between the predevelopment water-table surface and bedrock. We explored dividing the model areas into three, five, and seven layers using an 8,000 ft spaced grid (fig. A-2) instead of the model's native 400 ft cell resolution, which was too fine for the calculations given our available computational resources.

To provide control for the layers, the grid was divided into initial layers of targeted thickness. For the three- and five-layer approaches, the grid cells were evenly divided from the top of the predevelopment surface to the bedrock. For the seven-layer approach, the top five layers were 15 ft thick and the remaining sixth and seventh layers were split to cover any remaining thickness. The function by which the optimal layers are defined is controlled by a regularization term that keeps the process from straying too far from these target thicknesses. The regularization term can be adjusted to keep the resulting layering closer to the target structure or loosened to allow more variability.

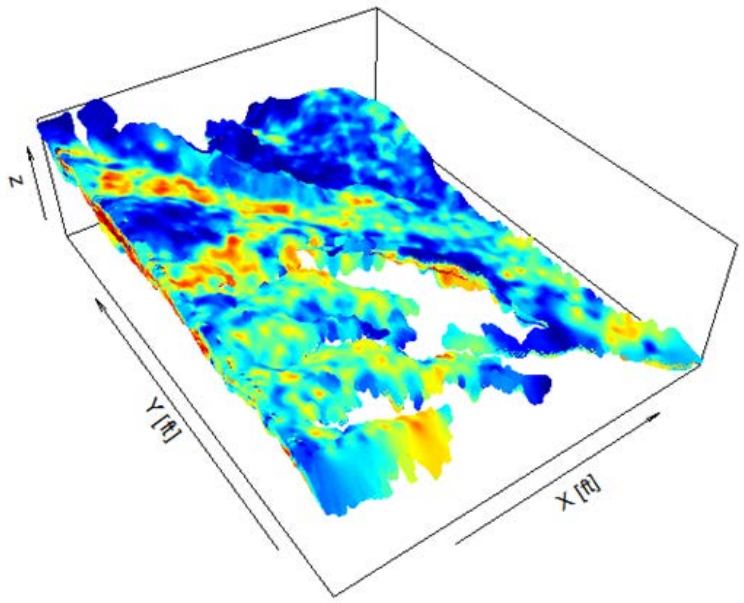

Figure A-1. Three-dimensional proportion-weighted average lithology categories. The dark blue colors indicate lower classes (finer materials) whereas light green to yellow and red represent higher classes (coarser materials).

A Monte Carlo process was used to find the optimal parameters for a thin-plate spline interpolation method. Forty-eight different realizations of the optimization process for each case—that being the number of layers, style of layering, and level of regularization—were run.

As example of the process, the initial structure of defining three layers across the model domain by trying to maximize the fine versus coarse material contrast between successive layers with the most restrictive regularization term has the following percentages:

Layer	% fine	% coarse
1 (top)	39	61
2	30	70
3 (bottom)	34	66

The optimization process starts with a thin-plate spline model and adjusts the interpolation based on more than 5,000 iterations in this case to establish layers of the following lithology category percentages:

Layer	% fine	% coarse
1	44	56
2	21	79
3	41	59

Figure A-2 shows the points that represent the center of the 8,000 ft grid cells where the logs are aggregated to produce a composite representation of all the logs within the grid cell. The composite logs are vertically averaged using 5 ft increments from which the layers are defined.

Cross sections of the layer definitions are shown from west to east (fig. A-3a) and south to north (fig. A-3b). In the cross section diagrams, the blue line represents the predevelopment water-table surface, the black line represents bedrock, and the red lines are the two internal surface contacts developed by the optimization process. The color scale represents the proportions of the "coarse" lithology categories (e.g., dark red is composed entirely of categories 3, 4, and/or 5).

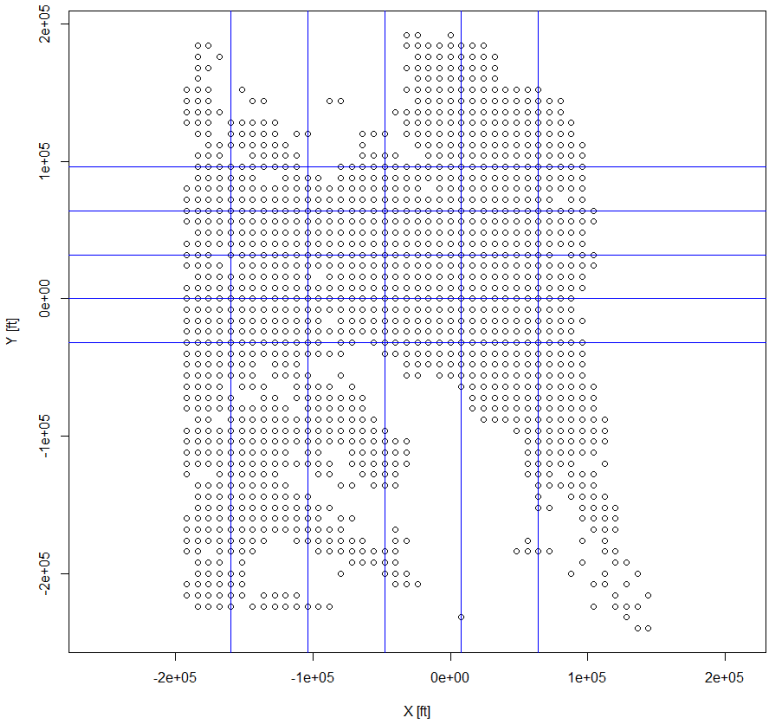

Figure A-2. Center points of the 8000 ft grid cells

The "optimal" spline model for the two internal surfaces (red lines in fig. A-3) was applied to generate surfaces over the model's native grid. As shown in fig. A-4, the upper left panel represents the total thickness divided by 3, which is the target thickness for each layer under the regularization term. Layers 1 to 3 are shown in their respective panels. Gray areas represent zero thickness, dark blue represents 1 ft of thickness and red equals at least 100 ft thickness. Each defined layer is absent in some place; when layers 1 and 2 are absent, layer 3 occupies the entire available thickness.

Initial findings of using lithology-based categories to vertically define layers across the model area indicate:

1. The drillers' logs are dominated by "coarse" descriptions, which may require expanding the five lithologic categories to better account for distinctions unique to south-central Kansas.
2. There does not appear to be a clear, consistent vertical structure, in terms of layers of predominantly coarse or fine material, across the entire model area.
3. The predominant fine/coarse trend is lateral rather than vertical, with a greater concentration of coarse material in the core regions of the model (active area) and finer material along the fringes.

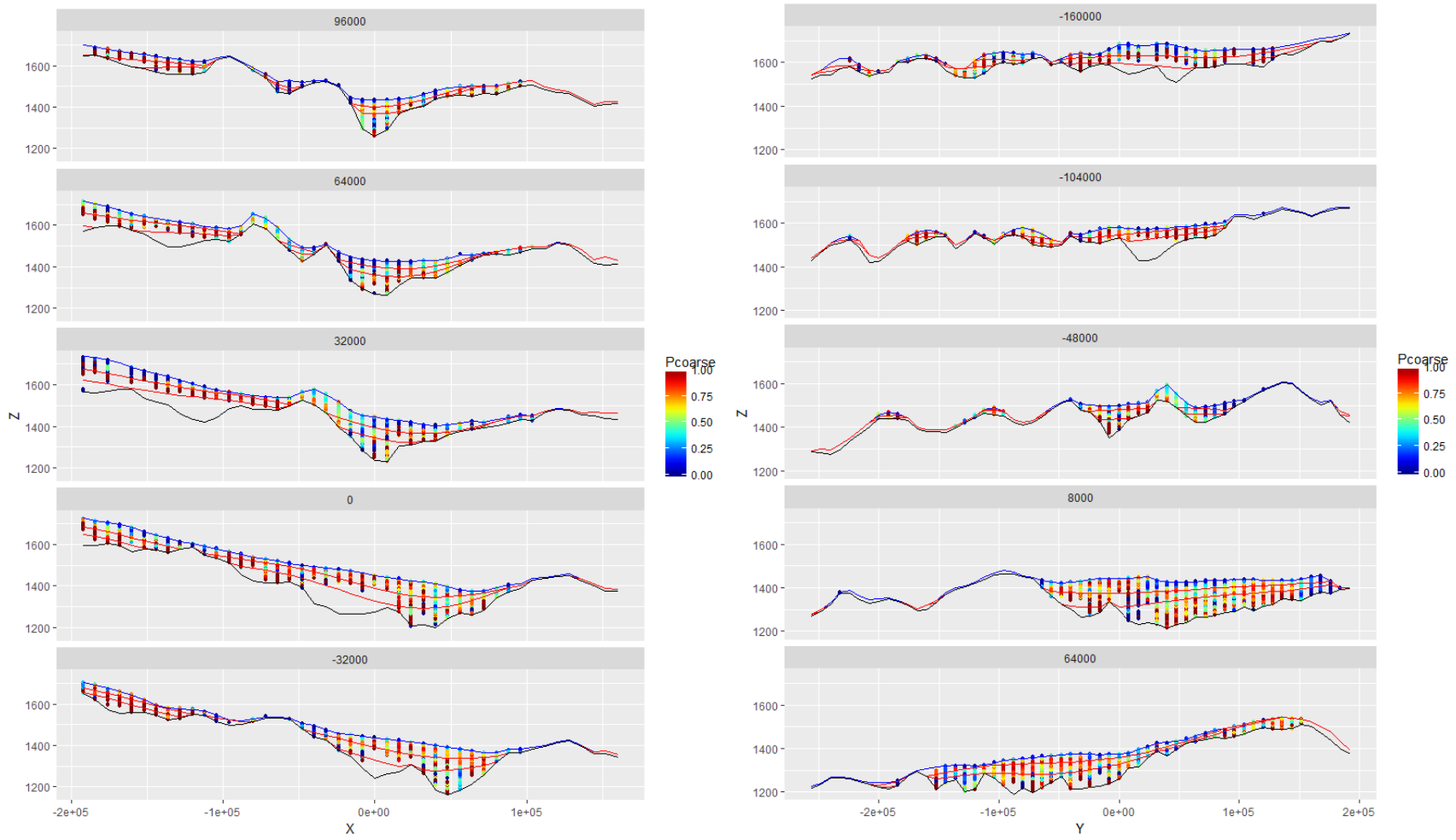

(a) west-to-east cross sections (b) south-to-north cross sections

Figure A-3. Cross sections of defined layers based on maximum fine versus coarse material contrast between successive layers.

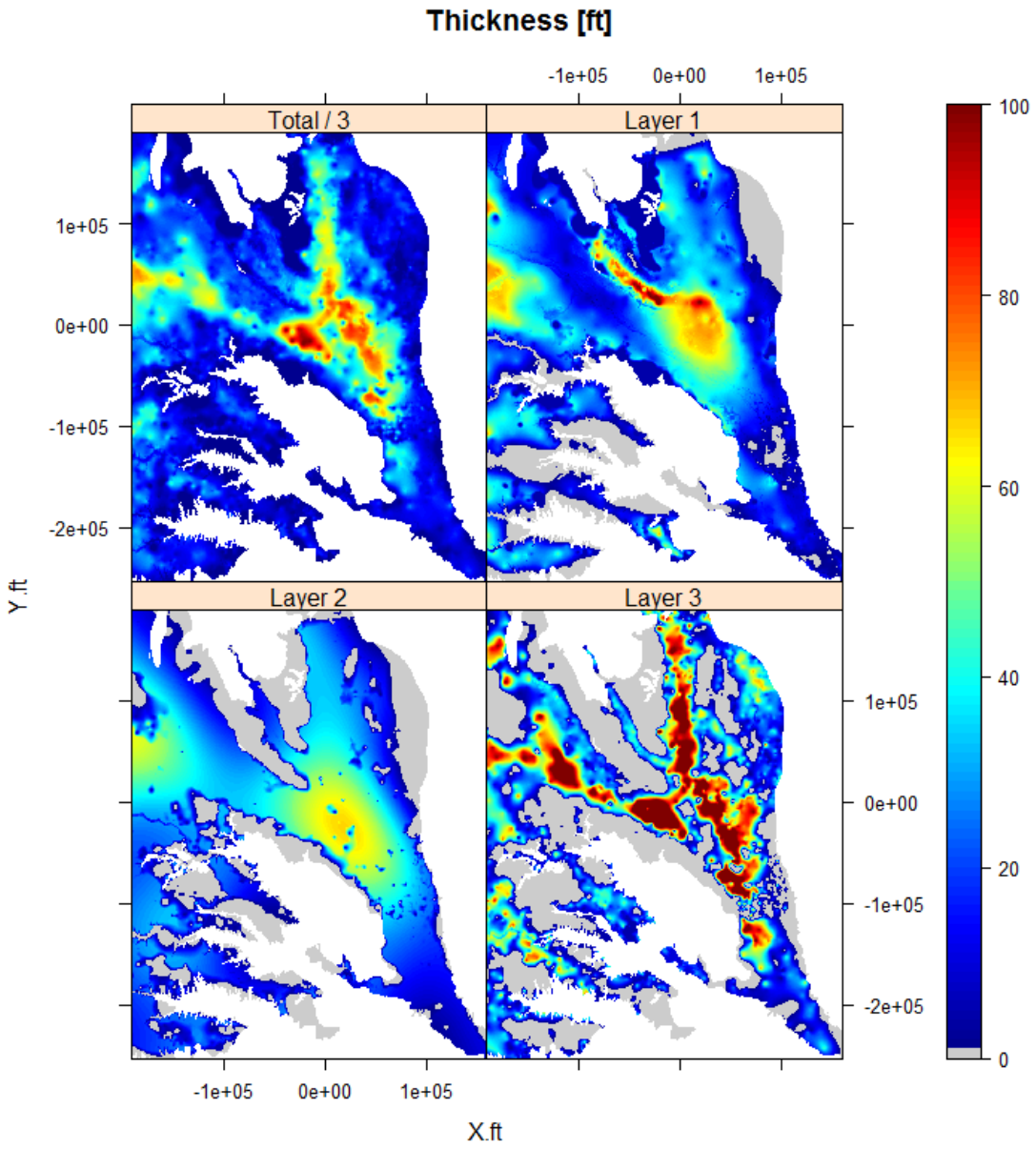

Figure A-4. Example of defined layer thickness using the optimal contrast of fine versus coarse materials between successive layers.

REFERENCES

Bayne, C. K., 1956, Geology and ground-water resources of Reno County, Kansas: Kansas Geological Survey, Bulletin 120, 130 p.

Bayne, C. K., 1960, Geology and ground-water resources of Harper County, Kansas: Kansas Geological Survey, Bulletin 143, 184 p.

Bohling, G. G., 2016, User's Guide to Hydra_translate.xlsm: An Excel Workbook for Quantification of Water Well Driller's Logs. Kansas Geological Survey, Open-File Report 2016-30, 26p.

Butler, J. J., Jr., Whittemore, D. O., and Wilson, B. B., 2017, Equus Beds Groundwater Management District No. 2 sustainability assessment: Kansas Geological Survey, Open-File Report 2017-3, 93 p.

Doherty, J., 2004, PEST—Model-Independent Parameter Estimation. User Manual, 5th Edition.Watermark Numerical Computing, 333 p.

Fent O. S., 1950, Geology and ground-water resources of Rice County, Kansas: Kansas Geological Survey, Bulletin 85, 143 p.

Harbaugh, A. W., Banta, E. R., Hill, M. C., and McDonald, M. G., 2000, MODFLOW-2000, the U.S. Geological Survey modular ground-water model—User guide to modularization concepts and the ground-water flow process: U.S. Geological Survey, Open-File Report 00-92, 121 p.

Kelly, B. P., Pickett, L. L., Hansen, C. V., and Ziegler, A. C., 2013, Simulation of groundwater flow, effects of artificial recharge, and storage volume changes in the Equus Beds aquifer near the city of Wichita, Kansas well field, 1935–2008: U.S. Geological Survey Scientific Investigations Report 2013–5042, 90 p.

Lane, C. W., 1960, Geology and ground-water resources of Kingman County, Kansas: Kansas Geological Survey, Bulletin 144, 174 p.

Lane, C. W., and Miller, E. M., 1965, Geohydrology of Sedgwick County, Kansas: Kansas Geological Survey, Bulletin 176, 100 p.

Liu, G., Wilson, B. B., Whittemore, D. O., Wei Jin, W., and Butler, J. J., Jr., 2010, Ground-water model for Southwest Kansas Groundwater Management District No. 3: Kansas Geological Survey, Open-File Report 2010-18, 106 p.

Macfarlane, P. A., and Wilson, B. B., 2006, Enhancement of the bedrock-surface map beneath the Ogallala portion of the High Plains aquifer, western Kansas: Kansas Geological Survey, Technical Series Report 20, 28 p.

Niswonger, R. G., Panday, S., and Ibaraki, M., 2011, MODFLOW-NWT, A Newton formulation for MODFLOW-2005: U.S. Geological Survey Techniques and Methods 6–A37, 44 p.

Prudic, D. E., Konikow, L. F., and Banta, E. R., 2004, A new streamflow-routing (SFR1) package to simulate stream-aquifer interaction with MODLFOW-2000: U.S. Geological Survey, Open-File Report 2004-1042, 104 p.

Stone, M. L., Klager, B. J., and Ziegler, A. C., 2019, Water-quality and geochemical variability in the Little Arkansas River and Equus Beds aquifer, south-central Kansas, 2001–16: U.S. Geological Survey Scientific Investigations Report 2019–5026, 79 p.

Walters, K. L., 1961, Geology and ground-water resources of Sumner County, Kansas: Kansas Geological Survey, Bulletin 151, 198 p.

Whittemore, D. O., Macfarlane, P. A., and Wilson, B. B., 2014, Water resources of the Dakota aquifer in Kansas: Kansas Geological Survey, Bulletin 260, 68 p.

Williams, C. C., and Lohman, S.W., with analyses by Hess, H. H., 1949, Geology and ground-water resources of a part of south-central Kansas: Kansas Geological Survey Bulletin 79, 455 p.

Wilson, B. B., and Bohling, G. C., 2003, Assessment of reported water use and total annual precipitation, State of Kansas: Kansas Geological Survey, Open-File Report 2003-55C, 39 p.

Wilson, B. B., Liu, G., Bohling, G. C., Whittemore, D. O., and Butler, J. J., Jr., 2015, West Central Kansas GMD1 Model: Kansas Geological Survey, Open-File Report 2015-33, 137 p.

Wilson, B. B., Liu, G., Whittemore, D. O., and Butler, J. J., Jr., 2008, Smoky Hill River ground-water model: Kansas Geological Survey, Open-File Report 2008-20, 99 p.